UC Riverside

UC Riverside Electronic Theses and Dissertations

Title

Investigating the Roles of Small RNAs in Plant-Bacterial Interactions

Permalink

https://escholarship.org/uc/item/28s5v6t9

Author

Lii, Yifan Eve

Publication Date

2016

Copyright Information

This work is made available under the terms of a Creative Commons Attribution-NonCommercial-NoDerivatives License, availalbe at https://creativecommons.org/licenses/by-nc-nd/4.0/

Peer reviewed|Thesis/dissertation

eScholarship.org Powered by the California Digital Library
University of California

UNIVERSITY OF CALIFORNIA
RIVERSIDE

Investigating the Role of Small RNAs in Plant-Bacterial Interactions

A Dissertation submitted in partial satisfaction
of the requirements for the degree of

Doctor of Philosophy

in

Genetics, Genomics, and Bioinformatics

by

Yifan Eve Lii

August 2016

Dissertation Committee:
Dr. Hailing Jin, Chairperson
Dr. Shou-wei Ding
Dr. Thomas Eulgem

Copyright by
Yifan Eve Lii
2016

The Dissertation of Yifan Eve Lii is approved:

Committee Chairperson

University of California, Riverside

ACKNOWLEDGEMENTS

None of this would have been possible without my advisor and dissertation committee chairperson Dr. Hailing Jin, who has provided me numerous opportunities for progress, learning, excelling, and personal growth during my time in her lab. She accommodated me during my pregnancies and maternity leaves, and supported me to continue and finish graduate school, for which I am so thankful.

Many others in the UCR community have also supported and guided me through these years—from just having simple daily conversations or stimulating scientific discussions with me, to teaching me procedures and helping me with experiments in the lab, to providing general guidance on getting through graduate school. To all of you, thank you so much; you have touched my life more profoundly than you know (not listed in any particular order): My dissertation committee members Dr. Shou-wei Ding and Dr. Thomas Eulgem, who have always supported my progress in graduate school; My qualifying committee members Dr. Thomas Eulgem, Dr. Shou-wei Ding, Dr. Joel Sachs, Dr. Isgouhi Kaloshian, and Dr. Yinshen Wong, who all pushed me to be the best graduate student I could be; every single current and former member of the Jin Lab, who shaped my day-to-day lab life and have helped me in so many aspects of my projects—specifically those taught me new protocols and techniques, Dr. Shang Gao, Dr. Xiaoming Zhang, Dr. Hongwei Zhao, Dr. Arne Weiberg, Dr. Ming Wang; All the professors of the graduate courses I have taken, who all instilled in me not only their knowledge of science but also their love for it; The NSF ChemGen IGERT director Dr. Julia Bailey-Serres and assistant director Dr. Sean Cutler, who gave me the wonderful opportunity to participate

in this program; All the ChemGen IGERT and Genetics, Genomics, and Bioinformatics (GGB) professors, who provided advice for my projects as well for graduate life; All the former ChemGen IGERT graduate students and current and former GGB graduate students for your camaraderie and for making graduate school fun; All the undergraduate and postgraduate research assistants, who volunteered their time to help me in all my projects and gave me the opportunity to teach, whom I will list by name—Elizabeth Yoon, who was with me the longest and helped me tremendously in my DNA methylation project; Kimberly Van, who assisted in lab duties and various experiments; Eric Kelley Jr., who helped me with a lot of the *SCRL5* work and various lab duties; and Nicole Durbin-Henderson Salvador, who helped me with the *SCRL5* work; Blair Clark, who complete a large part of chemical screening; Olivia Onejeme, who also assisted in the chemical screening and sowing plant seeds; Administrative staff members GGB student services supervisor Deidra Kornfeld, ChemGen IGERT grant coordinators Ronly Schlenk and Matthew Collin, who have tremendously helped me navigate the logistics and paperwork (and so much more!) of graduate school.

Chapter 2 of this dissertation is a reprint (with edited formatting of the references and figure labeling) of the publication: Dongdong Niu, Yifan E. Lii, Padmanabhan Chellappan, Lei Lei, Karl Peralta, Chunhao Jiang, Jianhua Guo, Gitta Coaker, & Hailing Jin (2016) Nature Communications 7, 11324. H.J. conceived the idea and designed the project; D.N., Y.E.L., P.C., L.L., C.J. and K.P. performed the experiments; H.J., D.N., Y.E.L., P.C., J.G. and G.C. analysed and interpreted the data; H.J., Y.E.L. and D.N. wrote the manuscript. We thank David Baulcombe for providing *rdr6-15* mutant seeds;

Johnathan Clark for providing *se-1* mutant seeds; and Artur Jarmolowski and Michael Prigge for providing SE-OE lines. H.J., D.N., Y.E.L. and P.C. were supported by grants from the National Institute of Health (R01 GM093008), the National Science Foundation (IOS-1557812) and an AES-CE Award (PPA-7517H) awarded to H.J. G.C. and L.L. were supported by grants from the National Science Foundation (MCB-1054298), and the National Institutes of Health (R01-GM092772) awarded to G.C. C.J. and J.G. were supported by a grant from Joint Research Fund for Overseas, Hong Kong, and Macao Scholars (31228018) awarded to J.G. and H.J.

The whole genome bisulfite sequencing in Chapter 3 of this dissertation was done in collaboration with Dr. Joe Ecker at the Salk Institute (La Jolla, CA). His staff and lab members were so helpful and accommodating during my time in his lab, especially Mark Urich, who taught me how to prepare the bisulfite libraries; Joseph Nery, who performed the Illumina sequencing runs; and Dr. Mathew Lewsey, who did the alignment, methylbase calling, and analysis of the sequences, provided thoughtful discussion, and helped answer so many of my questions related to this project. Dr. Rishi Aryal from our lab also helped in analyzing the sequences.

We thank Sean Cutler for providing us the LATCA small chemical library and Brian Stastawicz for providing the *Arabidopsis* transgenic seeds used for the forward chemical screen detailed in Chapter 4. The Keen Hall Core Facility academic coordinators Dr. Glenn Hicks and Dr. David Carter assisted me in setting up my chemical screen and taught me how to use the equipment. The figures used in this chapter were

previously used on a poster titled “Dissection of RNA Silencing Through Chemical Genomics” entered in the 2011 IGERT Poster Competition.

I was supported by funding from NSF-IGERT in Chemical Genomics (DGE0504249), from GGB, from TAships, and NIH and NSF grants awarded to Dr. Hailing Jin.

Outside of graduate school, I have had so much support and help. I want to thank all my family members and church friends, especially those in my home meeting, for their prayers and support. You all have lifted me up in the roughest times with God’s words and encouragement.

Lastly, I owe so much to my husband and companion, John, who stood by me through the thick and thin, sickness and health, highs and lows. I really could not have made it without you.

DEDICATION

To my children—my lights before the end of the tunnel

ABSTRACT OF THE DISSERTATION

Investigating the Roles of Small RNAs in Plant-Bacterial Interactions

by

Yifan Eve Lii

Doctor of Philosophy, Graduate Program in Genetics, Genomics, and Bioinformatics
University of California, Riverside, August 2016
Dr. Hailing Jin, Chairperson

Small RNAs are named for their small (20–24 nucleotide) size, but the impact of their function on nearly all organisms, including animals, plants, and fungi, is profound. Many studies have shown that these non-coding RNAs regulate gene expression by silencing genes during plant pathogen infection and determine the outcome—host survival or eventual death. In this dissertation, I present my studies investigating the role of small RNAs in the interactions between the plant *Arabidopsis thaliana* and the hemibiotrophic bacterial pathogen *Pseudomonas syringae*. Chapter 1 is an introduction to this dissertation and broadly covers relevant topics such as the plant immune system, small RNA biogenesis, the role of small RNAs in plant bacterial resistance, RNA-directed DNA methylation, and the role of DNA methylation in plant bacterial resistance. Chapter 2 is a reprint of our publication titled "miRNA863-3p sequentially targets negative immune regulator *ARLPKs* and positive regulator *SERRATE* upon bacterial infection". We discovered that miRNA863-3p is highly induced by *Pseuduomonas*

syringae pv. *tomato* containing effector gene *avrRpt2*, and it sequentially targets *ARLPKs*, which are receptor-like psuedokinases that have negative roles in plant defense, and SERRATE, which has a positive role in defense and a known role in miRNA biogenesis. Chapter 3 is a report on our finding that the *pol IV* mutant exhibits enhanced resistance to bacterial infection, but cannot be primed for systemic acquired resistance (SAR) with *Psuedomonas syrginae* pv. *maculicoli* (*Psm*), and whole genome bisulfite sequencing and further analysis revealed that *SCR-LIKE 5* (SCRL5) has increased DNA methylation and decreased relative expression after wild-type plants are pre-treated with *Psm*, but this change in methylation and gene expression is not seen in *pol IV*. Furthermore, SCRL5 is upregulated in local infections with *P. syringae* pv. *tomato,* suggesting that it may have a complex role in local and systemic defense. Lastly, Chapter 4 is a report of a forward chemical genetics screen conducted using "Library of AcTive Compounds on Arabidopsis to find small molecules that perturb a nat-siRNA pathway. We identified 11 small molecules possibly targeting this pathway that can be used for further testing.

TABLE OF CONTENTS

Chapter One: Overview

Introduction……..1
References……...18
Figures……...……..25
Tables……...…….……..26

Chapter Two: miRNA863-3p Sequentially Targets Negative Immune Regulator *ARLPKs* and Positive Regulator *SERRATE* Upon Bacterial Infection

Abstract……...32
Introduction…….....33
Results…….....35
Discussion…….....48
Methods……...53
References……...60
Figures……..……...68
Tables…….....90

Chapter Three: Polymerase IV-mediated RNA-directed DNA Methylation Regulates Systemic Acquired Resistance

Abstract……...91
Introduction…….92
Results…….....35
Discussion……100
Methods……103
References……106
Figures ……..…111
Tables……119

Chapter Four: Chemical Genetics Screen Targeting Small RNA Mediated Gene Silencing Pathways in *Arabidopsis Thaliana* yields several hit compounds

Abstract……120
Introduction……...121
Results……...122
Discussion……126
Methods……127
References……129
Figures ……..132

LIST OF FIGURES

Figure 1.1……24

Figure 2.1……67
Figure 2.2……68
Figure 2.3……69
Figure 2.4……71
Figure 2.5……72
Figure 2.6……73
Figure 2.7……74
Figure 2.8……75
Figure 2.9……76
Figure 2.10……77
Figure 2.11……78
Figure 2.12……80
Figure 2.13……81
Figure 2.14……83
Figure 2.15……84
Figure 2.16……86
Figure 2.17……88

Figure 3.1……108
Figure 3.2……110
Figure 3.3……111
Figure 3.4……112
Figure 3.5……114

Figure 4.1……129
Figure 4.2……130
Figure 4.3……131

LIST OF TABLES

Table 1……...25
Table 2……..89
Table 3……116

CHAPTER 1

Overview

INTRODUCTION

Plants are affected by a myriad of pathogens—bacteria, fungi, oomycete, and viruses—all of which threaten global food security. It is estimated that 30-40% of crops are lost from the field to the market due to various plant diseases (Bebber and Gurr, 2015; Flood, 2010). From 2014-2016, it is estimated that 795 million people in the world (one in nine people) were undernourished (Food and Agriculture Organization of the United Nations., 2014). With the ever-increasing world population and demand for crop production comes the need for ongoing research in the field of plant immunity and plant health.

Plants have evolved an immune system that contains conserved features found in the innate immune systems of mammals and insects (Ausubel, 2005). Many studies have uncovered the signaling pathways, phytohormone modulation, and transcriptional changes involved in the plant immune response using the model plant *Arabidopsis thaliana* (Arabidopsis) and the bacterial pathogen *Pseudomonas syringae* pv. *tomato* DC3000 (*Pst*) and several reviews are available (Nishimura and Dangl, 2010; Buscaill and Rivas, 2014; Dodds and Rathjen, 2010; Pieterse et al., 2012). While, *Pst* is not a natural pathogen for Arabidopsis in the wild, through artificial methods (e.g. infiltration of the leaves with bacterial suspension), *Pst* can infect the leaves and causes water-soaked patches that become necrotic. The leaves may also exhibit diffuse chlorosis, or yellowing of the leaves (Katagiri et al., 2002).

Many studies have shown that small RNAs (sRNAs) regulate gene expression in many plant processes and pathways, including plant defense responses against pathogens and even pathogen virulence (Ding, 2010; Fei et al., 2013; Pumplin and Voinnet, 2013; Seo et al., 2013; Weiberg et al., 2015; Weiberg and Jin, 2015; Weiberg et al., 2014). They can silence genes by mediating mRNA transcript cleavage or translational inhibition or by recruiting other factors that induce chromatin modification or DNA methylation (Bologna and Voinnet, 2014; Borges and Martienssen, 2015). In this introduction, I will first present basic concepts about the plant immune system and then talk about sRNAs and epigenetics (RNA-directed DNA methylation and histone modification), as well as summarize findings of their role in plant defense, specifically against bacterial pathogens.

The many layers of the plant immune system

An important feature of the plant immune system is the recognition of pathogens. Pattern recognition receptors (PRRs) can recognize and become activated by pathogen-associated molecular patterns (PAMPs), which are conserved microbial molecules that distinguish the host from the pathogen. A well-studied example is flg22, a conserved 22-amino acid peptide derived from bacterial flagellin, which is recognized by transmembrane FLAGELLIN-SENSING 2 (FLS2) (Chinchilla et al., 2006). As not all microbes are pathogenic, PRRs can also recognize microbe-associated molecular patterns (MAMPS). Even endogenous plant molecules produced from pathogen invasion and damage, called damage-associated molecular patterns (DAMPS) can also elicit

PRRs (Lotze et al., 2007). Activation of PRRs leads to PAMP-triggered immunity (PTI) that is characterized by increase in intracellular calcium concentration, MAP kinase cascades, production of reactive oxygen species, transcriptional reprogramming, and production of antimicrobial compounds, all to limit the growth and multiplication of the pathogen. This line of defense offered by PTI is also termed basal resistance (Li et al., 2016).

Pathogens have in-turn evolved a multitude of effector proteins with various functions, all with the purpose to inhibit PTI responses. These effectors are delivered into host cells via type III-secretion systems. The action of effectors renders the plant susceptible to infection. To combat this, plants have evolved resistance (R) proteins that recognize pathogen effector proteins, constituting the second layer of the plant immune system: effector triggered immunity (ETI). An example of an effector-R gene pair is the effector *avrRpm1* and *R* gene *RPM1* (Ritter and Dangl, 1995). ETI is similar to PTI in its responses although it is faster and more robust. It also can result in the hypersensitive response (HR), which does not occur in PTI, in which plant cells in the site of infection undergo cell death to inhibit pathogen spread. ETI, thus can successfully render the plant resistant to the attack pathogen (Dodds and Rathjen, 2010).

In addition to these two layers of pathogen recognition, plants also exhibit a phenomenon named systemic acquired resistance (SAR), in which leaves infected with a pathogen confer long-lasting (up to several weeks), broad-spectrum (unspecific to the original infecting pathogen) resistance in uninfected tissue (Fu and Dong, 2013). It is known that the gene NONEXPRESSOR OF PATHOGENESIS-RELATED 1 (NPR1)

and the hormone salicylic acid (SA) are important for establishing SAR (Dong et al., 2001; Gaffney et al., 1993). Furthermore, several mobile signals that are transmitted from infected tissue to the uninfected have been proposed (Dempsey and Klessig, 2012).

Disease resistance is not only indicated by decreased growth of the pathogen within the host but also by the induced expression of marker genes. In the case of resistance to biotrophic (e.g. oomycete *Hyaloperonospora* arabidopsidis) pathogens, those that do not kill the host as a part of the infection process, and hemibiotrophic pathogens (e.g. *Pst*), those that only kill the host in latter stages of the infection process, SA-responsive genes (e.g. PATHOGENESIS RELATED-1, PR-1) are upregulated. In the case of necrotrophic pathogens, those that kill host cells to release and feed off of cell nutrients, (e.g. fungi *Botrytis cinerea* and *Plectosphaerella cucumeria*), jasmonic acid (JA)/ethylene-responsive genes (e.g. PLANT-DEFENSIN 1.2, PDF1.2) are upregulated (Glazebrook, 2005). There is evidence that the SA and JA pathways are antagonistic in certain conditions (Tsuda et al., 2009), and resistance to a biotrophic pathogen may render a plant susceptible to a necrotrophic pathogen, and vice versa (Spoel et al., 2007).

Despite their immune repertoire, plants still succumb to pathogen infection, as pathogens and hosts are perpetually in an evolutionary arms-race to outcompete one another—for the pathogen to evade host detection and for the plant to ensure recognition and prompt removal of the pathogen (Anderson et al., 2010). Thus, there is the need to understand the underlying molecular mechanisms of disease resistance and susceptibility in plants, as well as to develop or breed resistant crops.

Small RNAs and their role in plant defense

Plants have many different types of small RNAs of varied biogenesis pathways and functions with sizes ranging from 20–24 nucleotides (nt). While general functions and attributes of these sRNAs and associated proteins have been detailed, there are many exceptions to the rules, and new findings are continuing to broaden, as well as clarify, our view of RNA silencing. Briefly, most sRNAs are processed from longer double-stranded RNA (dsRNA) or single-stranded RNA (ssRNA) with a partial double-stranded structure due to foldback into short RNAs duplexes by DICER-LIKE (DCL) proteins, which possess RNase-III endnuclease activity. *Arabidopsis* contains four DCL proteins (DCL1–4), which produce sRNAs of differing sizes (Henderson et al., 2006; Rogers and Chen, 2013). In some cases, these dsRNAs are produced by RNA-DEPENDENT RNA POLYMERASES (RDR), of which *Arabidopsis* has six (RDR1–6). One strand of the duplex is selected for association with a catalytic effector protein called ARGONAUTE (AGO), forming a RNA-induced gene silencing complex (RISC) which targets complementary RNA sequences to mediate gene silencing. *Arabidopsis* encodes 10 ARGONAUTE (AGO1–10), which form three different clades, each with different sRNA-loading specificities and functions (Zhang et al., 2015). Depending on the sRNA involved and the ARGONAUTE protein, this can occur through transcript cleavage or translation inhibition (post-transcriptional gene silencing, PTGS), or recruitment of other factors to mediate DNA methylation or histone modification (transcriptional gene silencing, TGS) (Bologna and Voinnet, 2014; Borges and Martienssen, 2015; Zhang et al., 2015).

There are two categories of endogenous sRNAs: microRNAs (miRNAs) or small-interfering RNAs (siRNAs). They differ in their starting RNAs: miRNAs are derived from Polymerase II (Pol II) transcripts that form imperfect hairpin-like structures (called pri-miRNAs), which are processed into shorter stem-loop structures (pre-miRNAs) by DCL1. Other proteins have been found in a complex with DCL1, such as TOUGH, SERRATE, and HYPONASTIC LEAVES1 and enhance the accuracy and processing of pri-miRNAs by DCL1. The resulting miRNA (guide)/miRNA* (passenger) duplexes are stabilized via 2'-*O*-methylated by methyltransferase HEN1. One of the strands from the duplex is selected for association with an AGO protein (usually AGO1, though exceptions exist) and the passenger strand is degraded by the coordinated action of HEN1 SUPPRESSOR1 uridylation and SMALL RNA DEGRADING NUCLEASE activity. The miRNA/AGO RISC can then target complementary transcripts for cleavage transcripts or inhibit translation (Borges and Martienssen, 2015; Rogers and Chen, 2013; Vazquez et al., 2010).

There are many subcategories of plant endogenous siRNAs, which all derive from long dsRNAs of different forms: Natural antisense transcript-derived siRNAs (nat-siRNAs) are derived from Pol II (or possibly Pol IV) complementary sense and antisense transcripts from the same (*cis*-nat-siRNAs) or different (*trans*-nat-siRNAs) loci. These may require the action of RNA-dependent RNA polymerases (RDRs), and are diced by DCL1, 2, or 3 into 21–24-nt siRNAs that can mediate PTGS. Heterochromatic siRNAs (hc-siRNAs) are can be produced from a canonical Pol IV-dependent pathway in which Pol IV transcript are processed into dsRNA by RDR2 and

diced by DCL3 into 24-nt siRNAs that mediate RNA-directed DNA methylation (RdDM) of many transposable elements, repeat regions, and some genes (detailed in the next section). Or, there is a non-canonical pathway, occurring at certain new transposons or trans-acting siRNA-generating (*TAS*) loci, in which Pol II transcripts are processed into dsRNA by RDR6 and then processed by DCL2 or DCL4 into 21–22-nt siRNAs. These siRNAs can bind to AGO4/AGO6 to mediate RdDM in a Pol V-independent manner or associate with AGO1 to mediate PTGS (Matzke et al., 2015). Lastly, phased secondary siRNAs (phasiRNAs), originally termed *trans*-acting siRNAs (tasiRNAs) (Fei et al., 2013), result from miRNA/AGO1 (or AGO7)-phased cleavage of *TAS* transcripts and processing by RDR6 and DCL4 into 21-nt siRNAs, which mainly direct PTGS, but can also mediate TGS in some instances.

Many sRNAs of various crops and plants are crucial to host defense responses against many pathogens, such as viruses, bacteria, fungi, and oomycetes, as well as to pathogen virulence, and their roles are detailed in many recent reviews (Ding, 2010; Fei et al., 2013; Pumplin and Voinnet, 2013; Seo et al., 2013; Staiger et al., 2013; Weiberg et al., 2015; Weiberg and Jin, 2015; Weiberg et al., 2014). Several *Arabidopsis* miRNAs and siRNAs are involved in PTI and ETI against bacterial pathogen *Pst*. miR393, the first sRNA discovered to play a role in antibacterial defense, is induced upon flg22 treatment and contributes to PTI by silencing auxin signaling receptors (Navarro et al., 2006). miR160a, also induced by flg22, positively regulates PAMP-induced callose deposition by targeting auxin response factors (Li et al., 2010). The same study also found that miR398b and miR773, are downregulated by flg22, and both play negative

roles in PAMP-induced callose deposition and PTI. miR398b targets a cytochrome c oxidase and two copper superoxide dismutases, while miR773 targets *MET2*, a DNA methyltransferase (Li et al., 2010). The complementary strand of miR393, miR393*, once thought to be a useless passenger strand marked for degradation, regulates ETI during infection with *Pst* carrying effector gene *avrRpt2* by silencing a protein trafficking gene *MEMB12*, thus promoting the secretion of antimicrobial pathogenesis-related (PR) proteins (Zhang et al., 2011). Other siRNAs are also involved in defense against *Pst* (*avrRpt2*), such as a natsiRNAATGB2, a nat-siRNA which contributes to ETI mediated by *RPS2* by silencing a gene with pentatricopeptide repeats (Katiyar-Agarwal et al., 2006), and AtlsiRNA, a long siRNA which silences the *ARABIDOPSIS THALIANA RNA-BINDING DOMAIN ABUNDANT IN APICOPLEXANS* (*AtRAP*) gene, which has a negative role in defense (Katiyar-Agarwal et al., 2007). Recently, we found that miR863-3p, targets multiple genes with opposite roles in plant defense. Early after infection, it targets two putative psuedokinases, *ATYPICAL RECEPTOR-LIKE PSEUDOKINASE1* (*ARLPK1*) AND *ARLPK2*, both which have negative roles in defense. Later during infection, it targets SE, which has a positive role in defense and miRNA biogenesis, forming a feed-back loop to downregulate miR863-3p. The functions of *ARLPK1* and *ARLPK2* are thus far unknown, but they interact with another functional kinase ARLPK1-interacting receptor-like kinase 1 (AKIK1), which also plays a negative role in disease resistance (Niu et al., 2016). Altogether, these studies show that these small RNAs have a large impact on the global health of crops and plants.

RNA-directed DNA methylation and its role in plant defense

DNA methylation occurs in plants, animals, fungi, and bacteria, and is important for many processes. It is a stable, heritable mark in which the DNA base cytosine (also adenine in bacteria) base is modified with a methyl group (Law and Jacobsen, 2010; Low et al., 2001; Matzke and Mosher, 2014; Matzke et al., 2015). While in animals methylation only occurs in the CG context, in plants it occurs in all three contexts—CG, CHG, and CHH (where H is any base other than G). In Arabidopsis, CHH methylation can be mediated by 24-nt hc-siRNAs RNAs in a pathway called RdDM. Pol IV, a plant-specific RNA polymerase related to Pol II, transcribes DNA at the loci to be methylated, and these transcripts are processed into dsRNA by RDR2, which are then processed into 24-nt siRNAs by DCL3. One strand of the siRNA is selected for association with AGO4, and the complex is directed to nascent scaffold transcripts of Pol V via base-pairing. AGO4 works cooperatively and sequentially with AGO6, which has a distinct function, to mediate RdDM, and AGO9 acts specifically in the reproductive tissue. AGO4/AGO6 also interact with Pol IV (Duan et al., 2015). Pol V transcription and chromatin association is mediated by several proteins, one of which is DEFECTIVE IN RNA-DIRECTED DNA METHYLATION 1 (DRD1). RNA-DIRECTED DNA METHYLATION 1 (RDM1) then interacts with AGO4 and links it to DOMAINS REARRANGED METHYLTRANSFERASE 2 (DRM2), a homologue of mammalian DNA METHYLTRANSFERASE 3 (DNMT3), that catalyses *de novo* methylation at the target loci (Matzke et al., 2015; Matzke and Mosher, 2014). Many other recruiting and

interacting proteins are involved in this process, but the ones mentioned here are those relevant to the pathogen infection studies as described later.

In contrast to *de novo* methylation, which methylates cytosines at new loci, maintenance methylation adds methylation in daughter strands after DNA replication. At CG loci, methylation is maintained by DNA METHYLTRANSFERASE 1 (MET1), a homologue of mammalian DNMT1; and at CHG loci, it is maintained by CHROMOMETHYLASE (CMT3), a plant-specific methyltransferase. Because CHH loci are asymmetrical, they cannot be maintained without the presence of an siRNA trigger; thus, they are maintained by DRM2 through persistent *de novo* methylation (Law and Jacobsen, 2010; Matzke et al., 2015). Methylation can also be removed through active demethylation mediated by a family of DNA glycosylases including REPRESSOR OF SILENCING 1 (ROS1), DEMETER-LIKE 2 (DML2), and DML3, which work via base excision repair (Zhang and Zhu, 2012) (Figure 1.1).

Transposons that reside in euchromatic regions of the genome are silenced by RdDM to maintain genome integrity. However, most of the transposons are located in pericentromeric heterochromatin, and DNA methylation there is not maintained or established by RdDM and is siRNA-independent. Rather, DECREASED DNA METHYLATION 1 (DDM1), a chromatin remodeler, is responsible for stably silencing transposons while RdDM represents a more dynamic methylation process (Zemach et al., 2013; Matzke, et al. 2014). It has been shown that loss of methylation at certain transposons results in reactivation of not only the transposons themselves but also nearby genes. Also, reactivated transposons may reinsert elsewhere into the genome to

disrupt function of other genes (Ito et al., 2011). DNA methylation is also involved in germ cell specification, genome imprinting, paramutation, response to abiotic stress (e.g. heat, drought, UV radiation), and response to biotic stress (e.g. pathogen infection) (Matzke and Mosher, 2014). Thus, DNA methylation is a dynamic process that changes in response to endogenous and environmental cues and has a great impact in many cellular processes. Knowing the dynamics of methylation during pathogen infection in infected tissue as well as systemic tissue would help point us to genes that are involved in the immune response.

DNA methylation does not act alone to affect gene expression and is often very closely linked to histone modifications. DNA is wrapped around four core histone proteins to form nucleosomes that are packaged to form chromatin. Covalent modification (e.g. methylation, acetylation, ubiquitination, etc.) of the histone protein tails can change the structure of chromatin and have profound effects on gene expression (Prakash et al., 2014). Unsurprisingly, histone modification is also involved in abiotic stress (Chen and Tian, 2007) and, as covered below, biotic stress. Histone 3 lysine 9 methylation (H3K9me) and non-CG methylation form self-reinforcing loop that perpetuates the establishment of both epigenetic marks (Bernatavichute et al., 2008). Some RdDM loci require histone-modifying enzymes in order to maintain the DNA methylation and promote methylation of H3K9 (Matzke and Mosher, 2014). Thus, changes in one epigenetic mark due to environmental cues affects the other and both should be studied concomitantly.

A study in 2006 found that Arabidopsis plants infected with *Pst* exhibited DNA hypomethylation and decondensed chromocenters. This hypomethylation was not associated with cell death during pathogen infection, as it took place before chlorosis or cell death occurred. It was also not associated with DNA replication or a loss of maintenance DNA methylation, implying an active demethylation process is occurring during pathogen infection (Pavet et al., 2006). Since this study, several groups have found that mutations in components of the RdDM pathway and maintenance methylation affect disease resistance. A summary of the findings is shown in Table 1. The thought is that under non-infection conditions, methylation silences immune defense genes to preserve resources for plant growth and propagation. During biotic stress, methylation is removed to turn on these specific defense genes to prevent pathogen multiplication. While most of the evidence confirms this hypothesis, several studies show the contrary.

Knock-out mutants with defects in components of the RdDM pathway—Pol IV, RDR2, DCL3, Pol V, DRD1, DRM1, and DRM2—all exhibit decreased CHG and CHH methylation to varying degrees and also are affected in disease phenotype compared to wild-type plants. In short, most of the evidence suggests that a decrease in methylation results in enhanced disease resistance to *Pst*, a hemibiotrophic pathogen, and *H. arabidopsidis*, a biotrophic pathogen, both of which activate the SA signaling pathway and lead to increased PR1 gene expression (Dowen et al., 2012; Lopez et al., 2011). At the same time, these mutants exhibit enhanced disease susceptibility to necrotrophic pathogens *B. cinerea* and *P. cucumeria* and decreased JA-responsive PDF1.2 gene

(Lopez et al., 2011). One study found that mutations in a subunit of Pol IV, but not Pol V, rendered the plants more resistant to *Pst* (Dowen et al., 2012), while another study found that Pol V, but not Pol IV, plays a role in resistance to *Pst*, *B. cinerea*, or *P. cucumeria* (Lopez et al., 2011). The latter study also showed that although there was no DNA methylation at the promoter of PR1, there were increased histone 3 lysine 4 trimethylation (H3K4me3) and histone 3 lysine 9 acetylation (H3K9ac) marks, which are associated with actively expressed genes, in Pol V and only slightly increased in Pol IV (Lopez et al., 2011). While *rdr1* and *rdr6* both exhibited enhanced resistance to *Pst* (Dowen et al., 2012), *rdr2* showed mixed results (Agorio and Vera, 2007; Dowen et al., 2012; Lopez et al., 2011). *drd1* mutants also showed mixed results, but two studies agreed with one another—the mutants are more resistant to *Pst* (Dowen et al., 2012) but more susceptible to *P. cucumeria* (Lopez et al., 2011). Differences in reported disease phenotypes may have resulted from differing plant growth or pathogen infection conditions or possibly slight differences in the wild-type control plants. It is important to note that sometimes single mutants of genes with family members that have overlapping or redundant functions did not reveal anything. DCL3 knock-out mutants did not have any disease phenotype differing from wild-type (Agorio and Vera, 2007), but the triple mutant *dcl2 dcl3 dcl4* showed enhanced disease resistance to *Pst* (Dowen et al., 2012). The *drm1 drm2* double mutant did not reveal changes in one study (Agorio and Vera, 2007) but showed enhanced resistance to *Pst* in another (Dowen et al., 2012). Two different mutant alleles of CMT3 did not reveal anything from two separate studies (Dowen et al., 2012; Yu et al., 2013). However, the triple mutant *drm1 drm2 cmt3* (*ddc*)

exhibited highly enhanced resistance to *Pst* and *H. arabidopsidis* as well as increased expression of PR1. (Dowen et al., 2012; Luna et al., 2012; Yu et al., 2013). Mutants of the CG maintenance methyltransferase MET1 show a dramatic reduction in CG and CHH methylation. Furthermore, they show greatly enhanced resistance to *Pst*, *Pst* (*avrPphB*), and *Pst* (*hrcC*-) (Dowen et al., 2012; Yu et al., 2013).

The DNA glycosylase mutant *ros1* has more methylation at certain tested loci (Morales-Ruiz et al., 2006), and this is sufficient to render the mutant slightly more susceptible to *Pst* infection (Yu et al., 2013). The single mutants of DML2 and DML3 do not have any affect on pathogen resistance, possibly because ROS1 controls most of the demethylation activity. It would be interesting to see whether mutation in *ros1* would cause the plant to be more resistant to necrotrophic fungi. The triple mutant *ros1 dml2 dml2* (*rdd*), while it does not have overall more methylation than wild-type, does have more methylation at certain loci (Lister et al., 2008).

The development of bisulfite treatment to reveal methylated cytosines and the advancement of high-throughput genome and transcriptome sequencing has allowed researchers to look at the methylation pattern across the genome (methylome) and determine whether changes in methylation are followed by changes in gene expression. One such study revealed that plants showed widespread dynamic changes in CG, CHG, and CHH methylation in response to *Pst*, *Pst* (*avrPphB*), or SA treatments, and RNA-seq revealed that the methylation patterns are coupled to differential gene expression. Specifically, methylation within transposons controls the expression of the transposons and proximal genes in response to stress (Dowen et al., 2012).

Put together, all the data point to an important role that DNA methylation and histone modification have in mediating gene expression changes during pathogen attack. The results may be further confirmed using other mutants in the RdDM pathway not already tested, as well as measuring the expression of marker genes and histone modification and/or DNA methylation at promoters of marker genes. Methylome sequencing of these various mutants would reveal the extent of the effect of the mutation on the methylation pattern, and RNA-seq could be used to determine which genes are actually affected in expression. There may be an overlap of induced genes among the methylation mutants, but there also may be uniquely induced or downregulated genes (due to transposon reinsertions) that account for differences in the plant immune response.

Epigenetic changes are by definition heritable so it is expected that the methylation changes that occur during pathogen attack to increase the disease resistance would be passed to the progeny of infected plants, rendering them more resistant. One group has shown that progeny of *Pst*-treated plants were primed to activate SA-inducible defense responses and were more resistant to *H. arabidopsidis* compared to progeny of untreated plants (Luna et al., 2012). This transgenerational priming was sustained over one stress-free generation. They also showed that the *ddc* mutants mimicked the transgenerational phenotype, even prior to priming, suggesting that the transgenerational phenotypeis transmitted by hypomethylated genes that prime SA-dependent defenses. These results agree with the phenotypes seen in the students mentioned earlier. The

progeny of the Pst-treated plants did not have reduced fitness or seed production; thus, the priming of defenses did not negatively impact plant growth.

A study of the temporal changes in pathogen-induced methylation of target genes should be useful for determining a precise initiation timing of methylation over the course of infection. As there are cell-to-cell differences in epigenetic changes, looking at single-cell changes in methylation would uncouple cell-autonomous and non-cell autonomous DNA methylation dynamics. There are still many important questions to be answered. Some of my preliminary data (Chapter 3) suggests that DNA methylation has a role in SAR. It is known that 24-nt siRNAs can travel through phloem to mediate transcriptional silencing (Melnyk et al., 2011; Molnar et al., 2010). 21-nt siRNAs can also move cell-to-cell to execute posttranscriptional silencing of complementary mRNA targets (Dunoyer et al., 2010). Various sRNAs can migrate to silence transposons during germline development. Could these 24-nt siRNAs that mediate RdDM travel cell-to-cell to establish methylation in tissues in a systemic manner? These questions could be answered by profiling the sRNAs in infected and systemic tissues.

Lastly, coming back to the topic of increased demand for crop production mentioned in the beginning of this Introduction, could priming be successfully used in agriculture? Could seeds of infected crops be used for the next season? Since induced defenses are correlated with reduced fitness and reproduction (Heil and Baldwin, 2002), we need to weigh the costs vs. benefits of this method. Induction of SA-inducible defenses renders plants more susceptible to necrotrophic fungi. Perhaps we would need

to consider the natural pathogens of the crops and whether their pathogens differ by region.

Interest in the role of epigenetics in plant immunity has only emerged in the last several years, spurred on by our understanding of RdDM and methylation dynamics as well as the advancement in sequencing technology and bioinformatics processing power. This remains a field to be further investigated, as many more questions and avenues can be explored.

REFERENCES

Agorio, A., and Vera, P. (2007). ARGONAUTE4 is required for resistance to Pseudomonas syringae in Arabidopsis. Plant Cell *19*, 3778-3790.

Anderson, J.P., Gleason, C.A., Foley, R.C., Thrall, P.H., Burdon, J.B., and Singh, K.B. (2010). Plants versus pathogens: an evolutionary arms race. Functional plant biology : FPB *37*, 499-512.

Ausubel, F.M. (2005). Are innate immune signaling pathways in plants and animals conserved? Nature immunology *6*, 973-979.

Bebber, D.P., and Gurr, S.J. (2015). Crop-destroying fungal and oomycete pathogens challenge food security. Fungal genetics and biology : FG & B *74*, 62-64.

Bernatavichute, Y.V., Zhang, X., Cokus, S., Pellegrini, M., and Jacobsen, S.E. (2008). Genome-wide association of histone H3 lysine nine methylation with CHG DNA methylation in Arabidopsis thaliana. PloS one *3*, e3156.

Bologna, N.G., and Voinnet, O. (2014). The diversity, biogenesis, and activities of endogenous silencing small RNAs in Arabidopsis. Annu Rev Plant Biol *65*, 473-503.

Borges, F., and Martienssen, R.A. (2015). The expanding world of small RNAs in plants. Nature reviews Molecular cell biology *16*, 727-741.

Buscaill, P., and Rivas, S. (2014). Transcriptional control of plant defence responses. Curr Opin Plant Biol *20*, 35-46.

Chan, S.W., Henderson, I.R., Zhang, X., Shah, G., Chien, J.S., and Jacobsen, S.E. (2006). RNAi, DRD1, and histone methylation actively target developmentally important non-CG DNA methylation in arabidopsis. PLoS genetics *2*, e83.

Chan, S.W., Zilberman, D., Xie, Z., Johansen, L.K., Carrington, J.C., and Jacobsen, S.E. (2004). RNA silencing genes control de novo DNA methylation. Science *303*, 1336.

Chen, Z.J., and Tian, L. (2007). Roles of dynamic and reversible histone acetylation in plant development and polyploidy. Biochimica et biophysica acta *1769*, 295-307.

Chinchilla, D., Bauer, Z., Regenass, M., Boller, T., and Felix, G. (2006). The Arabidopsis receptor kinase FLS2 binds flg22 and determines the specificity of flagellin perception. Plant Cell *18*, 465-476.

Dempsey, D.A., and Klessig, D.F. (2012). SOS - too many signals for systemic acquired resistance? Trends Plant Sci *17*, 538-545.

Ding, S.W. (2010). RNA-based antiviral immunity. Nature reviews Immunology *10*, 632-644.

Dodds, P.N., and Rathjen, J.P. (2010). Plant immunity: towards an integrated view of plant–pathogen interactions. Nature Review Genetics *11*, 539-548.

Dong, X., Li, X., Zhang, Y., Fan, W., Kinkema, M., and Clarke, J. (2001). Regulation of systemic acquired resistance by NPR1 and its partners. Novartis Foundation symposium *236*, 165-173; discussion 173-165.

Dowen, R.H., Pelizzola, M., Schmitz, R.J., Lister, R., Dowen, J.M., Nery, J.R., Dixon, J.E., and Ecker, J.R. (2012). Widespread dynamic DNA methylation in response to biotic stress. Proceedings of the National Academy of Sciences of the United States of America *109*, E2183-2191.

Duan, C.G., Zhang, H., Tang, K., Zhu, X., Qian, W., Hou, Y.J., Wang, B., Lang, Z., Zhao, Y., Wang, X.*, et al.* (2015). Specific but interdependent functions for Arabidopsis AGO4 and AGO6 in RNA-directed DNA methylation. The EMBO journal *34*, 581-592.

Dunoyer, P., Schott, G., Himber, C., Meyer, D., Takeda, A., Carrington, J.C., and Voinnet, O. (2010). Small RNA Duplexes Function as Mobile Silencing Signals Between Plant Cells. Science *328*, 912-916.

Fei, Q., Xia, R., and Meyers, B.C. (2013). Phased, secondary, small interfering RNAs in posttranscriptional regulatory networks. Plant Cell *25*, 2400-2415.

Flood, J. (2010). The importance of plant health to food security. Food Secur *2*, 215-231.

Food and Agriculture Organization of the United Nations. (2014). The state of food insecurity in the world (Rome, Italy: Food and Agriculture Organization of the United Nations), pp. v.

Fu, Z.Q., and Dong, X. (2013). Systemic acquired resistance: turning local infection into global defense. Annu Rev Plant Biol *64*, 839-863.

Gaffney, T., Friedrich, L., Vernooij, B., Negrotto, D., Nye, G., Uknes, S., Ward, E., Kessmann, H., and Ryals, J. (1993). Requirement of salicylic Acid for the induction of systemic acquired resistance. Science *261*, 754-756.

Glazebrook, J. (2005). Contrasting mechanisms of defense against biotrophic and necrotrophic pathogens. Annu Rev Phytopathol *43*, 205-227.

Heil, M., and Baldwin, I.T. (2002). Fitness costs of induced resistance: emerging experimental support for a slippery concept. Trends Plant Sci *7*, 61-67.

Henderson, I.R., Zhang, X., Lu, C., Johnson, L., Meyers, B.C., Green, P.J., and Jacobsen, S.E. (2006). Dissecting Arabidopsis thaliana DICER function in small RNA processing, gene silencing and DNA methylation patterning. Nature genetics *38*, 721-725.

Ito, H., Gaubert, H., Bucher, E., Mirouze, M., Vaillant, I., and Paszkowski, J. (2011). An siRNA pathway prevents transgenerational retrotransposition in plants subjected to stress. Nature *472*, 115-119.

Kanno, T., Mette, M.F., Kreil, D.P., Aufsatz, W., Matzke, M., and Matzke, A.J. (2004). Involvement of putative SNF2 chromatin remodeling protein DRD1 in RNA-directed DNA methylation. Current biology : CB *14*, 801-805.

Katagiri, F., Thilmony, R., and He, S.Y. (2002). The Arabidopsis thaliana-pseudomonas syringae interaction. The Arabidopsis book / American Society of Plant Biologists *1*, e0039.

Katiyar-Agarwal, S., Gao, S., Vivian-Smith, A., and Jin, H. (2007). A novel class of bacteria-induced small RNAs in Arabidopsis. Genes Dev *21*, 3123-3134.

Katiyar-Agarwal, S., Morgan, R., Dahlbeck, D., Borsani, O., Villegas, A., Jr., Zhu, J.K., Staskawicz, B.J., and Jin, H. (2006). A pathogen-inducible endogenous siRNA in plant immunity. Proc Natl Acad Sci USA *103*, 18002-18007.

Lahmy, S., Pontier, D., Cavel, E., Vega, D., El-Shami, M., Kanno, T., and Lagrange, T. (2009). PolV(PolIVb) function in RNA-directed DNA methylation requires the conserved active site and an additional plant-specific subunit. Proceedings of the National Academy of Sciences of the United States of America *106*, 941-946.

Law, J.A., and Jacobsen, S.E. (2010). Establishing, maintaining and modifying DNA methylation patterns in plants and animals. Nature reviews Genetics *11*, 204-220.

Li, B., Meng, X., Shan, L., and He, P. (2016). Transcriptional Regulation of Pattern-Triggered Immunity in Plants. Cell host & microbe *19*, 641-650.

Li, Y., Zhang, Q., Zhang, J., Wu, L., Qi, Y., and Zhou, J.M. (2010). Identification of microRNAs involved in pathogen-associated molecular pattern-triggered plant innate immunity. Plant Physiol *152*, 2222-2231.

Lister, R., O'Malley, R.C., Tonti-Filippini, J., Gregory, B.D., Berry, C.C., Millar, A.H., and Ecker, J.R. (2008). Highly integrated single-base resolution maps of the epigenome in Arabidopsis. Cell *133*, 523-536.

Lopez, A., Ramirez, V., Garcia-Andrade, J., Flors, V., and Vera, P. (2011). The RNA silencing enzyme RNA polymerase v is required for plant immunity. PLoS genetics *7*, e1002434.

Lotze, M.T., Zeh, H.J., Rubartelli, A., Sparvero, L.J., Amoscato, A.A., Washburn, N.R., Devera, M.E., Liang, X., Tor, M., and Billiar, T. (2007). The grateful dead: damage-associated molecular pattern molecules and reduction/oxidation regulate immunity. Immunological reviews *220*, 60-81.

Low, D.A., Weyand, N.J., and Mahan, M.J. (2001). Roles of DNA adenine methylation in regulating bacterial gene expression and virulence. Infection and immunity *69*, 7197-7204.

Luna, E., Bruce, T.J., Roberts, M.R., Flors, V., and Ton, J. (2012). Next-generation systemic acquired resistance. Plant physiology *158*, 844-853.

Matzke, M., Kanno, T., Huettel, B., Daxinger, L., and Matzke, A.J. (2006). RNA-directed DNA methylation and Pol IVb in Arabidopsis. Cold Spring Harbor symposia on quantitative biology *71*, 449-459.

Matzke, M.A., Kanno, T., and Matzke, A.J. (2015). RNA-Directed DNA Methylation: The Evolution of a Complex Epigenetic Pathway in Flowering Plants. Annu Rev Plant Biol *66*, 243-267.

Matzke, M.A., and Mosher, R.A. (2014). RNA-directed DNA methylation: an epigenetic pathway of increasing complexity. Nature reviews Genetics *15*, 394-408.

Melnyk, C.W., Molnar, A., Bassett, A., and Baulcombe, D.C. (2011). Mobile 24 nt small RNAs direct transcriptional gene silencing in the root meristems of Arabidopsis thaliana. Current biology : CB *21*, 1678-1683.

Molnar, A., Melnyk, C.W., Bassett, A., Hardcastle, T.J., Dunn, R., and Baulcombe, D.C. (2010). Small silencing RNAs in plants are mobile and direct epigenetic modification in recipient cells. Science *328*, 872-875.

Morales-Ruiz, T., Ortega-Galisteo, A.P., Ponferrada-Marin, M.I., Martinez-Macias, M.I., Ariza, R.R., and Roldan-Arjona, T. (2006). DEMETER and REPRESSOR OF SILENCING 1 encode 5-methylcytosine DNA glycosylases. Proceedings of the National Academy of Sciences of the United States of America *103*, 6853-6858.

Navarro, L., Dunoyer, P., Jay, F., Arnold, B., Dharmasiri, N., Estelle, M., Voinnet, O., and Jones, J.D.G. (2006). A plant miRNA contributes to antibacterial resistance by repressing auxin signaling. Science *312*, 436-439.

Nishimura, M.T., and Dangl, J.L. (2010). Arabidopsis and the plant immune system. Plant Journal *61*, 1053-1066.

Niu, D., Lii, Y.E., Chellappan, P., Lei, L., Peralta, K., Jiang, C., Guo, J., Coaker, G., and Jin, H. (2016). miRNA863-3p sequentially targets negative immune regulator ARLPKs and positive regulator SERRATE upon bacterial infection. Nature communications *7*, 11324.

Nuthikattu, S., McCue, A.D., Panda, K., Fultz, D., DeFraia, C., Thomas, E.N., and Slotkin, R.K. (2013). The initiation of epigenetic silencing of active transposable elements is triggered by RDR6 and 21-22 nucleotide small interfering RNAs. Plant physiology *162*, 116-131.

Pavet, V., Quintero, C., Cecchini, N.M., Rosa, A.L., and Alvarez, M.E. (2006). Arabidopsis displays centromeric DNA hypomethylation and cytological alterations of heterochromatin upon attack by Pseudomonas syringae. Molecular Plant-Microbe Interactions *19*, 577-587.

Pieterse, C.M., Van der Does, D., Zamioudis, C., Leon-Reyes, A., and Van Wees, S.C. (2012). Hormonal modulation of plant immunity. Annu Rev Cell Dev Biol *28*, 489-521.

Prakash, S., Singh, R., and Lodhi, N. (2014). Histone demethylases and control of gene expression in plants. Cellular and molecular biology *60*, 97-105.

Pumplin, N., and Voinnet, O. (2013). RNA silencing suppression by plant pathogens: defence, counter-defence and counter-counter-defence. Nature reviews Microbiology *11*, 745-760.

Ritter, C., and Dangl, J.L. (1995). The avrRpm1 gene of Pseudomonas syringae pv. maculicola is required for virulence on Arabidopsis. Molecular plant-microbe interactions : MPMI *8*, 444-453.

Rogers, K., and Chen, X. (2013). Biogenesis, turnover, and mode of action of plant microRNAs. Plant Cell *25*, 2383-2399.

Seo, J.K., Wu, J., Lii, Y., Li, Y., and Jin, H. (2013). Contribution of small RNA pathway components in plant immunity. Molecular plant-microbe interactions : MPMI *26*, 617-625.

Spoel, S.H., Johnson, J.S., and Dong, X. (2007). Regulation of tradeoffs between plant defenses against pathogens with different lifestyles. Proceedings of the National Academy of Sciences of the United States of America *104*, 18842-18847.

Staiger, D., Korneli, C., Lummer, M., and Navarro, L. (2013). Emerging role for RNA-based regulation in plant immunity. The New phytologist *197*, 394-404.

Tsuda, K., Sato, M., Stoddard, T., Glazebrook, J., and Katagiri, F. (2009). Network properties of robust immunity in plants. PLoS genetics *5*, e1000772.

Vazquez, F., Legrand, S., and Windels, D. (2010). The biosynthetic pathways and biological scopes of plant small RNAs. Trends Plant Sci *15*, 337-345.

Weiberg, A., Bellinger, M., and Jin, H.L. (2015). Conversations between kingdoms: small RNAs. Curr Opin Biotech *32*, 207-215.

Weiberg, A., and Jin, H. (2015). Small RNAs-the secret agents in the plant-pathogen interactions. Curr Opin Plant Biol *26*, 87-94.

Weiberg, A., Wang, M., Bellinger, M., and Jin, H. (2014). Small RNAs: a new paradigm in plant-microbe interactions. Annu Rev Phytopathol *52*, 495-516.

Xie, Z., Johansen, L.K., Gustafson, A.M., Kasschau, K.D., Lellis, A.D., Zilberman, D., Jacobsen, S.E., and Carrington, J.C. (2004). Genetic and functional diversification of small RNA pathways in plants. PLoS biology *2*, E104.

Yu, A., Lepere, G., Jay, F., Wang, J., Bapaume, L., Wang, Y., Abraham, A.L., Penterman, J., Fischer, R.L., Voinnet, O.*, et al.* (2013). Dynamics and biological relevance of DNA demethylation in Arabidopsis antibacterial defense. Proceedings of the National Academy of Sciences of the United States of America *110*, 2389-2394.

Zemach, A., Kim, M.Y., Hsieh, P.H., Coleman-Derr, D., Eshed-Williams, L., Thao, K., Harmer, S.L., and Zilberman, D. (2013). The Arabidopsis nucleosome remodeler DDM1 allows DNA methyltransferases to access H1-containing heterochromatin. Cell *153*, 193-205.

Zhang, H., Xia, R., Meyers, B.C., and Walbot, V. (2015). Evolution, functions, and mysteries of plant ARGONAUTE proteins. Curr Opin Plant Biol *27*, 84-90.

Zhang, X., Zhao, H., Gao, S., Wang, W.C., Katiyar-Agarwal, S., Huang, H.D., Raikhel, N., and Jin, H. (2011). Arabidopsis Argonaute 2 regulates innate immunity via miRNA393(*)-mediated silencing of a Golgi-localized SNARE gene, MEMB12. Mol Cell *42*, 356-366.

Zheng, X., Zhu, J., Kapoor, A., and Zhu, J.K. (2007). Role of Arabidopsis AGO6 in siRNA accumulation, DNA methylation and transcriptional gene silencing. The EMBO journal *26*, 1691-1701.

Zhu, J., Kapoor, A., Sridhar, V.V., Agius, F., and Zhu, J.K. (2007). The DNA glycosylase/lyase ROS1 functions in pruning DNA methylation patterns in Arabidopsis. Current biology : CB *17*, 54-59.

Zilberman, D., Cao, X., and Jacobsen, S.E. (2003). ARGONAUTE4 control of locus-specific siRNA accumulation and DNA and histone methylation. Science *299*, 716-719.

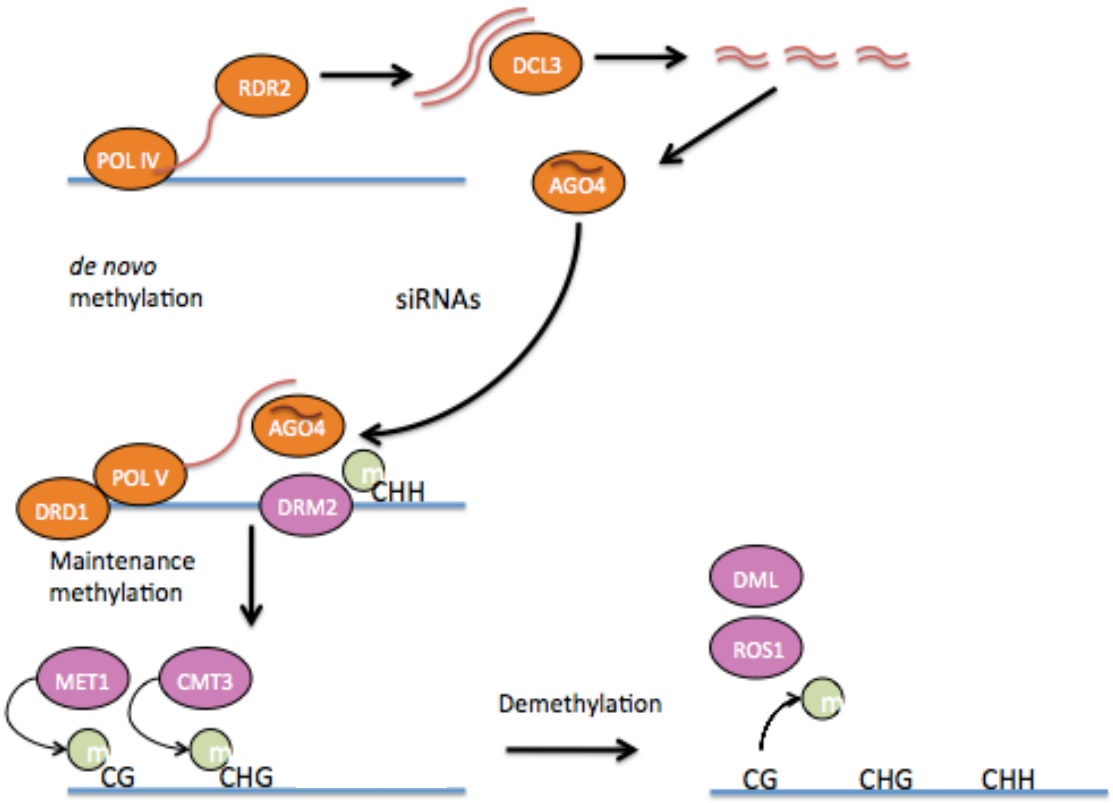


Figure 1.1. Simplified scheme of RNA-directed DNA methylation (RdDM), maintenance methylation, and demethylation. POL IV: Polymerase IV, RDR2: RNA-DEPENDENT RNA POLYMERASE, DCL3: DICER-LIKE 3, AGO4: ARGONAUTE 4, DRD1: DEFECTIVE IN RNA-DIRECTED DNA METHYLATION 1, POL V: Polymerase V, DRM2: DOMAINS REARRANGED METHYLTRANSFERASE 2, MET1: DNA METHYLTRANSFERASE 1, CMT3: CHROMOMETHYLASE 3, DML: DML: DEMETER-LIKE, ROS1: REPRESSOR OF SILENCING 1

Table 1. List of methylation pathway components and methylome and immune response analysis of mutants

Methylation pathway component	Function	Mutant allele tested	Effect of mutant on methylation	Effect of mutation on immunity
AGO4	Binds 24-nt siRNAs to direct RdDM	*ago4-1*	Dramatic reduction of CHG and CHH methylation (Zilberman et al., 2003)	Enahnced susceptibility to *Pst*, *Pst* (*avrRpm1*), and *Ps tabaci (*Agorio and Vera, 2007)
		ago4-2		No effect on resistance to *Pst (*Dowen et al., 2012)
				Enahnced susceptibility to *Pst*, *Pst* (*avrRpm1*), and *Ps tabaci (*Agorio and Vera, 2007)
				Enhanced susceptibility to *B. cinerea (*Lopez et al., 2011)
AGO6	Functionally redundant with AGO4	*ago6-2*		No effect on resistance to *Pst (*Dowen et al., 2012)
CMT3	CHG maintenance methylation	*cmt3-7*	Dramatic reduction of CHG methylation (Zheng et al., 2007)	No effect on resistance to *Pst* (Agorio and Vera, 2007)
		cmt3-11	N/A	No effect on resistance to *Pst (*Yu et al*., 2013)*
		see *ddc*		
DCL2, DCL, and DCL3	Processing of dsRNA into 22-nt, 24-nt, and 21-nt siRNAs	*dcl2-1 dcl3-1 dcl4-2*	N/A	Highly enhanced resistance to *Pst*; enhanced resistance *Pst* (*avrPphB*) and *Pst* (*hrcC*) (Dowen et al., 2012)
DCL3	Processing of	*dcl3-1*	Reduced	No effect on resistance to

	dsRNA into 24-nt siRNAs in RdDM		methylation at FWA locus (Chan et al., 2004)	*Pst* (Agorio and Vera, 2007)
DDM1	Nucleosome remodeler	*ddm1-8*	Little change in CG methylation; dramatic reduction of CHG and CHH methylation (Zemach et al., 2013)	Enhanced resistance to *Pst (*Dowen et al., 2012)
		ddm1-10		Enhanced resistance to *Pst* (Dowen et al., 2012)
DML2	DNA glycosylase; removal of methlyation	*dml2-1*	N/A	No effect on resistance to *Pst* (Yu et al., 2013)
		see rdd		
DML3	DNA glycosylase; removal of methlyation	*dml3-1*	N/A	No effect on resistance to *Pst* (Yu et al., 2013)
		see *rdd*		
DRD1	Chromatin remodeler, unwinding activity allowing for Pol V transcription	*drd1-6*	Reduction of non-CG methylation at certain loci; methlyation at centromeric regions unaffected (Kanno et al., 2004)	Enhanced resistance to *Pst* (Dowen et al., 2012)
				Enhanced susceptibility to *Pst* (Agorio and Vera, 2007)
				Enhanced susceptibility to *P. cucumeria* (Lopez et al., 2011)
DRM1 and DRM2	*de novo* methyltrasferase	*drm1-1 drm2-2*	Prevents establishment of maintenance of gene silencing at certain loci	No effect on resistance to *Pst* (Agorio and Vera, 2007)
				Enhanced resistance to *Pst* (Yu et al., 2013)

			(Lister et al., 2008)	Enhanced susceptibility to *P. cucumeria* (Lopez et al., 2011)
		drm1-1 drm2-1 cmt3-11 (*ddc*)	CG methylation unaffected; dramatic reduction of CHG methylation; 80% reduction of CHH methylation (Lister et al., 2008)	Enhanced resistance to *Pst* (Dowen et al., 2012)
				High enhanced resistance to *Pst*, enhanced induction of PR-1 (Yu et al., 2013)
				Enhanced resistance to *H. arabidopsidis* WACO9; enhanced induction of PR-1 (Luna et al., 2012)
MET1	CG maintenance methylation	*met1-3*	Dramatic reduction of CG methylation; 50% reduction of CHH methylation; little change in CHG methylation (Lister et al., 2008)	Highly enhanced resistance to *Pst*; enhanced resistance *Pst* (*avrPphB*), and *Pst* (*hrcC*) (Dowen et al., 2012)
				Enhanced resistance to *Pst* (Yu et al., 2013)
		met1-3 nrpd2-2	N/A	Highly enhanced resistance to *Pst*; enhanced induction of PR-1; constitutive cell death resembling HR (Yu et al., 2013)
Pol IV	Production of ssRNA transcript in RdDM, guides CHH methylation to genomic sites	*nrpd1a-4*	Methylation is lost at 50-60% of CHH sites, but gained at new CHH sites (Matzke et al.,	Enhanced resistance to *Pst*; no change in PR-1 induction (Dowen et al., 2012)
				Enhanced susceptibility to *P. cucumeria*; no effect on

			2006)	resistance to *B. cinerea*; slightly decreased induction of PDF1.2 (Lopez et al., 2011)
				No effect on resistance to *Pst*; no DNA methylation footprint at PR-1; increased histone activation marks H3K4me3 and H3K9ac at and decreased histone repressive marks at PR-1 promoter (Lopez et al., 2011)
		nrpd1-4 nrpde1-11	N/A	Enhanced resistance to *Pst (*Lopez et al., 2011)
		see *nrpd2* mutants (*mutation is in subunits shared between Pol IV and Pol V)		
		nrpd2a2b	N/A	No effect on resistance to *Pst (*Dowen et al., 2012)
Pol V	Production of scaffold RNA in RdDM, recruits DRM2; guides CHH methylation to genomic sites	*nrpd1b-11/nrpe1-11*	Methylation is lost at 50-60% of CHH sites, but gained at new CHH sites (Lahmy et al., 2009)	No effect on resistance to *Pst (*Dowen et al., 2012)
				Enhanced resistance to *Pst*, increased induction of PR-1; increase in H3K4me3 and H3K9ac at PR-1 promoter (Lopez et al., 2011)
				Enhanced susceptibility to *B. cinerea*; decreased induction of PDF1.2 (Lopez et al., 2011)
		*nrpd2-2**	N/A	Highly enhanced susceptibility to *B. cinerea*, enhanced susceptibility to *P. cucumeria*; decreased

				induction of PDF1.2 (Lopez et al., 2011)
				Enhanced resistance to *Pst*; increased induction of PR-1; no DNA methylation footprint at PR-1; increase in histone activation marks H3K4me3and H3K9ac and decrease of histone repressive marks at PR-1 promoter (Lopez et al., 2011)
				Enhanced resistance to *Pst(Lopez et al., 2011)* (Yu et al., 2013)
		*nrpd2-53**	N/A	Enhanced susceptibility to *B. cinerea*, decreased induction of PDF1.2 (Lopez et al., 2011)
RDR1	Formation of virus-derived siRNAs	*rdr1-1*	*de novo* silencing normal at FWA gene (Chan et al., 2006)	Enhanced resistance to *Pst (*Dowen et al., 2012)
RDR2	Formation of dsRNA in the biogenesis of hc-siRNAs	*rdr2-1*	Reduction of heterochromatic formation (Xie et al., 2004)	Enhanced resistance to *Pst (*Dowen et al., 2012)
				No effect on resistance to *Pst* (Agorio and Vera, 2007)
				Enhanced susceptibility to *P. cucumeria (*Lopez et al., 2011)
RDR6	Formation of dsRNA involved in non-canonical RdDM pathway	*rdr6-15*	Reduction of methylation at select transposons	Enhanced resistance to *Pst (*Dowen et al., 2012)

			(Nuthikattu et al., 2013)	
ROS1	DNA glycosylase; removal of methlyation	*ros1*	Increased methylation at certain loci (Zhu et al., 2007)	Mild enhanced susceptibility to *Pst* (Yu et al., 2013)
		ros1-3 dml2-1 dml3-1 (*rdd*)	Over all little change in context and numbers of methylation; however, methylation is at least 2-fold greater in certain regions (Lister et al., 2008)	N/A

CHAPTER TWO

miRNA863-3p sequentially targets negative immune regulator *ARLPKs* and positive regulator *SERRATE* upon bacterial infection

ABSTRACT

Plant small RNAs play important roles in gene regulation during pathogen infection. Here we show that miR863-3p is induced by the bacterial pathogen *Pseudomonas syringae* carrying various effectors. Early during infection, miR863-3p silences two negative regulators of plant defence, atypical receptor-like pseudokinase 1 (*ARLPK1*) and *ARLPK2*, both lacking extracellular domains and kinase activity, through mRNA degradation to promote immunity. ARLPK1 associates with, and may function through another negative immune regulator ARLPK1-interacting receptor-like kinase 1 (AKIK1), an active kinase with an extracellular domain. Later during infection, miR863-3p silences SERRATE, which is essential for miRNA accumulation and positively regulates defence, through translational inhibition. This results in decreased miR863-3p levels, thus forming a negative feedback loop to attenuate immune responses after successful defence. This is an example of a miRNA that sequentially targets both negative and positive regulators of immunity through two modes of action to fine-tune the timing and amplitude of defence responses.

INTRODUCTION

During pathogen infection, plants undergo reprogramming and fine-tuning of gene expression to activate innate immune responses, and small RNAs (sRNAs) are important regulators in this process (Katiyar-Agarwal and Jin, 2010; Padmanabhan et al., 2009; Weiberg and Jin, 2015; Weiberg et al., 2014). As the first layer of defence, plant pattern-recognition receptors detect conserved pathogen features called pathogen-associated molecular patterns (PAMPs), leading to PAMP-triggered immunity (PTI) (Macho and Zipfel, 2014). Some pathogens deliver effector proteins to attenuate PTI; however, in resistant hosts, Nod-like receptor (NLR) proteins recognize cognate effectors and activate effector-triggered immunity (ETI), which is more specific, robust and rapid than PTI. ETI is often characterized by the hypersensitive response (HR), a type of cell death, at the site of infection (Dodds and Rathjen, 2010; Li et al., 2015). One well-studied effector-NLR model in *Arabidopsis* is the effector AvrRpt2 from the bacterial pathogen *Pseudomonas syringae* pv. *tomato* (*Pst*) DC3000 and its cognate plant host NLR protein RPS2 (Kunkel et al., 1993; Yu et al., 1993).

sRNAs are critical regulators of plant defence responses and pathogen virulence (Katiyar-Agarwal and Jin, 2010; Padmanabhan et al., 2009; Weiberg and Jin, 2015; Weiberg et al., 2014; Weiberg et al., 2013). These microRNAs (miRNAs) and short interfering RNAs (siRNAs) are processed by Dicer or Dicer-like (DCL) proteins and then incorporated into Argonaute (AGO) proteins to form RNA-induced silencing complex to target genes with full or partial complementary sequences. sRNAs can

induce gene silencing by guiding post-transcriptional gene silencing via mRNA degradation or translational inhibition, or transcriptional inhibition via DNA methylation or chromatin modification (Martinez de Alba et al., 2013). During infection with *Pst* DC3000 carrying the effector gene *avrRpt2*, the natural antisense transcript-associated siRNA natsiRNAATGB2 silences a gene with pentatricopeptide repeats, which acts as a negative regulator of ETI mediated by *RPS2* (Katiyar-Agarwal et al., 2006). A long siRNA, AtlsiRNA, also induced by *Pst* (*avrRpt2*), silences the *AtRAP* gene (*Arabidopsis thaliana RNA*-binding domain abundant in apicomplexans), which has a negative role in defence (Katiyar-Agarwal et al., 2007). miR393 contributes to PTI by targeting auxin signalling receptors upon elicitor flg22 treatment or after infection with virulent *Pst* DC3000 (Navarro et al., 2006). The complementary strand of miR393 within the sRNA duplex, miR393*, regulates ETI during infection of *Pst* (*avrRpt2*) by targeting a protein trafficking gene *MEMB12* (Membrin 12) to promote the secretion of antimicrobial PR (pathogenesis-related) proteins (Zhang et al., 2011). miR160a enhances PAMP-induced callose deposition by targeting auxin response factors (Li and Tax, 2013). In addition to these examples of sRNAs that are induced by pathogen infection, some sRNAs are downregulated by infection. For example, miR398b, which targets a cytochrome c oxidase and two copper superoxide dismutases, and miR773, which targets a DNA methyltransferase, *MET2*, both negatively regulate PAMP-induced callose deposition, as well as PTI against *Pst* (EV) and *Pst* (Δ*hrcC*) (Li and Tax, 2013). Collectively, these studies highlight the importance of sRNAs that target critical plant genes involved in

immune signalling. However, no sRNAs are reported to target genes with antagonistic roles in plant immunity or any other cellular processes.

We previously identified miRNAs and siRNAs that are differentially expressed on infection with various bacterial *Pst* strains (Zhang et al., 2011). One of these miRNAs, miR863-3p, was highly upregulated by the avirulent strain *Pst* (*avrRpt2*); thus, we hypothesized that this miRNA may play an important role in ETI, and sought to characterize its targets and their function. Here we show that miR863-3p targets the putative pseudokinases, atypical receptor-like pseudokinase 1 (*ARLPK1*) and *ARLPK2*, early on during infection to boost plant defence. ARLPK1 interacts with ARLPK1-interacting receptor-like kinase (AKIK1), an active kinase that also negatively regulates defence. Later during infection, miR863-3p silences SERRATE (SE)—a protein important for miRNA processing and accumulation (Dong et al., 2008; Fang and Spector, 2007; Lobbes et al., 2006; Yang et al., 2006) and for defence—to form a negative feedback loop to regulate the level of miRNA863-3p. Attenuation of immune responses after successful defence is possibly to conserve host resources for growth and reproduction.

RESULTS

miR863-3p is induced by infection with avirulent *Pst* strains

To identify miRNAs involved in regulating immune responses to bacterial infection, we previously profiled sRNAs from plants challenged with virulent and avirulent bacterial

strains, *Pst* (EV) and *Pst* (*avrRpt2*), respectively (Zhang et al., 2011). We found that miR863-3p was highly upregulated during *Pst* (*avrRpt2*) infection. miR863-3p is a 21-nucleotide (nt) miRNA originating from the 3′-arm of the precursor miRNA (.1a) (Meyers et al., 2008). Northern blot analysis confirmed that miR863-3p was induced by an avirulent strain *Pst* (*avrRpt2*), but not by the virulent strain *Pst* carrying an empty vector (EV), a strain that has a mutation in its type III secretion system—*Pst* (Δ*hrcC*), or mock solution (10 mM $MgCl_2$; Figure 2.2a). miR863-3p levels are also upregulated by avirulent strains *Pst* (*avrRpm1*) and *Pst* (*avrRps4*), although to a lesser degree compared with *Pst* (*avrRpt2*) (Figure 2.1b). Interestingly, miR863-5p, the complementary strand of miR863-3p, was not induced by any of these *Pst* strains, and thus is not likely to be involved in defence against *Pst* (Figure 2.2b).

Biogenesis of miRNAs depends on DCL1, which processes pri-miRNAs, and is aided by interacting RNA-binding proteins HYL1 and SE to promote accurate processing (Dong et al., 2008). Northern blot analysis revealed that miR863-3p accumulation is dependent on DCL1 and SE, but independent of RDR6, which is involved in the biogenesis and amplification of siRNAs (Figure 2.1c) (Martinez de Alba et al., 2013). These results indicate that miR863-3p is indeed a true miRNA instead of a siRNA. Taken together, our results show that miR863-3p is dependent on DCL1 and SE, and it is induced by challenge with avirulent *Pst* strains, especially *Pst* (*avrRpt2*). Its complementary strand was not detected in our experiments, showing that miR863-3p is the stable miRNA strand during pathogen infection.

miR863-3p targets two ARLPKs and SE

We hypothesized that miR863-3p targets genes involved in immune responses, but since miR863-3p has no validated targets in existing databases, we predicted its potential targets (Methods). miR863-3p potentially targets the coding sequences of two atypical receptor-like kinases (RLKs), *ARLPK1* and *ARLPK2*, belonging to the leucine-rich repeat (LRR) III RLK subfamily (Shiu et al., 2004), as well as the 3′-untranslated region (UTR) of *SE*, which encodes a zinc-finger protein found in both the miRNA biogenesis DCL1 complex (Fang and Spector, 2007), and the nuclear cap-binding protein complex (Raczynska et al., 2014) (Figure 2.3a). Typical RLKs have an extracellular ligand-binding domain, a single transmembrane region and an intracellular kinase domain (Shiu et al., 2004). Both *ARLPK1* and *ARLPK2* have a signal peptide sequence overlapping with their N-terminal transmembrane domain (Figure 2.4a,b) and lack extracellular domains (Shiu et al., 2004). They also have variations in the conserved features of functional kinase domains such as the glycine-rich loop, VAIK motif and HRD motif (Figure 2.5), and are thus predicted pseudokinases (Boudeau et al., 2006). Because ARLPK1 and ARLPK2 are missing conserved key residues in the consensus motifs and are lacking extracellular domains, we named them atypical receptor-like pseudokinases (*ARLPK1*, At5g61570; and *ARLPK2*, At5g07620). miR863-3p is also predicted to target a third gene *SE*, which is involved in the accumulation of miRNAs, including miR863-3p (Figure 2.2c). During *Pst* (*avrRpt2*) infection, the mRNA levels of the two *ARLPKs* are downregulated compared with mock-infected plants;

however, *SE* mRNA levels are upregulated. In contrast, the levels of all three transcripts do not change significantly during *Pst* (EV) or *Pst* (Δ*hrcC*) infection (Figure 2.3b).

To confirm that *ARLPK1* and *ARLPK2* are true targets of miR863-3p, we performed *Agrobacterium*-mediated transient co-expression assays in *Nicotiana benthamiana* using wild-type (wt) and mutated (m) kinase genes. The mutated kinases have an altered miR863-3p target site, yet the predicted amino-acid sequence is unchanged (Figure 2.3a). MIR863 co-expression with wtARLPK1 or wtARLPK2 resulted in a decrease of the mRNA levels of both kinases, while co-expression with mARLPK1 or mARLPK2 did not affect the mRNA levels of *mARLPK1* or*mARLPK2* (Figure 2.3c). In addition, we performed RNA-ligase mediated 5' rapid amplification of cDNA ends (RLM-RACE) in *Pst* (*avrRpt2*)-infected *Arabidopsis* to map miR863-3p-guided cleavage sites in *ARLPK* mRNA. As expected, the majority of the 5′-RACE cloned products mapped to the predicted target site in *ARLPK1* and *ARLPK2* mRNAs (Figure 2.3d). These data indicate *ARLPK1* and *ARKPL2* are direct targets of miR863-3p, and they are silenced via mRNA cleavage and degradation.

In plants, most miRNAs silence their targets by directing mRNA cleavage and degradation, while others mediate translational inhibition (Rogers and Chen, 2013). In mammals, most miRNA target sites for translational inhibition are located in the 3′-UTR, and the target site of miR863-3p in *SE* is also at the beginning of the 3′-UTR. *SE* mRNA levels are not downregulated by miR863-3p (Figure 2.3b), even though the nucleotide alignment shows very few mismatches (Figure 2.3a). Thus, it is possible

that miR863-3p silences SE through translational inhibition. In mammals, target mRNAs silenced by RNA-induced silencing complex via translational repression are delivered to and accumulate in processing (P)-bodies (Liu et al., 2005). Thus, it is possible that we see elevated *SE* transcripts not only because of continual transcription of *SE* due to the absence of SE protein product but also because of the accumulation of sequestered *SE* mRNAs in P-bodies. To test that hypothesis, we generated constructs of green fluorescent protein (GFP) fused to a wt version of truncated *SE* that includes only the 3′-UTR (GFP-wtSE-3′-UTR) or a mutated truncated version of *SE* with an altered miRNA target site (GFP-mSE-3′-UTR; Figure 2.3a). We co-expressed the fusions with MIR863 in *N. benthamiana*, and western blotting revealed that GFP-wtSE-3′-UTR, but not GFP-mSE-3′-UTR, levels were downregulated (Figure 2.3e). To confirm this result *in vivo*, we obtained an anti-SE antibody and detected SE protein levels in *Arabidopsis* plants challenged with *Pst* strains. Western blot analysis revealed that SE protein levels are downregulated by *Pst* (*avrRpt2*) but not by *Pst* (Δ*hrcC*) or *Pst* (EV) (Figure 2.3f). These results suggest that miR863-3p targets and silences SE by inhibiting its translation. Thus, miR863-3p uses two different modes of action to silence its targets—it suppresses the two *ARLPKs* via mRNA cleavage and degradation and inhibits *SE* by translational inhibition.

ARLPKs are negative regulators of disease resistance

To investigate the role of miR863-3p during plant immune responses, we created transgenic plants overexpressing MIR863 under the control of the cauliflower mosaic

virus 35S promoter. Figure 2.6a shows nine such overexpression (OE) lines. The lines with very high miR863-3p expression (such as MIR863-OE1 and -OE2 lines) resembled the *serrate* mutant phenotype (Clarke et al., 1999), further supporting that SE is indeed a miR863-3p target (Figure 2.6b). Only a slight increase of miR863-3p was observed after infection with *Pst* (*avrRpt2*) in the OE lines, most likely because miR863-3p levels are already very high (Figure 2.7). We also detected very low levels of miR863-5p in some of the OE lines (Figure 2.6a). We chose two transgenic lines with high miR863-3p levels, MIR863-OE1 and -OE2, and one with lower levels, MIR863-OE3, for functional analyses (Figure 2.6a). MIR863-OE1 and -OE2 plants were slightly smaller than Col-0 WT plants (Figure 2.6b, upper panels). In the MIR863 overexpression lines, *ARLPK1* and *ARLPK2* mRNA levels are downregulated while *SE* mRNA levels are elevated, as shown by real-time reverse transcription–PCR (RT–PCR) results (Figure 2.6c). *SE* mRNA levels are elevated just as in *Pst* (*avrRpt2*)-infected plants (Figure 2.3a), most likely due to feedback compensation to increase transcription and also sequestering of transcripts in P-bodies (Liu et al., 2005). SE protein levels in the overexpression lines are significantly lower compared with Col-0 WT, especially in MIR863-OE1 and -OE2 (Figure 2.6d). Interestingly, even though the target genes were downregulated, the MIR863 overexpression lines showed no altered disease resistance to *Pst* (EV) or *Pst* (*avrRpt2*) compared with Col-0 WT plants (Figure 2.6e).

To understand why overexpressing MIR863 did not have an effect on the defence response, we decided to study the function of miR863-3p targets individually. First, we focused on the functional analysis of the two ARLPKs and obtained the null

mutants SALK_144635 (*arlpk1-1*) and SALK_040744C (*arlpk2-1*) (Alonso et al., 2003). Each mutant contains a T-DNA insertion in the first exon (Figure 2.8a), as confirmed by RT–PCR (Figure 2.8b). The single mutants were developmentally similar to Col-0 WT plants (Figure 2.8c) and did not differ from Col-0 WT in defence response to infection with *Pst* (EV) or *Pst* (*avrRpt2*) (Figure 2.8d). This lack of disease phenotype may be due to functional redundancy, so we generated the *arlpk1-1 arlpk2-1* double mutant. The *arlpk1-1 arlpk2-1* plants were smaller compared with Col-0 WT (9a), and when infected with *Pst* (EV) and *Pst* (*avrRpt2*), *arlpk1-1 arlpk2-1* plants exhibited less bacterial growth in both cases (Figure 2.9b). To confirm the phenotype of enhanced resistance in the double mutant, we measured the expression of antimicrobial pathogenesis-related protein, PR1, a marker for salicylic acid-dependent disease responses. At 12 h post inoculation (h.p.i.), *arlpk1-1 arlpk2-1* showed higher PR1 protein expression compared with Col-0 WT after infection with *Pst* (EV) and *Pst* (*avrRpt2*) (Figure 2.9c), indicating that ARLPK1 and ARLPK2 are functionally redundant and negatively regulate plant immune responses.

We furthermore generated transgenic *Arabidopsis* overexpressing ARLPK1 with a mutation in the miR863-target site (mARLPK1-OE, as in Figure 2.3a) in the Col-0 WT background. We selected two overexpression lines, mARLPK1-OE1 and -OE2, exhibiting high *ARLPK1* transcript levels as detected by real-time RT–PCR for further functional analysis (Figure 2.9d). Both lines are more susceptible to *Pst* (EV) and *Pst* (*avrRpt2*) compared with Col-0 WT, further supporting that ARLPKs are

negative regulators of plant immunity (Figure 2.9e). miR863-3p-mediated silencing of*ARLPK1* during bacterial infection is important to promote plant defence responses.

ARLPKs are putative pseudokinases

As noted above, ARLPK1 and ARLPK2 have variations in the conserved motifs of functional kinase domains such as the glycine-rich loop (GXGXXG), VAIK motif and HRD motif (Figure 2.5), and are thus predicted pseudokinases. The glycine loop is located in subdomain I near the catalytic domain and is found in many nucleotide-binding proteins as well as in protein kinases (Boudeau et al., 2006). Both ARLPK1 and ARLPK2 have a serine substitution for the second glycine in the loop. The VAIK, HRD and DFG motifs are all found in the catalytic domain. The lysine in the VAIK motif in subdomain II interacts with ATP (Boudeau et al., 2006). ARLPK1 and ARLPK2 have a VRVL and an IRVL motif, respectively, and are thus missing the lysine residue; it has not been demonstrated that these motifs can bind ATP. The aspartic acid in the HRD motif in subdomain IV is the base acceptor for proton transfer (Boudeau et al., 2006). However, both pseudokinases have a HGN motif containing an uncharged asparagine. Finally, the aspartic acid in the DFG motif, which is found in catalytic domains and binds Mg^{2+} ions that coordinate the phosphates of ATP in the ATP-binding cleft (Boudeau et al., 2006), is conserved in ARLPK1 and ARLPK2 (Figure 2.5). As predicted, we were unable to detect autophosphorylation *in vitro* using recombinant ARLPK1 and ARLPK2 proteins (Figure 2.9f). In contrast, we were able to clearly detect kinase activity for the RPM1-induced protein kinase (RIPK), which was used as a

positive control (Liu et al., 2011). These data support that ARLPK1 and ARLPK2 are most likely pseudokinases.

ARLPK1 interacts with AKIK1 to regulate plant immunity

Both ARLPKs have a predicted transmembrane domain, so we determined their subcellular localization in *N. benthamiana* with confocal microscopy. However, the endoplasmic reticulum (ER) signal peptide in ARLPK1 and ARLPK2 overlaps with the predicted transmembrane domain (Figure 2.4). We originally thought that the pseudokinases would be localized in the plasma membrane (PM) and we used a PM-localized protein RLK (At5g23740)-cyan fluorescent protein (CFP) as control. To our surprise, we found that both ARLPK1-yellow fluorescent protein (YFP) and ARLPK2-YFP predominantly localize in the ER (Figure 2.10). We confirmed this using a mCherry-tagged ER organelle marker (ER-mCherry) (Nelson et al., 2007) as a control. ARLPK1-YFP and ARLPK-YFP overlapped with ER-mCherry in merged images, and Hechtian strands were not visible after plasmolysis treatment (Figure 2.11a, upper panels). These results only show the steady-state localization of these fluorescently tagged proteins. Trafficking or movement of some RLKs during pathogen challenge is often observed, as in the case of FLS2, which undergoes endocytosis upon flg22 treatment (Robatzek et al., 2006). We also checked the localization of ARLPKs after *Pst* (*avrRpt2*) challenge; however, we did not see any changes in the localization after *Pst* (*avrRpt2*) infection, both with and without plasmolysis treatment (Figure 2.11a, lower panels).

Because these two kinases are putative pseudokinases that lack an extracellular domain, we hypothesized that ARLPK1 and ARLPK2 function with another RLK to perceive and/or regulate extracellular signals. We searched for interacting proteins on the Arabidopsis Interactions Viewer (Geisler-Lee et al., 2007) (http://bar.utoronto.ca/), and found AT5G59650, a LRR I subfamily RLK, which may interact with ARLPK1. Thus, we named it AKIK1. Owing to non-complementarity in the nucleotide alignment, AKIK1 is not likely to be targeted by miR863-3p. AKIK1 contains a malectin domain and two LRR domains in its predicted extracellular region (Figure 2.12a,b). We found that AKIK1-CFP also predominantly localizes in the ER in untreated and pathogen-treated plants, both with and without plasmolysis treatment, as seen in the merged image with ER-mCherry (Figure 2.11b, left panels), and it also co-localizes with ARLPK1-YFP (Figure 2.11b, right panels).

We confirmed by co-immunoprecipitation (Co-IP) that ARLPK1, but not ARLPK2, interacts with AKIK1 (Figure 2.13a). We hypothesized that due to its association with ARLPK1, AKIK1 also has a role in plant defence. We obtained two T-DNA insertion mutant lines, *akik1-1* (SALK_022711C) and *akik1-2* (CS848612), which have T-DNA insertions in the fourth and ninth introns of AKIK1, respectively (Figure 2.14a). These two lines are both null mutants of *AKIK1*, as confirmed by RT–PCR (Figure 2.14b), and neither had any obvious developmental phenotypes compared with Col-0 WT (Figure 2.14c). Both *akik1-1* and *akik1-2* were more resistant to infection with *Pst* (EV) and *Pst* (*avrRpt2*) compared with Col-0 WT plants (Figure 2.13b).

Because both mutants showed the same disease phenotypes, we used *akik1-1* for further analysis. In agreement with the bacterial growth assays, PR1 protein levels were higher in *akik1-1* compared with Col-0 WT 12 h.p.i. with *Pst* (EV) and *Pst* (*avrRpt2*), although to a lesser extent with *Pst* (EV) (Figure 2.13c). To confirm the roles of ARLPK1, ARLPK2 and AKIK1 in PTI, we performed assays that measured PAMP responses to flg22 treatment. We measured PTI-responsive gene flg22-induced receptor-like kinase 1 (*FRK1*) by real-time RT–PCR after treatment with flg22. In agreement with the bacterial growth assay results, the double mutant *arlpk1-1 arlpk2-1* and the *akik1-1* mutant showed highly increased *FRK1* expression compared with Col-0 WT (Figure 2.13d). Mitogen-activated protein kinase 3 (MPK3) and MPK6 are two kinases involved in the MAP kinase signalling cascade, which act downstream of FLS2 to confer disease resistance (Asai et al., 2002). The *arlpk1-1 arlpk2-1* double mutant and the *akik1-1* mutant showed significantly higher MPK3 and MPK6 levels compared with Col-0 WT after flg22 treatment (Figure 2.13e). Unlike ARLPK1 and ARLPK2, AKIK1 does possess conserved catalytic residues in its kinase domain (Figure 2.5). The kinase domain of AKIK1 was expressed and purified from *Escherichia coli* and subjected to an *in vitro* radiolabelled kinase assay. Consistent with its conserved catalytic residues, we were able to detect autophosphorylation activity for AKIK1, demonstrating that it is an active kinase (Figure 2.13f). Taken together, the results show ARLPK1, ARLPK2 and AKIK1 all negatively regulate ETI and PTI.

SE is a positive regulator of plant immunity

SE was originally identified as a C_2H_2-type zinc-finger protein important in leaf and meristem development, inflorescence architecture and phase transition (Clarke et al., 1999; Prigge and Wagner, 2001). Since then, it has been shown to play a role in a crucial step of miRNA maturation and accumulation (Dong et al., 2008; Fang and Spector, 2007; Lobbes et al., 2006; Yang et al., 2006), pre-mRNA splicing (Laubinger et al., 2008) and alternative splicing (Raczynska et al., 2014). We hypothesized that as a target of miR863, *SE* should have a role in disease resistance; however, nothing has been uncovered so far regarding its function in antibacterial defence in plants.

We obtained the *se-1* mutant (CS3257), which contains an X-ray-induced 7-base deletion, for analysis (Clarke et al., 1999; Lobbes et al., 2006; Prigge and Wagner, 2001). The *se-1* mutant is smaller, has serrated leaves and exhibits pleotropic defects in shoot and leaf development (Clarke et al., 1999). We inoculated the *se-1* plants with *Pst* (EV), *Pst* (*avrRpt2*) and a mock solution to determine the role of SE in disease resistance. The *se-1* mutant showed increased disease susceptibility manifested as stronger chlorosis, or yellowing of the leaves, 3–4 d.p.i. (days post inoculation) compared with Col-0 WT plants. Infection with pathogen does not stunt growth of *se-1* mutants (Figure 2.15a). The *se-1* mutant also showed delayed HR after infection with *Pst* (*avrRpt2*), indicating a weaker or slower RPS2-mediated defence response against *Pst* (*avrRpt2*) (Figure 2.15b). We included *Pst* (EV) infection as a control, which did not trigger HR; however, at 48 h.p.i., the *se-1* mutant showed chlorosis of the leaves (Figure 2.15b) while Col-0 WT did not. We also measured the bacterial titre in *se-*

1 mutant and found that both *Pst* (EV) and *Pst* (*avrRpt2*) growth was greater in the mutants compared with Col-0 WT plants (Figure 2.15c). Consistent with the bacterial growth assays, PR1 protein expression is lower in *se-1* mutant than in Col-0 WT after infection with *Pst* (EV) and *Pst* (*avrRpt2*) (Figure 2.15d). *FRK1* transcript level (Figure 2.15e) and MPK6 and MPK3 protein levels (Figure 2.15f) are lower in *se-1* after flg22 treatment than in Col-0 WT. Furthermore, we obtained *Arabidopsis* transgenic lines overexpressing *SE* CDS in the *se-1* background (SE-OE) (Lobbes et al., 2006; Raczynska et al., 2014) that have a complemented leaf phenotype and are slightly smaller than Col-0 WT plants (Figure 2.15g). We confirmed the overexpression of *SE* in these lines (Figure 2.15h), and found that they show enhanced disease resistance to *Pst* (EV) and *Pst* (*avrRpt2*) (Figure 2.15i). Taken together, these data further support SE is a positive regulator of disease resistance.

miR863 sequentially silences its targets to regulate defence

Our results showed that the three confirmed targets of miR863 have opposite roles in plant immunity. While the ARLPKs are negative regulators of defence, SE is a positive regulator, thus explaining why overexpressing miR863 has no clear effect on disease resistance (Figure 2.6e). Thus far, known miRNAs involved in immunity target either negative or positive regulators of plant immunity, not both. To find out why miR863-3p silences targets with opposite cellular functions, we performed a time course experiment and examined the levels of the targets during early and late stages after infection with *Pst* (*avrRpt2*). Because high inoculum concentration of avirulent *Pst* can trigger

HR and thus affect the expression levels of many genes, we used a lower concentration (2×10^6 colony-forming units (c.f.u.) per ml) that would not trigger macroscopic HR at 15 h.p.i., but could still induce miR863-3p levels. Real-time RT–PCR and western blot analysis revealed the kinases are downregulated early, just at 4 h.p.i. (Figure 2.16a), while SE protein levels are downregulated much later, around 12 h.p.i. (Figure 2.16b). It may be that SE is not targeted by miR863 during earlier stages of infection because a higher level of miR863 is required for translation inhibition of SE, which is not achieved until the late stage of infection. After SE protein levels decrease, the accumulation of miR863-3p also decreases in the later stages of infection (Figure 2.16c). We probed miR393 and miR319 as well and found that the levels of both also decrease in latter stages of infection similar to that of miR863-3p, showing that downregulation of SE protein does indeed affect miRNA accumulation (Figure 2.17a). We also performed the time course experiment with *Pst* (EV) infection and found that the levels of *ARLPK1* and *ARLPK2* mRNA, miR863-3p and SE protein did not significantly change over time (Figure 2.17b). These results show that miR863-3p temporal regulation of its targets is more predominant in ETI, although ARLPK1, ARLPK2 and AKIK1 all have roles in negative regulation of both ETI and PTI.

DISCUSSION

The initiation, timing and amplitude of plant defence responses are tightly controlled. Cellular reprogramming that occurs during pathogen infection is energy consuming;

thus, a trade-off exists between plant growth and defence (Belkhadir et al., 2014). In recent years, several miRNAs and siRNAs with important roles in plant immunity have been discovered. However, no sRNAs that target genes with antagonistic roles in response to the same environmental or developmental cues have been reported in any cellular processes within any organisms. Here we identified miR863-3p, which is highly induced by *Pst* (*avrRpt2*) infection and sequentially silences negative and positive regulators of plant immunity through two different modes of action. miR863-3p first suppresses negative regulators—ARLPK1 and ARLPK2—via mRNA degradation to boost defence responses quickly after infection. ARLPK1 interacts with AKIK1, which also functions as a negative regulator. Then, during later stages of infection, miR863-3p downregulates SE via translational inhibition to attenuate defence signalling by bringing down the level of miR863-3p, of which accumulation is dependent on SE (Figure 2.16c,d), thus forming a negative feedback loop to attenuate plant immunity. Thus, miR863-3p plays a critical role in regulating and fine-tuning the timely upregulation of plant defences on pathogen infection, as well as the attenuation of immune responses after successful defence. Just as the timely upregulation of plant defences on pathogen infection is crucial for survival, the attenuation of immune responses after successful defence may also be important to conserve host resources for growth and reproduction.

Even though miR863-3p regulates ARLPK1, ARLPK2 and SE during ETI, all targets, as well as AKIK1, are regulators of not only ETI but also PTI. A recent systematic study of network characteristics in ETI and PTI revealed that both share a large subnetwork of genes and interactors that most likely functions to favour plant

defence over growth (Dong et al., 2015). However, the organization of defence response modules in ETI is independent, rather than cohesive as it is in PTI, due to the evolutionary demand for a rapid and robust response to pathogen effectors (Dong et al., 2015).

The RLK/Pelle family has over 600 members and is the largest group of protein kinases in *Arabidopsis* (Shiu et al., 2004). Many RLKs are extensively involved in signalling pathways in development and plant immunity (Antolin-Llovera et al., 2012; Li and Tax, 2013; Monaghan and Zipfel, 2012). In the recent years, several RLKs that play a role in negative regulation of plant defence have been discovered, such as growth-promoting phytosulfokine (PSK) receptors PSKR1 and PSY1R (Igarashi et al., 2012; Mosher et al., 2013), and BAK1-interactors BIR1 (Gao et al., 2009) and BIR2 (Halter et al., 2014). Interestingly, the BIR2 kinase domain is missing conserved motifs and exhibits no kinase activity (Halter et al., 2014). Nearly 20% of *Arabidopsis* RLKs are predicted to be pseudokinases and can have phosphorylation-independent mechanisms of mediating signal transduction (Castells and Casacuberta, 2007). Many pseudokin ses have important functions in humans (Reiterer et al., 2014), plants (Chevalier et al., 2005; Lewis et al., 2013; Nimchuk et al., 2011; Wang et al., 2015) and bacteria (Childers et al., 2014; Gee et al., 2012), and still possess kinase catalytic activity or bind nucleotides and/or cations. They can act as scaffolding proteins or regulate the activity of functional kinases (Boudeau et al., 2006). Neither ARLPK1 nor ARLPK2 exhibited detectable autophosphorylation *in vitro* (Figure 2.9f) and may thus function as

scaffolding proteins or modulate the activity of AKIK1 or other kinases to regulate immune signalling.

Most studied RLKs, including PSKY1 (Ladwig et al., 2015), PSY1R (Fuglsang et al., 2014), BIR1 (Gao et al., 2009), and BIR2 (Halter et al., 2014), localize in the plasma membrane, but we found that ARLPK1, ARLPK2 and AKIK1 were all predominantly localized to the ER (Figure 2.10, 1.11). ARLPK1 and ARLPK2 both have predicted signal peptides that overlap with their transmembrane domains (Figure 2.4); thus, it is possible that the sequences are not true signal peptides. In contrast, AKIK1 has a clear signal peptide (Figure 2.12). It is possible that AKIK1 also localizes in other cellular organelles. Future experiments would involve obtaining native antibodies specific to AKIK1, ARLPK or ARLPK2, to determine their subcellular localization *in vivo*. The multigene family of hormone ethylene receptor kinases—including ETR1, ERS1, CTR1 and EIN2—are ER-membrane bound. Ethylene plays a role in many plant growth and development processes, as well as responses to environmental stresses, and its gaseous nature may explain why its receptors can localize in the ER (Merchante et al., 2013). *Arabidopsis* hormone cytokinin receptors—AHK2, AHK3 and CRE1/AHK4—which play roles in plant growth and formation, as well as in biotic and abiotic stress responses, are all membrane-bound kinases that mainly localize in the ER. These receptors may be localized in the ER for crosstalk or for close proximity to the nucleus for downstream signalling (Wulfetange et al., 2011). On the other hand, *Arabidopsis* AtIre1-1 and AtIre1-2 are transmembrane receptor kinases located in the ER and most likely function in ER unfolded protein response

signalling, like their yeast and mammalian homologue Ire1 (Koizumi et al., 2001). How the roles of ARLPK1, ARLPK2 and AKIK1 are related to their subcellular localization in the ER remains to be determined. Finding their downstream components or other interacting partners may shed light on this question.

The role of SE in antibacterial plant defence has not been previously uncovered. However, *dcl1*, *hyl1* and *hen1*, the mutants defective in miRNA accumulation, have decreased basal defence (Katiyar-Agarwal et al., 2006; Navarro et al., 2006). One study showed that SE might be involved in the cuticle integrity pathway, and related to that, *se-1* mutants are more susceptible to necrotrophic fungal infection (Voisin et al., 2009). SE has been proposed to regulate gene expression by modifying chromatin structure (Prigge and Wagner, 2001). As a component of the nuclear cap-binding complex, SE also has a role in pre-mRNA splicing (Laubinger et al., 2008). This distinguishes SE from DCL1 and HYL1, which participate in only miRNA processing (Raczynska et al., 2014). Other SE-dependent miRNAs are also likely to be involved during later infection stages to returning the host immune system to a normal state. Future research focusing on the role of additional SE-related miRNAs as well as ARLPK1 and ARLPK2 targets will enhance our understanding of temporal immune signalling.

METHODS

Plant materials and growth conditions

Arabidopsis and *N. benthamiana* plants were grown in a controlled growth room at 23±1 °C in a 12-h light/12-h dark photoperiod. All experiments were performed on 4-week-old *Arabidopsis* plants and 3-week-old *N. benthamiana* plants. The following mutants seeds were used in this study: *dcl1-7/fwf2* (Katiyar-Agarwal et al., 2007), *rdr6-15* (Allen et al., 2005), *se*-1 (Clarke et al., 1999), and SALK lines *arlpk-1* (SALK_144635), *arlpk-1* (SALK_040744), *akik1-1* (SALK_022711C) and *akik1-2* (CS848612) (Alonso et al., 2003). Homozygous mutants plants were identified by RT–PCR, and primers are listed in Table 1.1. All mutants were in the Columbia (Col-0) background, except for *dcl1-7/fwf2*, which was in the Landsberg *erecta* (L*er*) background.

Identification of target proteins of miR863

To identify miR863-3p target genes, a set of computational rules for target prediction was adapted from Allen *et al*. (Allen et al., 2005) and modified. The miRNA-target duplex must contain four or less unpaired bases, four or less G:U pairs, up to one single-nucleotide bulge and seven or fewer unpaired plus G:U positions. Nucleotides at positions 10 and 11 of the miRNA must be a perfect match with its target. Mismatched pairs or single-nucleotide bulges were given a score of 1; G:U pairs were given a score

of 0.5. Mismatched and G:U pair scores were doubled if they were located within the core segment (positions 2–13). A maximum of three continuous mismatches was allowed if the mismatch region contained at least two G:U pairs, and the penalty score of the region was multiplied by 1.5. We used 5.5 as the cutoff score for selecting the miRNA targets.

Bacterial infection

Bacterial strains used include the following: *Pseudomonas syringae* pv. *tomato* DC3000 carrying broad host range vector pVSP61 (EV) (Innes et al., 1993); or pVSP61 plasmid containing avirulence gene *avrRpt2* (Innes et al., 1993), *avrRpm1* (Bisgrove et al., 1994)(or *avrRps4* (Hinsch and Staskawicz, 1996); and a strain that has a mutation in its type III secretion system (Δ*hrcC*) (Yuan and He, 1996). For bacterial growth assays, 4-week-old *Arabidopsis* plants were syringe-infiltrated with a 5×10^5 c.f.u. per ml bacterial suspension. Leaves were collected 3 d.p.i. using a cork borer, and bacterial titre was determined by serial dilution, plating and counting the colonies. At least 15 leaf discs were collected for each growth assay. Three biological repeats were performed with similar results. Student's *t*-test was used to determine the significant differences between mutants and control plants. For northern and western blots and the HR assay, a 1×10^7 c.f.u. per ml bacterial suspension was used. A total of 18 leaves were infected for the HR assay and monitored for the appearance of HR symptoms. For the time course, a 2×10^6 c.f.u. per ml bacterial suspension was used.

Generation of transgenic plants

To generate the construct for the MIR863-OE lines, the miR863 precursor was cloned using a miR319 backbone (Schwab et al., 2006) into a pEarleyGate (pEG) 100 destination vector (Earley et al., 2006) using LR clonase II (Invitrogen). To generate the mARLPK1-OE lines, the mutated (m) ARLPK1 CDS was cloned into pEG104. *Arabidopsis* plants were transformed using floral dip method with *Agrobacterium tumefaciens* strain GV3101 carrying the carrying cloned vectors.

Protein extraction and analysis

Tissue sample was ground in liquid nitrogen and total proteins were extracted using 2 × SDS loading buffer. The samples were resolved on a 12% SDS–PAGE gel and transferred onto nitrocellulose membranes using a Tris-Glycine transfer buffer. The blots were probed with the appropriate antibodies: monoclonal mouse anti-GFP, which also recognizes YFP (Roche, 11814460001, 1:2,000 dilution); monoclonal mouse anti-FLAG (Sigma-Aldrich, F3165, 1:2,000 dilution); monoclonal mouse anti-α tubulin (Sigma-Aldrich, T6074, 1:4,000 dilution); polyclonal rabbit anti-PR1 (obtained from Xinnian Dong (Wang et al., 2005), 1:2,000 dilution); polyclonal rabbit anti-SE (serum containing polyclonal antibodies was produced in rabbits immunized with peptide containing the first 200 amino acids of the SE protein, AbMax Biotechnology Co., Ltd., 1:1,000 dilution); rabbit serum was purified using Montage Antibody Purification kit,

Millipore); goat anti-mouse IgG-HRP (Santa Cruz Biotechnology, sc-2005, 1:4,000 dilution); and goat anti-rabbit IgG-HRP (Santa Cruz Biotechnology, sc-2030. 1:4,000 dilution).

Transient expression analysis in *N. benthamiana*

Transient co-expression and co-immunoprecipitation assays in *N. benthamiana* were performed by infiltrating 3-week-old *N. benthamiana* plants with *Agrobacterium* (OD_{600} (optical density at 600 nm)=1.0) harbouring constructs containing the miR863 precursor with *Agrobacterium* containing (OD_{600}=1.0) wtARLPK1 or mutated (m) ARLPK1 CDS (pEG104), wtARLPK2 or mARLPK2 CDS (pEG104), and GFP-wtSE-3′-UTR or GFP-mSE-3′-UTR (pEG103). Leaf tissue was collected 48 h.p.i. and processed as described above. AKIK1 (pEG202) was used for Co-IP assays with ARLPK1 and ARLPK2. ANTI-FLAG M2 affinity gel (Sigma-Aldrich, A2220) was used for pull downs.

5′-RACE of mRNA cleavage products

5′-RACE (Llave et al., 2002) was performed using FirstChoice RLM-5′-RACE kit (Ambion) following the manufacturer's instructions. Briefly, total RNA was extracted from *Pst* (*avrRpt2*)-infected tissue 10 h.p.i. and directly ligated to the RNA Oligo adaptor without further modification. Oligo (dT) primer was used to prime cDNA synthesis with reverse transcriptase. Gene-specific 5′-RACE reactions were done with the 5′ Nested Primer and gene-specific primers ARLPK1-R 5′-RACE and ARLPK2-R

5′-RACE as listed in Table 1.1. The 5′-RACE products were gel purified, cloned into pENTR (Invitrogen) vector and sequenced.

Site-directed mutagenesis

The wtARLPK1 CDS, ARLPK2 CDS and SE 3′-UTR sequences were cloned into pENTR (Invitrogen) vector. Point mutations were introduced using the GeneArt Site-Directed Mutagenesis System kit (Invitrogen) following the manufacturer's instructions. Primers used are listed in Table 1.1 as mARLPK1-F, mARLPK1-R, mARLPK2-F, mARLPK2-R, mSE 3′-UTR-F and mSE 3′-UTR-R. The final plasmids with the mutated sequences were cloned into the pEG104 (mARLPK1 and mARLPK2) or pEG103 (mSE-3′-UTR) destination vectors using LR Clonase II (Invitrogen).

Protein kinase assays

ARLPK1 and ARLPK2 were cloned into pMAL-C4X with N-terminal fusions to maltose-binding protein (MBP). MBP-ARLPK1, MBP-ARLPK2 and MBP-RIPK were induced with 0.3 mM isopropyl-β-D-thiogalactoside for 3 h at 28 °C and purified by amylose affinity chromatography from *E. coli*. The kinase domain of AKIK1 (547–892 aa) was cloned into pDEST-15 (Invitrogen) with an N-terminal fusion to glutathione *S*-transferase (GST). GST-AKIK1 was expressed in *E. coli* (BL21 strain) at 28 °C for 4 h and the recombinant protein purified with Glutathione Sepharose 4B (GE Healthcare). Kinase assays were performed using 3 μg of recombinant protein with [γ-^{32}P]-ATP. The

assay was initiated by adding 1 ml (10 μCi) ^{32}P-ATP and incubated for 40 min at 30 °C. The reaction was terminated by the addition of 3 × laemmli loading buffer and subsequent incubation at 95 °C for 5 min. The proteins were separated on a 12% SDS–PAGE gel and signals were visualized by X-ray film exposure[30].

RNA extraction and analysis

Fresh tissue was ground in liquid nitrogen and RNA was extracted using TRIzol Reagent (Invitrogen) following the manufacturer's instructions. RNA is resolved on a 17% denaturing 8 M urea-PAGE gel and then transferred and chemically crosslinked onto a Hybond N^+ membrane (GE Healthcare Life Sciences) using *N*-(3-Dimethylaminopropyl)-*N*′(3-Dimethylaminopr hydrochloride. miRNAs were detected using end-labelled oligonucleotide probes and exposed to a phosphor imager screen. ImageQuant TL 7.0 analysis software (GE Healthcare Life Sciences) was used to measure relative abundance levels. For quantification of relative gene expression, cDNA was synthesized using Superscript III (Invitrogen), and real-time RT–PCR was performed using SYBR green dye (Bio-Rad) on a MyiQ detection system (Bio-Rad). The primers for all experiments are listed in Table 1.1.

MAPK activity assay

Two-week-old seedlings grown on half-strength Murashige and Skoog medium were treated with 10 μM flg22 containing 0.01% Silwet L-77. Samples were collected at 0, 5, 10, 15 and 30 min, and analysed by western blotting using monoclonal rabbit phospho-p44/42 MAPK (Erk1/2) (Thr202/Tyr204)(D13.14.4E) XP antibodies (Cell Signaling

Technology, #4370S, 1:2,000 dilution).α-tubulin was used as a loading control using monoclonal mouse anti-α tubulin (Sigma-Aldrich, T6074, 1:4,000 dilution).

Subcellular localization

Subcellular localization of fluorescent-tagged proteins was determined using confocal microscopy. Three-week-old *N. benthamiana* plants were infiltrated with *Agrobacterium* carrying constructs ARLPK1-YFP, ARLPK2-YFP, AKIK1-CFP, RLK-CFP, ER-mCherry (ER-rk; *CD3-959*) or empty GFP vector. Untreated tissue was collected 48 h.p.i. Plants were treated with *Pst* (*avrRpt2*) 48 h.p.i. after infiltration with *Agrobacterium* and tissue was collected 12 h.p.i. For the plasmolysis treatment, tissue was treated with 5% NaCl for 5–10 min before visualization (+NaCl), or with water as a control (–NaCl). The ER marker is the mCherry fluorescent protein with the signal peptide of *Arabidopsis* wall-associated kinase 2 (AtWAK2) at the N terminus and the ER retention signal His-Asp-Glu at the C terminus (Nelson et al., 2007). The plasma membrane marker is an RLK (At4g23740) fused to CFP at the C terminus (Caplan et al., 2009).

REFERENCES

Allen, E., Xie, Z., Gustafson, A.M., and Carrington, J.C. (2005). microRNA-directed phasing during trans-acting siRNA biogenesis in plants. Cell *121*, 207-221.

Alonso, J.M., Stepanova, A.N., Leisse, T.J., Kim, C.J., Chen, H., Shinn, P., Stevenson, D.K., Zimmerman, J., Barajas, P., Cheuk, R.*, et al.* (2003). Genome-wide insertional mutagenesis of Arabidopsis thaliana. Science *301*, 653-657.

Antolin-Llovera, M., Ried, M.K., Binder, A., and Parniske, M. (2012). Receptor kinase signaling pathways in plant-microbe interactions. Annu Rev Phytopathol *50*, 451-473.

Asai, T., Tena, G., Plotnikova, J., Willmann, M.R., Chiu, W.L., Gomez-Gomez, L., Boller, T., Ausubel, F.M., and Sheen, J. (2002). MAP kinase signalling cascade in Arabidopsis innate immunity. Nature *415*, 977-983.

Belkhadir, Y., Yang, L., Hetzel, J., Dangl, J.L., and Chory, J. (2014). The growth-defense pivot: crisis management in plants mediated by LRR-RK surface receptors. Trends Biochem Sci *39*, 447-456.

Bisgrove, S.R., Simonich, M.T., Smith, N.M., Sattler, A., and Innes, R.W. (1994). A disease resistance gene in Arabidopsis with specificity for two different pathogen avirulence genes. Plant Cell *6*, 927-933.

Boudeau, J., Miranda-Saavedra, D., Barton, G.J., and Alessi, D.R. (2006). Emerging roles of pseudokinases. Trends Cell Biol *16*, 443-452.

Caplan, J.L., Zhu, X., Mamillapalli, P., Marathe, R., Anandalakshmi, R., and Dinesh-Kumar, S.P. (2009). Induced ER chaperones regulate a receptor-like kinase to mediate antiviral innate immune response in plants. Cell host & microbe *6*, 457-469.

Castells, E., and Casacuberta, J.M. (2007). Signalling through kinase-defective domains: the prevalence of atypical receptor-like kinases in plants. J Exp Bot *58*, 3503-3511.

Chevalier, D., Batoux, M., Fulton, L., Pfister, K., Yadav, R.K., Schellenberg, M., and Schneitz, K. (2005). STRUBBELIG defines a receptor kinase-mediated signaling pathway regulating organ development in Arabidopsis. Proc Natl Acad Sci USA *102*, 9074-9079.

Childers, W.S., Xu, Q., Mann, T.H., Mathews, II, Blair, J.A., Deacon, A.M., and Shapiro, L. (2014). Cell fate regulation governed by a repurposed bacterial histidine kinase. PLoS biology *12*, e1001979.

Clarke, J.H., Tack, D., Findlay, K., Van Montagu, M., and Van Lijsebettens, M. (1999). The SERRATE locus controls the formation of the early juvenile leaves and phase length in Arabidopsis. Plant J *20*, 493-501.

Dodds, P.N., and Rathjen, J.P. (2010). Plant immunity: towards an integrated view of plant-pathogen interactions. Nat Rev Genet *11*, 539-548.

Dong, X.B., Jiang, Z.H., Peng, Y.L., and Zhang, Z.D. (2015). Revealing Shared and Distinct Gene Network Organization in Arabidopsis Immune Responses by Integrative Analysis. Plant Physiol *167*, 1186-1203.

Dong, Z., Han, M.H., and Fedoroff, N. (2008). The RNA-binding proteins HYL1 and SE promote accurate in vitro processing of pri-miRNA by DCL1. Proc Natl Acad Sci USA *105*, 9970-9975.

Earley, K.W., Haag, J.R., Pontes, O., Opper, K., Juehne, T., Song, K., and Pikaard, C.S. (2006). Gateway-compatible vectors for plant functional genomics and proteomics. Plant J *45*, 616-629.

Endicott, J.A., Noble, M.E., and Johnson, L.N. (2012). The structural basis for control of eukaryotic protein kinases. Annu Rev Biochem *81*, 587-613.

Fang, Y., and Spector, D.L. (2007). Identification of nuclear dicing bodies containing proteins for microRNA biogenesis in living Arabidopsis plants. Curr Biol *17*, 818-823.

Fuglsang, A.T., Kristensen, A., Cuin, T.A., Schulze, W.X., Persson, J., Thuesen, K.H., Ytting, C.K., Oehlenschlaeger, C.B., Mahmood, K., Sondergaard, T.E.*, et al.* (2014). Receptor kinase-mediated control of primary active proton pumping at the plasma membrane. Plant J *80*, 951-964.

Gao, M., Wang, X., Wang, D., Xu, F., Ding, X., Zhang, Z., Bi, D., Cheng, Y.T., Chen, S., Li, X.*, et al.* (2009). Regulation of cell death and innate immunity by two receptor-like kinases in Arabidopsis. Cell host & microbe *6*, 34-44.

Gee, C.L., Papavinasasundaram, K.G., Blair, S.R., Baer, C.E., Falick, A.M., King, D.S., Griffin, J.E., Venghatakrishnan, H., Zukauskas, A., Wei, J.R.*, et al.* (2012). A phosphorylated pseudokinase complex controls cell wall synthesis in mycobacteria. Sci Signal *5*, ra7.

Geisler-Lee, J., O'Toole, N., Ammar, R., Provart, N.J., Millar, A.H., and Geisler, M. (2007). A predicted interactome for Arabidopsis. Plant Physiol *145*, 317-329.

Halter, T., Imkampe, J., Mazzotta, S., Wierzba, M., Postel, S., Bucherl, C., Kiefer, C., Stahl, M., Chinchilla, D., Wang, X.*, et al.* (2014). The leucine-rich repeat receptor kinase BIR2 is a negative regulator of BAK1 in plant immunity. Curr Biol *24*, 134-143.

Hanks, S.K., and Hunter, T. (1995). Protein kinases 6. The eukaryotic protein kinase superfamily: kinase (catalytic) domain structure and classification. FASEB J *9*, 576-596.

Hanks, S.K., Quinn, A.M., and Hunter, T. (1988). The protein kinase family: conserved features and deduced phylogeny of the catalytic domains. Science *241*, 42-52.

Hinsch, M., and Staskawicz, B. (1996). Identification of a new Arabidopsis disease resistance locus, RPs4, and cloning of the corresponding avirulence gene, avrRps4, from Pseudomonas syringae pv. pisi. Mol Plant Microbe In *9*, 55-61.

Igarashi, D., Tsuda, K., and Katagiri, F. (2012). The peptide growth factor, phytosulfokine, attenuates pattern-triggered immunity. Plant J *71*, 194-204.

Innes, R.W., Bisgrove, S.R., Smith, N.M., Bent, A.F., Staskawicz, B.J., and Liu, Y.C. (1993). Identification of a disease resistance locus in Arabidopsis that is functionally homologous to the RPG1 locus of soybean. Plant J *4*, 813-820.

Katiyar-Agarwal, S., Gao, S., Vivian-Smith, A., and Jin, H. (2007). A novel class of bacteria-induced small RNAs in Arabidopsis. Genes Dev *21*, 3123-3134.

Katiyar-Agarwal, S., and Jin, H. (2010). Role of small RNAs in host-microbe interactions. Annu Rev Phytopathol *48*, 225-246.

Katiyar-Agarwal, S., Morgan, R., Dahlbeck, D., Borsani, O., Villegas, A., Jr., Zhu, J.K., Staskawicz, B.J., and Jin, H. (2006). A pathogen-inducible endogenous siRNA in plant immunity. Proc Natl Acad Sci USA *103*, 18002-18007.

Koizumi, N., Martinez, I.M., Kimata, Y., Kohno, K., Sano, H., and Chrispeels, M.J. (2001). Molecular characterization of two Arabidopsis Ire1 homologs, endoplasmic reticulum-located transmembrane protein kinases. Plant Physiol *127*, 949-962.

Kornev, A.P., and Taylor, S.S. (2010). Defining the conserved internal architecture of a protein kinase. Biochim Biophys Acta *1804*, 440-444.

Kunkel, B.N., Bent, A.F., Dahlbeck, D., Innes, R.W., and Staskawicz, B.J. (1993). RPS2, an Arabidopsis disease resistance locus specifying recognition of Pseudomonas syringae strains expressing the avirulence gene avrRpt2. Plant Cell *5*, 865-875.

Ladwig, F., Dahlke, R.I., Stuhrwohldt, N., Hartmann, J., Harter, K., and Sauter, M. (2015). Phytosulfokine Regulates Growth in Arabidopsis through a Response Module at the Plasma Membrane That Includes CYCLIC NUCLEOTIDE-GATED CHANNEL17, H+-ATPase, and BAK1. Plant Cell *27*, 1718-1729.

Laubinger, S., Sachsenberg, T., Zeller, G., Busch, W., Lohmann, J.U., Ratsch, G., and Weigel, D. (2008). Dual roles of the nuclear cap-binding complex and SERRATE in pre-mRNA splicing and microRNA processing in Arabidopsis thaliana. Proc Natl Acad Sci USA *105*, 8795-8800.

Lewis, J.D., Lee, A.H., Hassan, J.A., Wan, J., Hurley, B., Jhingree, J.R., Wang, P.W., Lo, T., Youn, J.Y., Guttman, D.S.*, et al.* (2013). The Arabidopsis ZED1 pseudokinase is required for ZAR1-mediated immunity induced by the Pseudomonas syringae type III effector HopZ1a. Proc Natl Acad Sci USA *110*, 18722-18727.

Li, J., and Tax, F.E. (2013). Receptor-like kinases: key regulators of plant development and defense. J Integr Plant Biol *55*, 1184-1187.

Li, X., Kapos, P., and Zhang, Y. (2015). NLRs in plants. Curr Opin Immunol *32*, 114-121.

Liu, J., Elmore, J.M., Lin, Z.J., and Coaker, G. (2011). A receptor-like cytoplasmic kinase phosphorylates the host target RIN4, leading to the activation of a plant innate immune receptor. Cell host & microbe *9*, 137-146.

Liu, J.D., Valencia-Sanchez, M.A., Hannon, G.J., and Parker, R. (2005). MicroRNA-dependent localization of targeted mRNAs to mammalian P-bodies. Nat Cell Bio *7*, 719-U118.

Llave, C., Xie, Z.X., Kasschau, K.D., and Carrington, J.C. (2002). Cleavage of Scarecrow-like mRNA targets directed by a class of Arabidopsis miRNA. Science *297*, 2053-2056.

Lobbes, D., Rallapalli, G., Schmidt, D.D., Martin, C., and Clarke, J. (2006). SERRATE: a new player on the plant microRNA scene. EMBO Rep *7*, 1052-1058.

Macho, A.P., and Zipfel, C. (2014). Plant PRRs and the activation of innate immune signaling. Mol Cell *54*, 263-272.

Martinez de Alba, A.E., Elvira-Matelot, E., and Vaucheret, H. (2013). Gene silencing in plants: a diversity of pathways. Biochim Biophys Acta *1829*, 1300-1308.

Merchante, C., Alonso, J.M., and Stepanova, A.N. (2013). Ethylene signaling: simple ligand, complex regulation. Curr Opin Plant Biol *16*, 554-560.

Meyers, B.C., Axtell, M.J., Bartel, B., Bartel, D.P., Baulcombe, D., Bowman, J.L., Cao, X., Carrington, J.C., Chen, X., Green, P.J.*, et al.* (2008). Criteria for annotation of plant MicroRNAs. Plant Cell *20*, 3186-3190.

Monaghan, J., and Zipfel, C. (2012). Plant pattern recognition receptor complexes at the plasma membrane. Curr Opin Plant Biol *15*, 349-357.

Mosher, S., Seybold, H., Rodriguez, P., Stahl, M., Davies, K.A., Dayaratne, S., Morillo, S.A., Wierzba, M., Favery, B., Keller, H.*, et al.* (2013). The tyrosine-sulfated peptide receptors PSKR1 and PSY1R modify the immunity of Arabidopsis to biotrophic and necrotrophic pathogens in an antagonistic manner. Plant J *73*, 469-482.

Navarro, L., Dunoyer, P., Jay, F., Arnold, B., Dharmasiri, N., Estelle, M., Voinnet, O., and Jones, J.D.G. (2006). A plant miRNA contributes to antibacterial resistance by repressing auxin signaling. Science *312*, 436-439.

Nelson, B.K., Cai, X., and Nebenfuhr, A. (2007). A multicolored set of in vivo organelle markers for co-localization studies in Arabidopsis and other plants. The Plant journal : for cell and molecular biology *51*, 1126-1136.

Nimchuk, Z.L., Tarr, P.T., and Meyerowitz, E.M. (2011). An evolutionarily conserved pseudokinase mediates stem cell production in plants. Plant Cell *23*, 851-854.

Padmanabhan, C., Zhang, X., and Jin, H. (2009). Host small RNAs are big contributors to plant innate immunity. Curr Opin Plant Biol *12*, 465-472.

Prigge, M.J., and Wagner, D.R. (2001). The arabidopsis serrate gene encodes a zinc-finger protein required for normal shoot development. Plant Cell *13*, 1263-1279.

Raczynska, K.D., Stepien, A., Kierzkowski, D., Kalak, M., Bajczyk, M., McNicol, J., Simpson, C.G., Szweykowska-Kulinska, Z., Brown, J.W., and Jarmolowski, A. (2014). The SERRATE protein is involved in alternative splicing in Arabidopsis thaliana. Nucleic Acids Res *42*, 1224-1244.

Reiterer, V., Eyers, P.A., and Farhan, H. (2014). Day of the dead: pseudokinases and pseudophosphatases in physiology and disease. Trends Cell Biol *24*, 489-505.

Robatzek, S., Chinchilla, D., and Boller, T. (2006). Ligand-induced endocytosis of the pattern recognition receptor FLS2 in Arabidopsis. Genes Dev *20*, 537-542.

Rogers, K., and Chen, X. (2013). Biogenesis, turnover, and mode of action of plant microRNAs. Plant Cell *25*, 2383-2399.

Schwab, R., Ossowski, S., Riester, M., Warthmann, N., and Weigel, D. (2006). Highly specific gene silencing by artificial microRNAs in Arabidopsis. Plant Cell *18*, 1121-1133.

Shiu, S.H., Karlowski, W.M., Pan, R., Tzeng, Y.H., Mayer, K.F., and Li, W.H. (2004). Comparative analysis of the receptor-like kinase family in Arabidopsis and rice. Plant Cell *16*, 1220-1234.

Sievers, F., Wilm, A., Dineen, D., Gibson, T.J., Karplus, K., Li, W., Lopez, R., McWilliam, H., Remmert, M., Soding, J.*, et al.* (2011). Fast, scalable generation of high-quality protein multiple sequence alignments using Clustal Omega. Molecular systems biology *7*, 539.

Voisin, D., Nawrath, C., Kurdyukov, S., Franke, R.B., Reina-Pinto, J.J., Efremova, N., Will, I., Schreiber, L., and Yephremov, A. (2009). Dissection of the complex phenotype in cuticular mutants of Arabidopsis reveals a role of SERRATE as a mediator. PLoS Genet *5*, e1000703.

Wang, D., Weaver, N.D., Kesarwani, M., and Dong, X.N. (2005). Induction of protein secretory pathway is required for systemic acquired resistance. Science *308*, 1036-1040.

Wang, G., Roux, B., Feng, F., Guy, E., Li, L., Li, N., Zhang, X., Lautier, M., Jardinaud, M.F., Chabannes, M.*, et al.* (2015). The Decoy Substrate of a Pathogen Effector and a Pseudokinase Specify Pathogen-Induced Modified-Self Recognition and Immunity in Plants. Cell host & microbe *18*, 285-295.

Weiberg, A., and Jin, H. (2015). Small RNAs-the secret agents in the plant-pathogen interactions. Curr Opin Plant Biol *26*, 87-94.

Weiberg, A., Wang, M., Bellinger, M., and Jin, H. (2014). Small RNAs: a new paradigm in plant-microbe interactions. Annu Rev Phytopathol *52*, 495-516.

Weiberg, A., Wang, M., Lin, F.M., Zhao, H., Zhang, Z., Kaloshian, I., Huang, H.D., and Jin, H. (2013). Fungal small RNAs suppress plant immunity by hijacking host RNA interference pathways. Science *342*, 118-123.

Wulfetange, K., Lomin, S.N., Romanov, G.A., Stolz, A., Heyl, A., and Schmulling, T. (2011). The Cytokinin Receptors of Arabidopsis Are Located Mainly to the Endoplasmic Reticulum. Plant Physiol *156*, 1808-1818.

Yang, L., Liu, Z.Q., Lu, F., Dong, A.W., and Huang, H. (2006). SERRATE is a novel nuclear regulator in primary microRNA processing in Arabidopsis. Plant J *47*, 841-850.

Yu, G.L., Katagiri, F., and Ausubel, F.M. (1993). Arabidopsis Mutations at the Rps2 Locus Result in Loss of Resistance to Pseudomonas-Syringae Strains Expressing the Avirulence Gene Avrrpt2. Mol Plant Microbe In *6*, 434-443.

Yuan, J., and He, S.Y. (1996). The Pseudomonas syringae Hrp regulation and secretion system controls the production and secretion of multiple extracellular proteins. J Bacteriol *178*, 6399-6402.

Zhang, W., Gao, S., Zhou, X., Chellappan, P., Chen, Z., Zhou, X., Zhang, X., Fromuth, N., Coutino, G., Coffey, M.*, et al.* (2011). Bacteria-responsive microRNAs regulate plant innate immunity by modulating plant hormone networks. Plant Mol Biol *75*, 93-105.

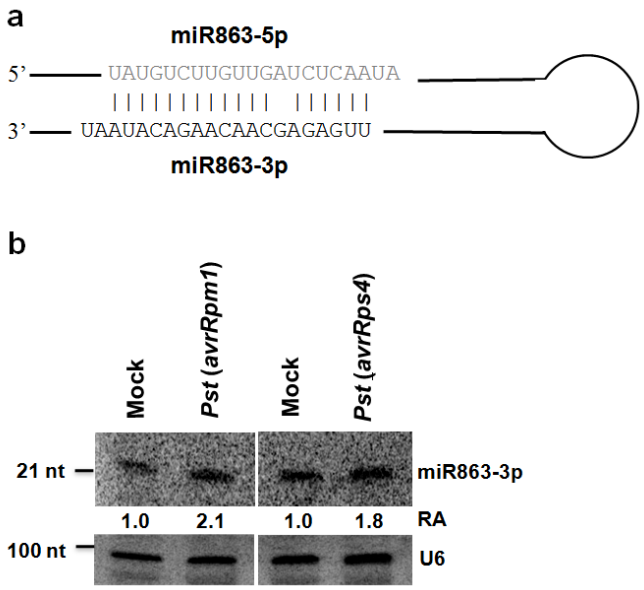


Figure 2.1: miR863-3p is induced by bacterial infection.
(a) miR863 precursor fold-back structure containing miR863-3p and -5p with 2' overhang. (b) miR863-3p levels in mock-, *Pst* (*avrRpm1*)- and *Pst* (*avrRps4*)-infected Col-0 WT plants were detected by Northern blot. Bacterial inoculum concentration: 1 x 10^7 CFU/ml. *Pst* (*avrRpm1*)- *Pst* (*avrRps4*)-infected leaf tissue was collected at 8 hpi and 24 hpi, respectively. U6 was used as a loading control. Relative abundance (RA) levels are indicated.

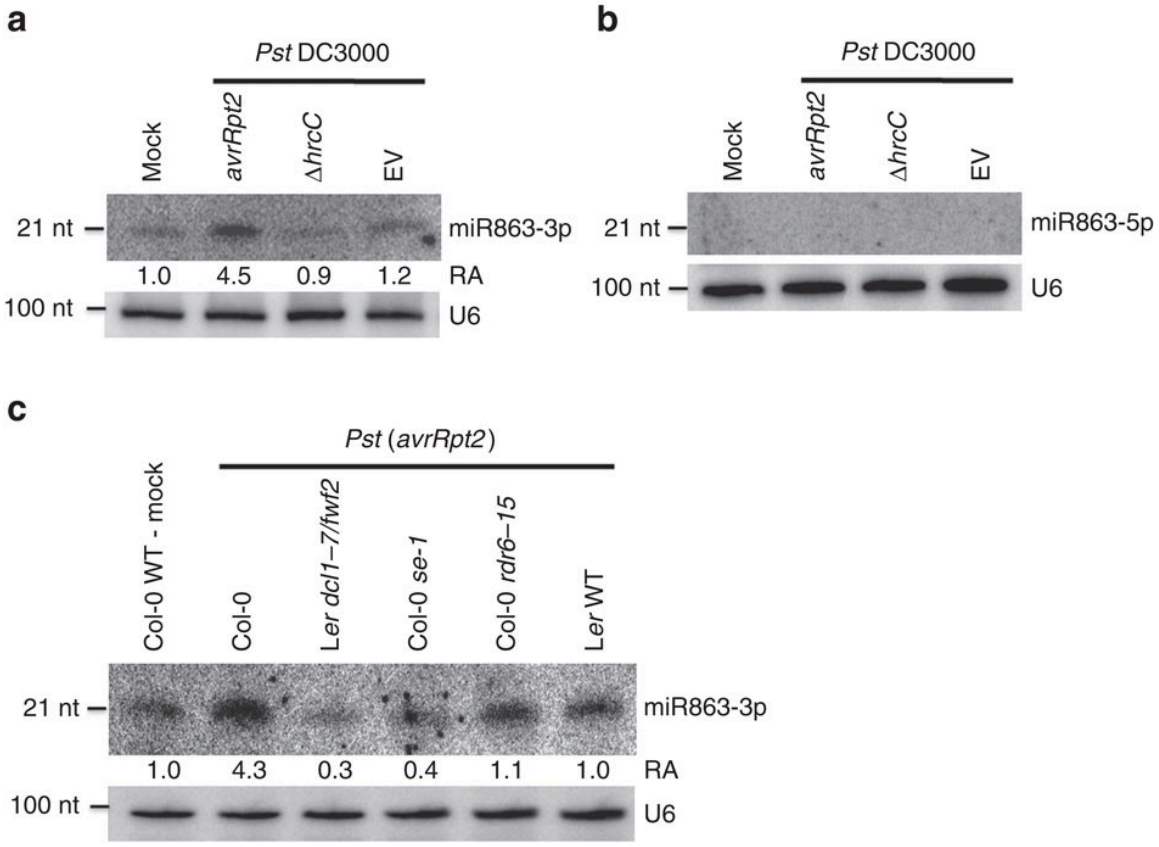


Figure 2.2: miR863-3p is induced by *Pst* carrying the effector avrRpt2.
(a) miR863-3p and (b) miR863-5p levels in mock-, *Pst* (*avrRpt2*)-, *Pst* (Δ*hrcC*)- and *Pst* (EV)-infected Col-0 WT plants were detected by northern blot analysis. Bacterial inoculum concentration: 1×10^7 c.f.u. per ml. Leaf tissue was collected at 14 h.p.i. U6 was used as a loading control. Relative abundance (RA) levels are indicated. Similar results were obtained from three biological replicates. (c) miR863-3p levels in various *Pst* (*avrRpt2*)-infected mutants defective in miRNA biogenesis (L*er dcl1-7/fwf2* and Col-0 *se-1*) or siRNA biogenesis (Col-0 *rdr6-15*) are detected by northern blot analysis. Mock-treated and *Pst* (*avrRpt2*)-infected Col-0 WT and *Pst* (*avrRpt2*)-infected L*er* WT were used as controls. Bacterial inoculum concentration: 1×10^7 c.f.u. per ml. Leaf tissue was collected at 14 h.p.i. U6 was used as a loading control. RA levels are indicated. Similar results were obtained from three biological replicates.

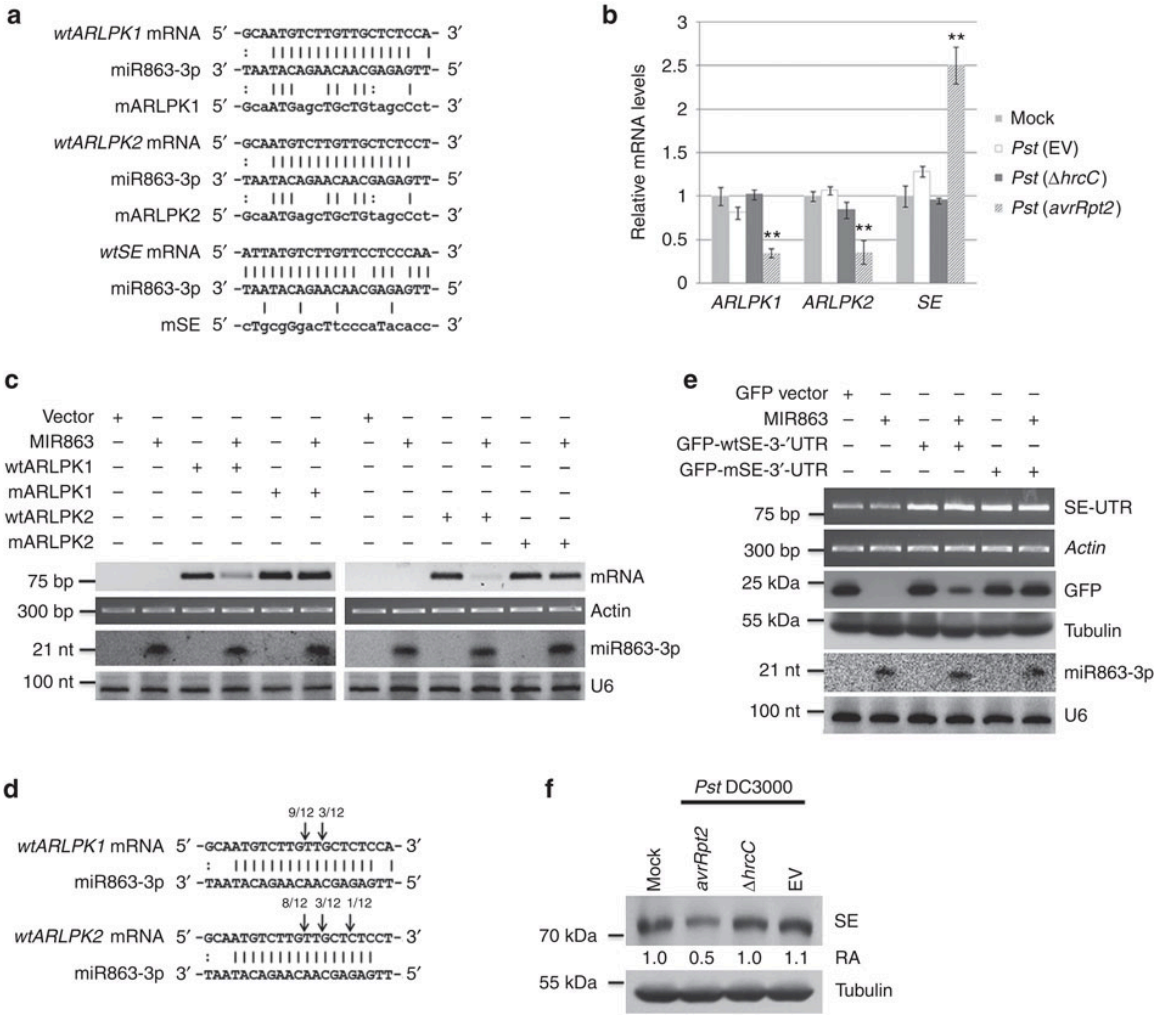
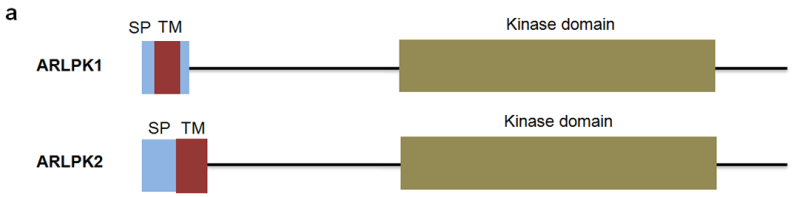


Figure 2.3: miR863-3p targets and silences *ARLPK1* and *ARLPK2* and SE by two modes of action.

(a) Nucleotide sequences of wt and mutated (m) versions of *ARLPK1*, *ARLPK2* and *SE* aligned against the miR863-3p sequence. (b) Relative expression levels of *ARLPK1*, *ARLPK2* and *SE* transcripts in mock- and *Pst* (EV), *Pst* (Δ*hrcC*) and *Pst* (*avrRpt2*)-infected Col-0 WT plants were detected by real-time RT–PCR. Bacterial inoculum concentration: 1×10^7 c.f.u. per ml. Leaf tissue was collected 14 h.p.i. Relative mRNA levels in mock-infected plants were set at 1. Error bars indicate s.d. from three technical replicates. Similar results were obtained from three biological replicates. ***P* value <0.01 (Student's *t*-test). (c) *Agrobacterium*-mediated transient co-expression assay with WT (wtARLPK1 and wtARLPK2) or mutated kinases (mARLPK1 and mARLPK2) and MIR863. mRNA levels of the wt and mutant kinases were detected by RT–PCR. rRNA was used as a loading control. miR863-3p levels were detected by northern blot analysis. U6 was used as a loading control. Similar results were obtained from two biological replicates. (d) Cleavage sites

of *ARLPK1* and *ARLPK2* mRNAs were revealed by mapping cloned RLM-5′-RACE products using *Pst* (*avrRpt2*)-infected WT *Arabidopsis* plants. Arrows indicate positions and proportions of clones mapping to the sites. (e) *Agrobacterium*-mediated transient co-expression assay with GFP-tagged wt (GFP-wtSE-3′-UTR) or mutated (GFP-mSE-3′-UTR) 3′-UTR SE fragment and MIR863. wtSE-GFP and mSE-GFP mRNA were detected by RT–PCR using primers specific to the SE 3′-UTR. Actin was used as a loading control. GFP protein levels were detected by western blot. α-Tubulin was used as a loading control. miR863-3p levels were detected by northern blot analysis. U6 was used as a loading control. Similar results were obtained from two biological replicates. (f) SE protein levels in mock-, *Pst* (*avrRpt2*)-, *Pst* (Δ*hrcC*)- and *Pst* (EV)-infected Col-0 WT plants were detected by western blot using an anti-SE antibody. Bacterial inoculum concentration: 1×10^7 c.f.u. per ml. Leaf tissue was collected at 14 h.p.i. α-Tubulin was used as a loading control. Relative abundance (RA) levels are indicated. Similar results were obtained from two biological replicates.



b

ARLPK1

Signal peptide Transmembrane domain

MRKSHLVKLILAVSLPTTFLIMIAIIIIFIFCRRTTTETNEVQYDVESPYEKQEFSDNGSETEEEL
IIFNGGEDLTICDILDAPGEVIGKSSYGTLYKATLQRSGKVRVLRFLRPLCAVNSDSKEFNGVI
ESLGFVRHDNLVPLLGFYVGNRGEKLMIHPFFGSSGNLSAFIKFLAGGDVDAHKWSNILSITI
GIAKALDHLHTGMQKPIVHGNLKSKNVLLDKSFRPRVSDFGLHLLLNLAAGQEVLEASAA
EGYKAPELIKMKEVSKESDVYSFGVIMLELVSGKEPTNKNPTGSVLDRNRLSDLYRPEIIRR
CLKDGNGVTEECVLEYFQLAMSCCSPSPTLRPSFKQVLRKLEEIRK

Kinase domain

ARLPK2

Signal peptide Transmembrane domain

MRKSLLLTLLLGVSLSAFLIVIFFIIFLRRKESSSTESDQYDVESLDHNKQGFSSETEELVIFQG
GEDLTICDILDAPGEVIGKSSYGTLYKASLQRSGKIRVLRFLRPVCTVRSDSKEFNGIIETLVR
HENLVPLLGFYAGNRGEKLMVHPFFGSGNLSDFIRSGDDESRKWINILRITIGISKALDHLHT
GMQKPIVHGNLKSKNVLLSSSFEPRISDFGLHLLLNLSAGQEILDVSAAEGYKAPELIKMKD
VSKESDVYSLGVIMLELVSGKEPINENATGDDEFYLPDFMRNAVLDHRLSDLYRPEILGSDD
NLSEECVLKYFQLAMSCCSPSPSLRPNVKQVLRKLEEIGKF

Kinase domain

Figure 2.4: ARLPK1 and ARLPK2 are atypical receptor-like kinases lacking extracellular domains.
(a) Diagrams of ARLPK1 and ARLPK2 with important predicted domains indicated. SP (blue box): signal peptide; TM (red box): transmembrane domain; kinase domain (brown box)
(b) Amino acid sequences of ARLPK1 and ARLPK2 with signal peptide (blue), transmembrane domain (highlighted in yellow), and kinase domain (brown) indicated.

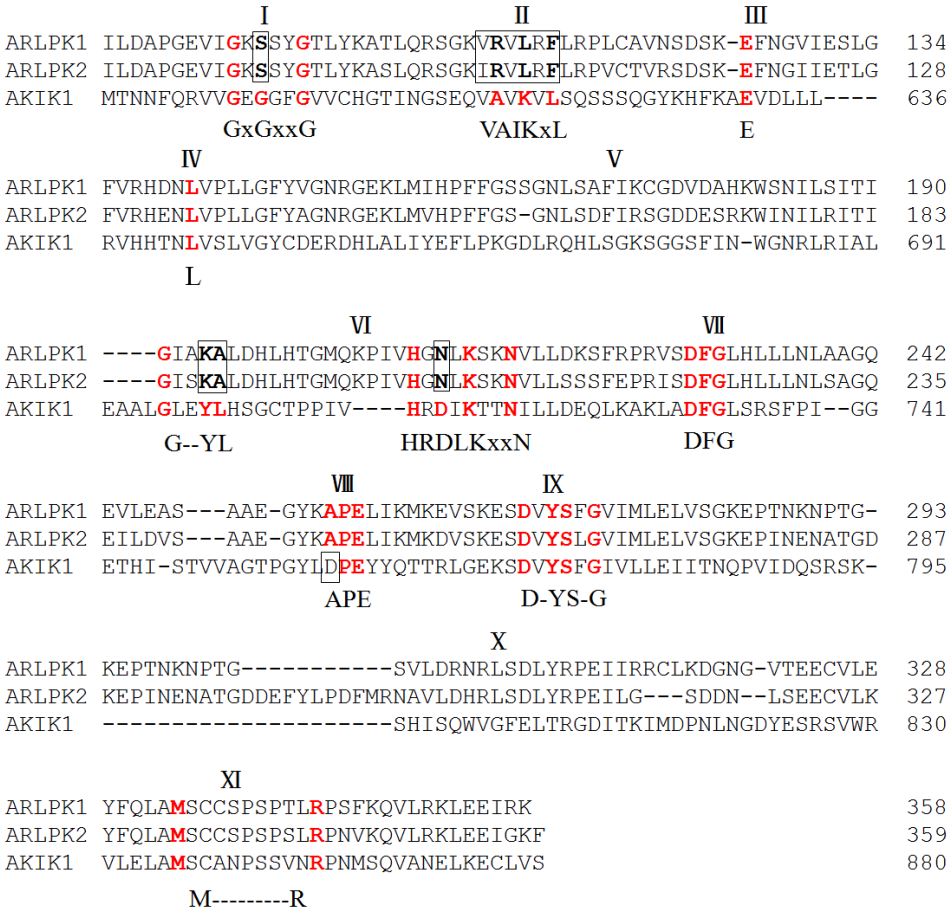


Figure 2.5: Amino acid alignments of ARLPK1, ARLPK2, and AKIK1 kinase domains.

Alignments were made using Clustal Omega (1.2.1)(Sievers et al., 2011). Consensus sequences of active receptor-like kinases are indicated below the alignments(Boudeau et al., 2006; Endicott et al., 2012; Hanks and Hunter, 1995; Hanks et al., 1988; Kornev and Taylor, 2010) and include: the glycine rich loop (GxGxxG), the Val-Ala-x-Lys-x-Leu (VA-K-L), glutamate (E), leucine (L), Gly-x-x-Tyr-Leu (GxxYL), His-Arg-Asp-Leu-Lys-x-x-Asn (HRDLKxxN) loop, Asp-Phe-Gly (DFG) motif,Ala-Pro-Glu (APE), Asp-x-Tyr-Ser-x-Gly (DxYSxG), andMet-x-x-x-x-x-x-x-x-x-Arg (MxxxxxxxxxR). Features and amino acids that are conserved in ARLPK1, ARLPK2, and AKIK1 are in red, while those that deviate from the consensus are boxed. Subdomains are indicated by Roman numerals.

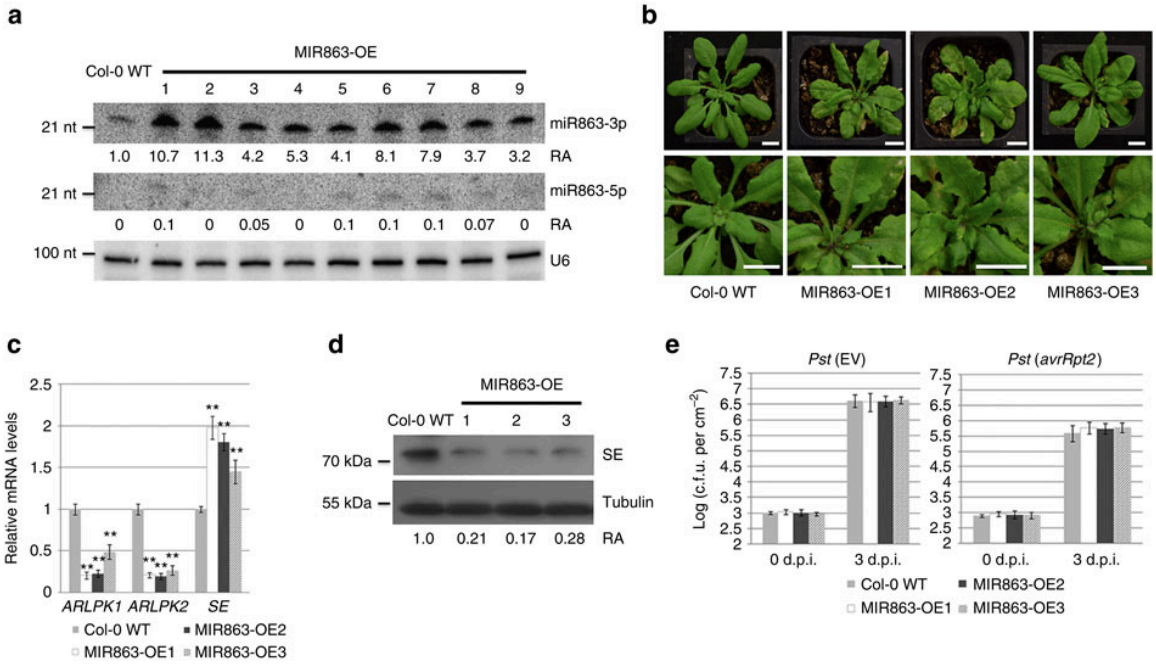


Figure 2.6: Plants overexpressing MIR863 show serrated leaves and have downregulated *ARLPK1* and *ARLPK2* mRNA and SE protein levels.
(**a**) miRNA863-3p and miRNA863-5p levels were detected in Col-0 WT and MIR863-OE lines #1–9. U6 was used as a loading control. Relative abundance (RA) levels are indicated. miRNA863-5p RA levels were measured compared with the miR863-3p levels in Col-0 WT. Similar results were obtained from two biological replicates. (**b**) Phenotypes of 4-week-old MIR863 OE plants. Out of the 20 lines tested, 4 highly expressed lines resembled the *serrate* mutant phenotype (MIR863-OE1 and -OE2 are shown), while 7 medium expressed lines showed a weak serrated leaf phenotype (MIR863-OE3 is shown). Scale bar, 10 mm. (**c**) *ARLPK1*, *ARLPK2* and *SE* transcript levels in Col-0 WT and MIR863-OE plants were detected by real-time RT–PCR. Error bars indicate s.d. from three technical replicates. Similar results were obtained from three biological replicates. ***P* value <0.01 (Student's *t*-test). (**d**) SE protein levels were detected in*Pst* (*avrRpt2*)-infected Col-0 WT and MIR863-OE plants by western blot analysis using an anti-SE antibody. Bacterial inoculum concentration: 1×10^7 c.f.u. per ml. Leaf tissue was collected at 14 h.p.i. α-Tubulin was used as a loading control. RA levels are indicated. Similar results were obtained from two biological replicates. (**e**) Bacterial growth in *Pst* (EV)- and *Pst* (*avrRpt2*)-infected Col-0 WT and MIR863-OE plants. Bacterial inoculum concentration: 5×10^5 c.f.u. per ml. Bacterial growth was measured at 3 d.p.i. Error bars represent s.d. for at least 15 leaf discs. Similar results were obtained from three biological replicates.

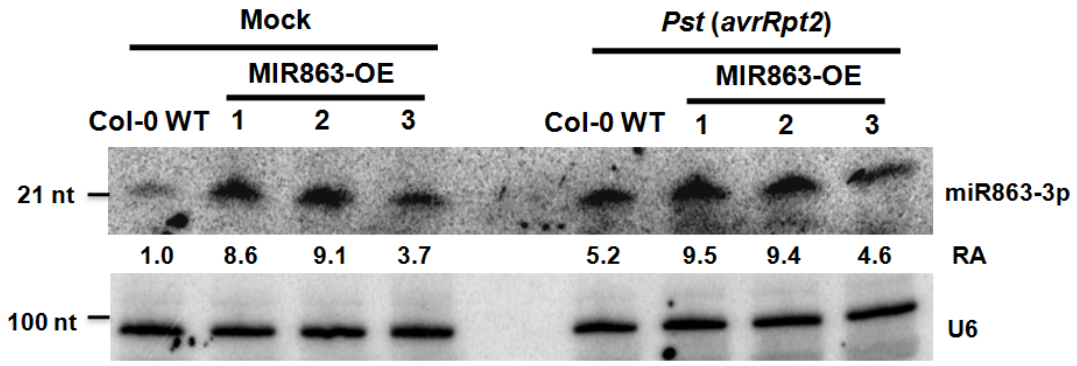


Figure 2.7: Expression of miR863-3p in MIR863-OE lines after mock- or *Pst (avrRpt2)* treatment.
miR863-3p levels in mock- and *Pst* (*avrRpt2*)-infected Col-0 WT and MIR863-OE plants were detected by Northern blot. Bacterial inoculum concentration: 1 x 10^7 CFU/ml. Leaf tissue was collected at 14 hpi. U6 was used as a loading control. Relative abundance (RA) levels are indicated.

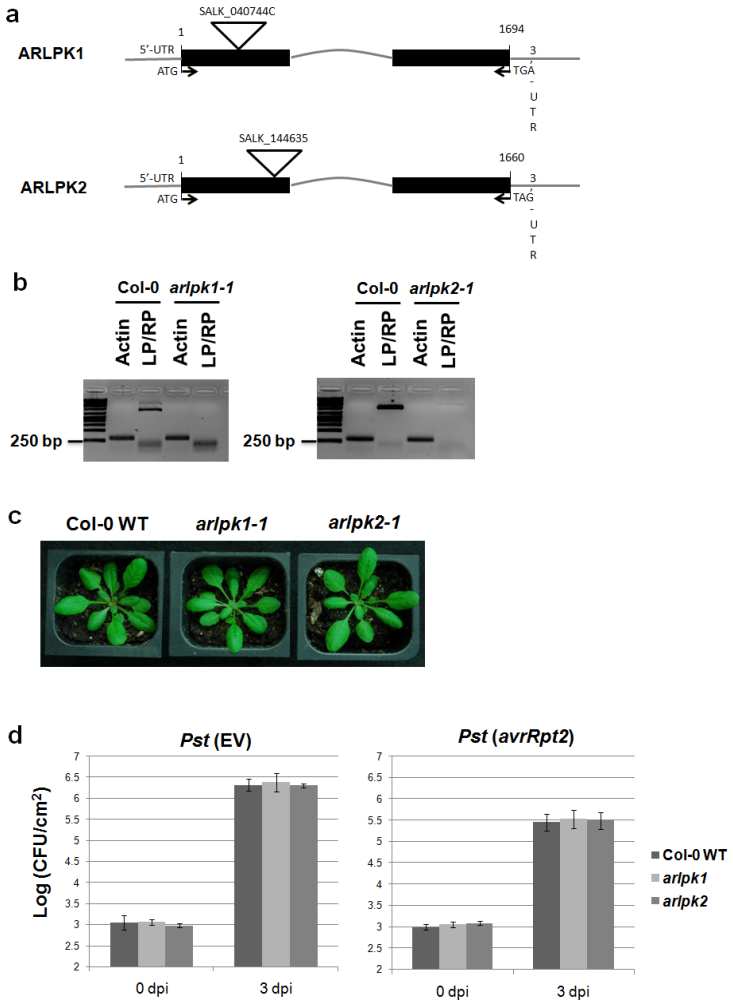


Figure 2.8: Analysis *arlpk1-1* and *arlpk2-1* single mutants.
(a) Gene structure of ARLPK1 and ARLPK2 with *arlpk1-1* (SALK_040744C) and *arlpk2-1* (SALK_144635) T-DNA insertion sites indicated, respectively. Black boxes: exons, curved lines: introns, lines: UTRs, triangles: T-DNA insertion sites. Nucleotide positions are indicated by the numbers.
(b) T-DNA insertions in *arlpk1-1* (SALK_144635) and *arlpk2-1* (SALK_040744) were confirmed by real-time RT-PCR. *Actin* was used as control.
(c) Phenotypes of 4-week-old *arlpk1-1* and *arlpk2-1*mutant plants compared with Col-0 WT plants.
(d) Bacteria growth in *Pst* (EV)- and *Pst* (*avrRpt2*)-infected Col-0 WT, *arlpk1*-2, and *arlpk2-1* mutants. Bacterial inoculum concentration: 5 x 10^5 CFU/ml. Bacterial growth was measured 3 dpi. Error bars represent standard deviation for at least 15 leaf discs.

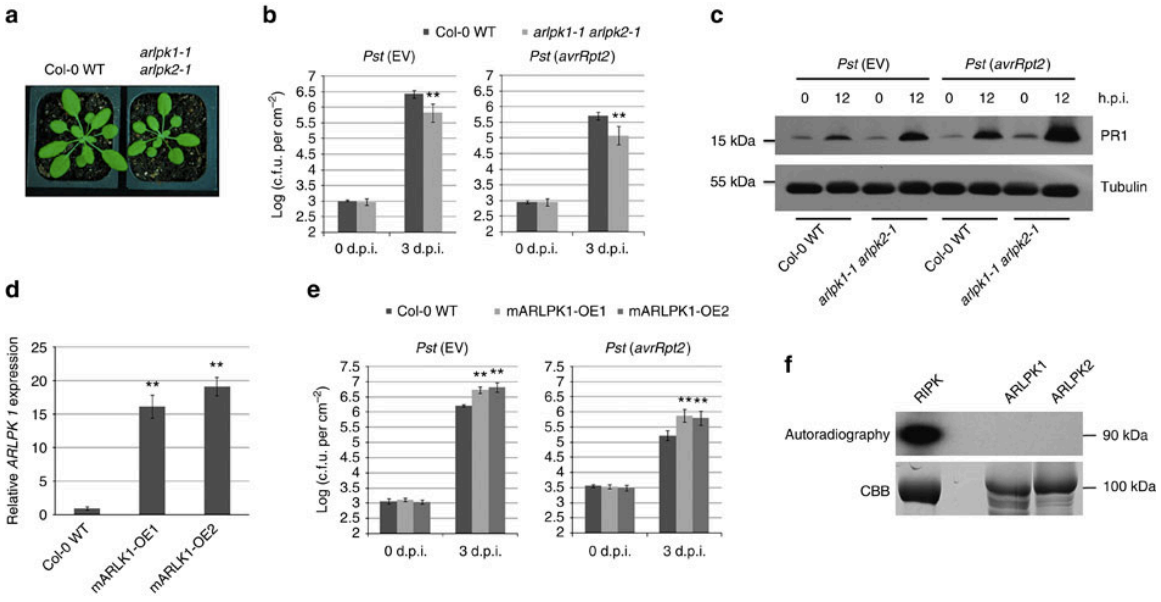


Figure 2.9: Analysis of the *arlpk1-1 arlpk2-1* double mutant.
(**a**) Phenotype of 4-week-old *arlpk1-1 arlpk2-1* double mutants compared with Col-0 WT plants. (**b**) Bacterial growth in *Pst* (EV)- and *Pst* (*avrRpt2*)-infected Col-0 WT and *arlpk1-1 arlpk2-1* double mutants. Bacterial inoculum concentration: 5×10^5 c.f.u. per ml. Bacterial growth was measured at 3 d.p.i. Error bars represent s.d. for at least 15 leaf discs. Similar results were obtained in three biological replicates. ***P* value <0.01 (Student's *t*-test). (**c**) PR1 protein levels were detected in *Pst* (EV)- and *Pst* (*avrRpt2*)-infected Col-0 WT and *arlpk1-1 arlpk2-1* double mutants by western blot using an anti-PR1 antibody. Bacterial inoculum concentration: 1×10^7 c.f.u. per ml. Samples were collected at 0 and 12 h.p.i. α-Tubulin was used as a loading control. Similar results were obtained from two biological replicates. (**d**) Levels of *ARLPK1* transcript in Col-0 WT, mARLPK1-OE1 and mARLPK1-OE2 lines were detected by real-time RT–PCR. Error bars indicate s.d. from three technical replicates. Similar results were obtained in three biological replicates. ***P* value <0.01 (Student's *t*-test). (**e**) Bacterial growth in*Pst* (EV)- and *Pst* (*avrRpt2*)-infected Col-0 WT and mARLPK1-OE plants. Bacterial inoculum concentration: 5×10^5 c.f.u. per ml. Bacterial growth was measured 3 d.p.i. Error bars represent s.d. for at least 15 leaf discs. Similar results were obtained from three biological replicates. ***P* value <0.01 (Student's *t*-test). (**f**) Recombinant MBP-tagged kinase domains of RIPK, ARLPK1 and ARLPK2 proteins were subjected to a radioactive kinase assay and kinase activity was detected using autoradiography. Bottom panel: SDS–PAGE gel stained with coomassie brilliant blue (CBB) demonstrating protein abundance. Similar results were obtained from two biological replicates.

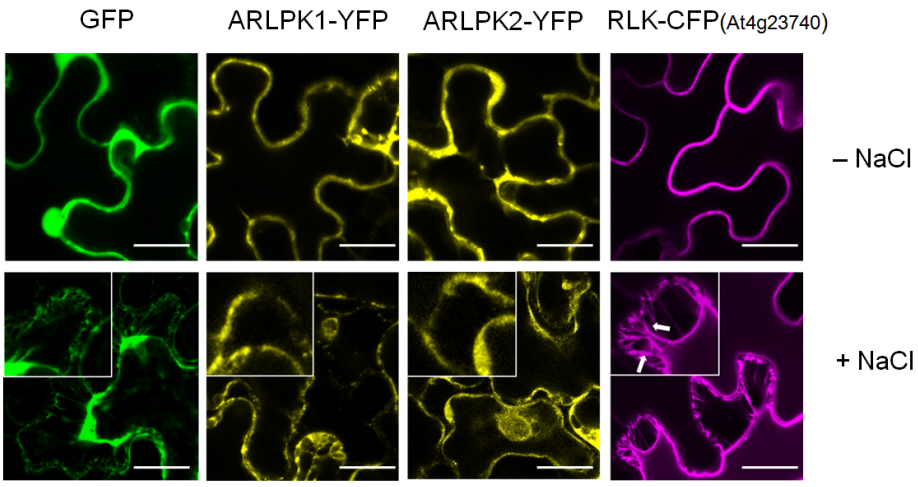


Figure 2.10: ARLPK1 and ARLPK2 localize in the endoplasmic reticulum. Subcellular localization of ARLPK1-YFP and ARLPK2-YFP in *N. benthamiana* was observed at 48 hpi with confocal microscopy. For the plasmolysis treatment, tissue was treated with 5% NaCl for 5-10 min before visualization (+ NaCl), or with water (– NaCl) as a control. GFP empty vector was used as control. RLK-CFP, a known plasma membrane (PM)-localized RLK (At4g23740) was fused to CFP at the C-terminus, was used as a PM-localization control. Arrows indicate Hechtian strands on the bottom panel. Fluorescent images were taken of the middle of the cell. Scale bars: 20 μm.

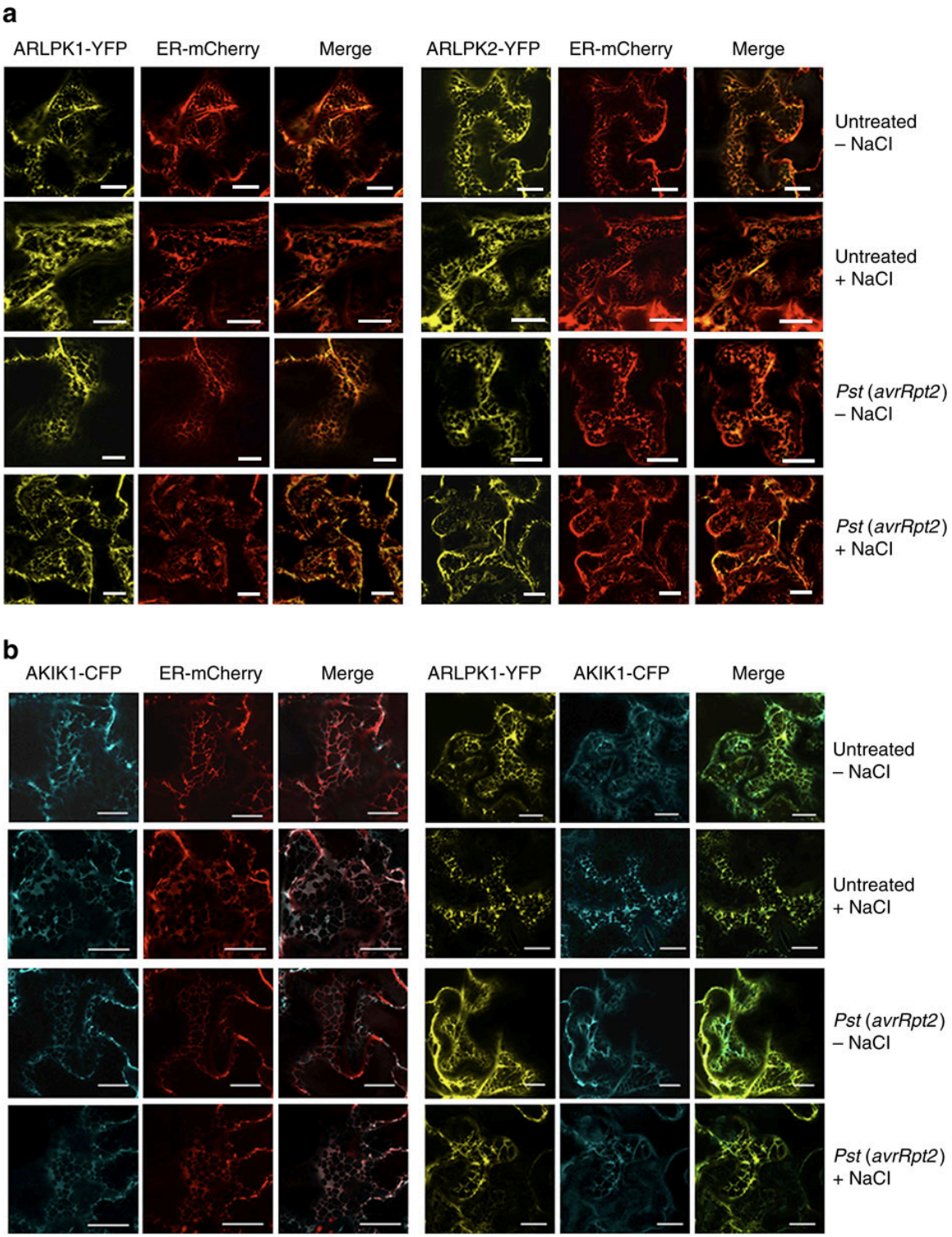

a
ARLPK1-YFP
ER-mCherry
Merge
ARLPK2-YFP
ER-mCherry
Merge
Untreated
– NaCl
Untreated
+ NaCl
Pst (avrRpt2)
– NaCl
Pst (avrRpt2)
+ NaCl
b
AKIK1-CFP
ER-mCherry
Merge
ARLPK1-YFP
AKIK1-CFP
Merge
Untreated
– NaCl
Untreated
+ NaCl
Pst (avrRpt2)
– NaCl
Pst (avrRpt2)
+ NaCl

Figure 2.11: ARLPKs and AKIK1 predominantly localize in the ER.
(**a**) Co-localization of ARLPK1-YFP or ARLPK2-YFP with ER-mCherry in *N. benthamiana* was observed with confocal microscopy. Untreated plants were visualized 60 h after co-infiltration. Treated plants were infected 48 h after co-infiltration with *Pst* (*avrRpt2*) and visualized 12 h.p.i. Bacterial inoculum concentration: 1×10^7 c.f.u. per ml. Fluorescent images of the middle of the cell were taken separately then merged. Samples were visualized without (−NaCl) and with (+NaCl) plasmolysis treatment (5% NaCl for 5–10 min). Scale bars: 20 μm. (**b**) Co-localization of AKIK1-CFP with ER-mCherry and ARLPK1-YFP with AKIK1-CFP in *N. benthamiana* was observed with confocal microscopy. Untreated plants were visualized 60 h after co-infiltration. Treated plants were infected 48 h after co-infiltration with *Pst* (*avrRpt2*) and visualized 12 h.p.i. Tissue was collected for imaging 12 h.p.i. Bacterial inoculum concentration: 1×10^7 c.f.u. per ml. Fluorescent images of the middle of the cell were taken separately then merged. Samples were visualized without (– NaCl) and with (+NaCl) plasmolysis treatment (5% NaCl for 5–10 min). Scale bars: 20 μm.

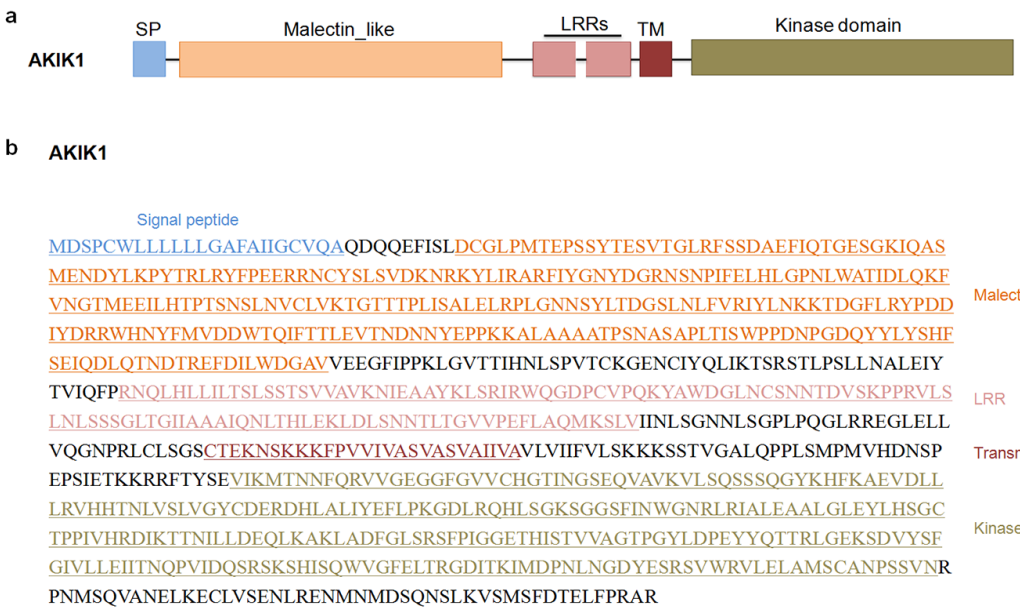


Figure 2.12: AKIK1 is a receptor-like kinase.
(a) Diagram of AKIK1 with important predicted domains indicated. SP (blue box): signal peptide; malectin-like (peach box); LRR (pink box): Leucine-rich repeat; TM (red box): transmembrane domain; kinase domain (brown box).
(b) Amino acid sequence of AKIK1 with signal peptide (blue), malectin-like domain (peach); LRR domains (pink), transmembrane domain (red), and kinase domains (brown) indicated.

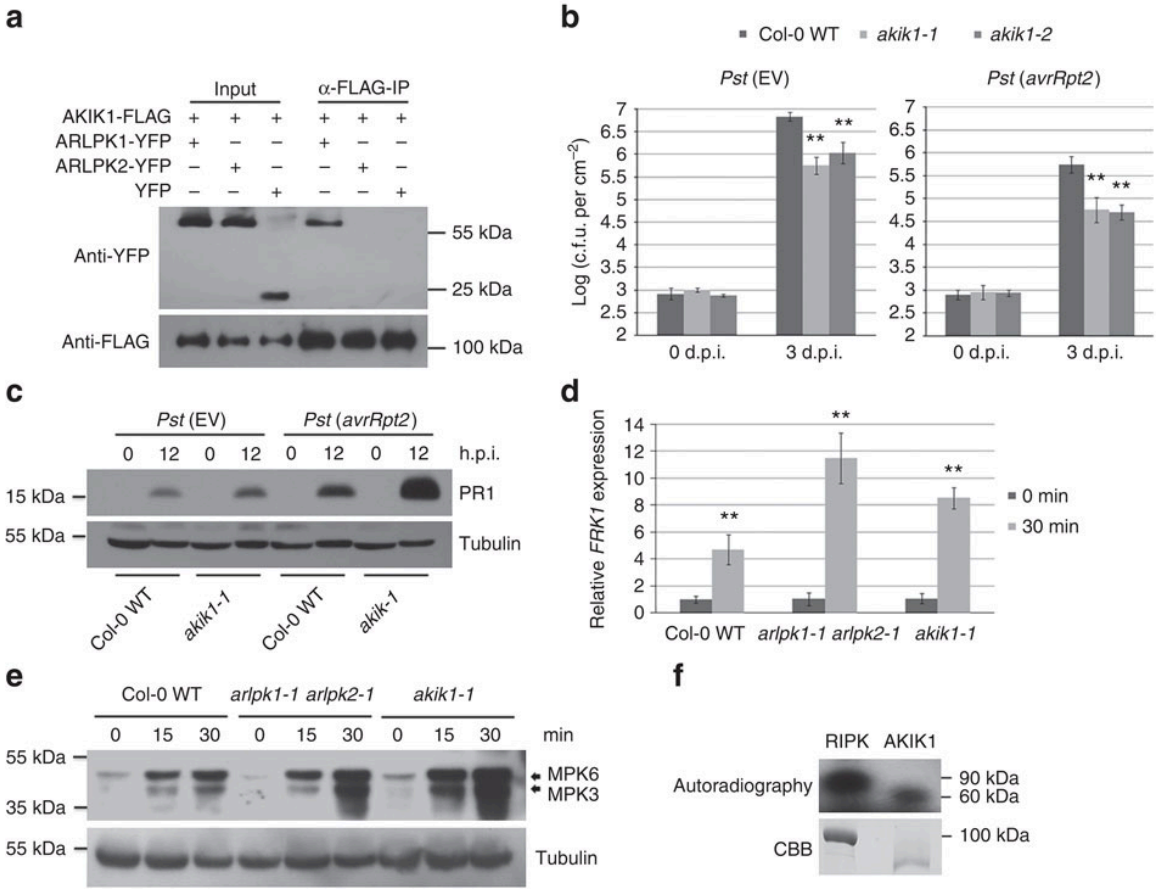


Figure 2.13: ARLPK1 interacts with AKIK1 that is also a negative regulator of disease resistance.

(**a**) AKIK1-FLAG co-IP with ARLPK1-YFP but not with ARLPK2-YFP. Total proteins (input) from *N. benthamiana* extracts were immunoprecipitated with ANTI-FLAG M2 affinity gel, and AKIK1-FLAG and ARLPK1-YFP proteins were detected by western blot using anti-FLAG and anti-YFP antibodies, respectively. Similar results were obtained from three biological replicates. (**b**) The *akik1-1* and *akik1-2* mutants are more resistance to bacterial *Pst* (EV) and *Pst* (*avrRpt2*), as compared with WT plants. Bacterial inoculum concentration: 5×10^5 c.f.u. per ml. Bacterial growth was measured 3 d.p.i. Error bars represent s.d. for at least 15 leaf discs. Similar results were obtained from three biological replicates. ***P* value <0.01 (Student's *t*-test). (**c**) PR1 protein levels in *Pst* (EV)- and *Pst*(*avrRpt2*)-infected Col-0 WT and *akik1-1* mutant were detected by western blot using an anti-PR1 antibody. Bacterial inoculum concentration: 1×10^7 c.f.u. per ml. Leaf tissue was collected 0 and 12 h.p.i. α-Tubulin was used as a loading control. Similar results were obtained from two biological replicates. (**d**) Relative expression levels of *FRK1* in flg22-treated Col-0 WT, *arlpk1-1 arlpk2-1* and *akik1-1* mutants were detected by real-time RT–PCR. Samples were collected 0 and 30 min after treatment. Error bars indicate s.d. from three technical replicates. Similar results were obtained from three biological replicates. ***P* value <0.01

(Student's *t*-test). (**e**) The levels of phosphorylated MPK3 and MPK6 in flg22-treated Col-0 WT, *arlpk1-1 arlpk2-1* and *akik1-1* mutants were detected by western blot using monoclonal rabbit phospho-p44/42 MAPK (Erk1/2) (Thr202/Tyr204)(D13.14.4E) XP antibody. Leaf tissue was collected 0, 15 and 30 min after treatment. α-Tubulin was used as a loading control. Similar results were obtained from three biological replicates. (**f**) Recombinant MBP-tagged RIPK kinase domain and GST-tagged AKIK1 kinase domain were subjected to a radioactive kinase assay and kinase activity was detected using autoradiography. Bottom panel: SDS–PAGE gel stained with coomassie brilliant blue (CBB) demonstrating protein abundance. Similar results were obtained from two biological replicates.

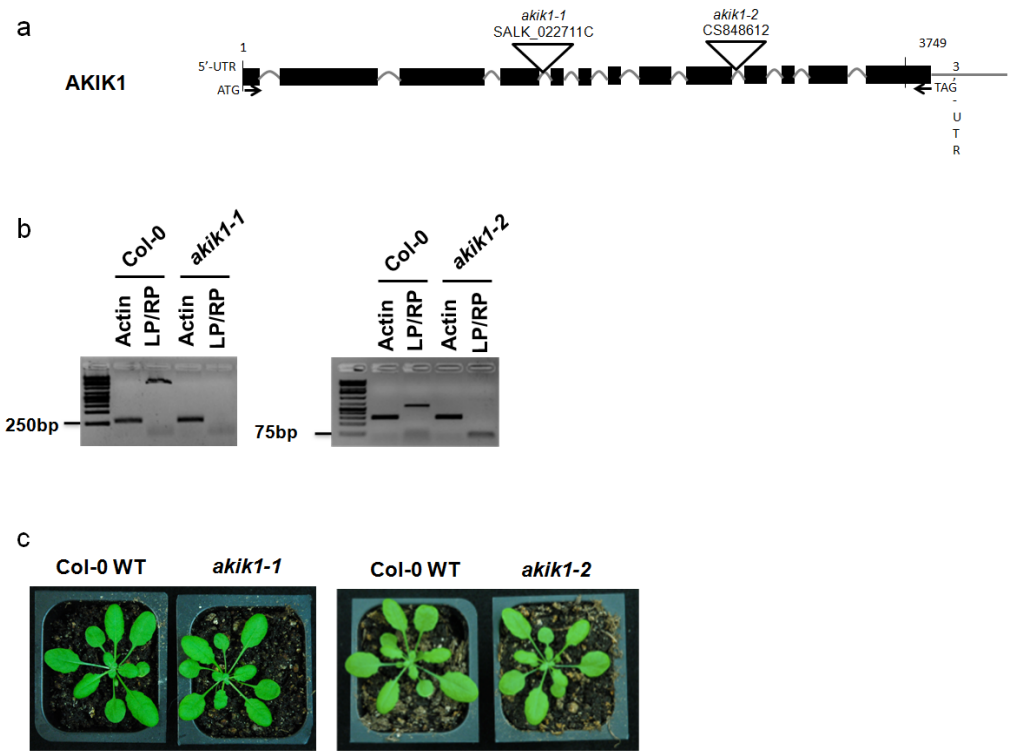


Figure 2.14. Analysis of *akik1-1* and *akik1-2* mutants.
(a) Gene structure of AKIK1 with *akik1-1* (SALK_022711C) and *akik1-2* (CS848612) T-DNA insertion sites indicated. Black boxes: exons, curved lines: introns, lines: UTRs, triangles: T-DNA insertion sites. Nucleotide positions are indicated by the numbers.
(b) T-DNA insertions in *akik1-1* and *akik1-2* were confirmed by real-time RT-PCR. Actin was used as control.
(c) Phenotypes of 4-week-old *akik1-1*and *akik1-2* mutants compared with Col-0 WT plants.

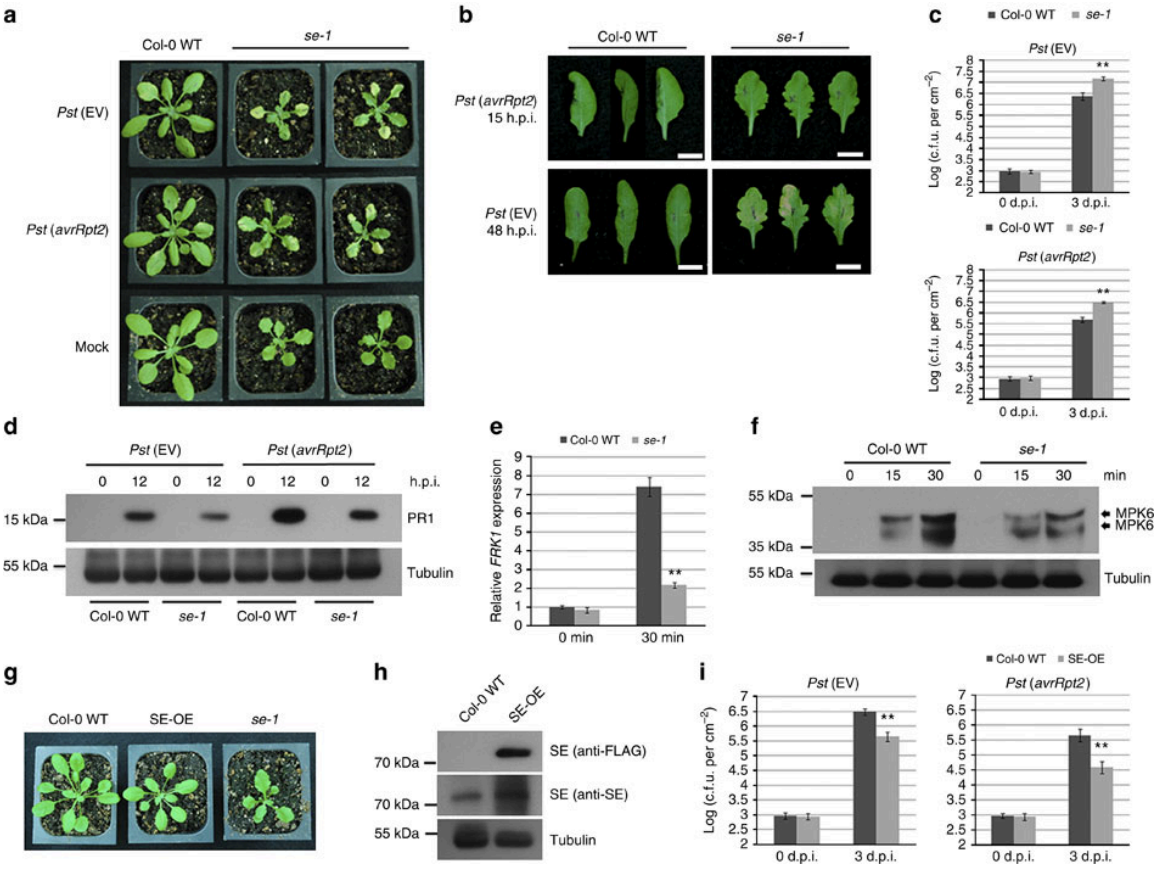


Figure 2.5: SE is a positive regulator of disease resistance.
(**a**) The *se-1* mutant displays enhanced disease susceptibility phenotype after *Pst* (EV) and *Pst* (*avrRpt2*) infection. Bacterial inoculum concentration: 5×10^5 c.f.u. per ml. Photos were taken 3 d.p.i. Mock-treated plants were used as controls. (**b**) The *se-1* mutant shows delayed HR after *Pst* (*avrRpt2*) infection, and enhanced disease phenotype after *Pst* (EV) infection. Pictures were taken 15 h.p.i. of *Pst* (*avrRpt2*) infection and 48 h.p.i. of *Pst* (EV) infection. In all, 16 out of 18 *Pst* (*avrRpt2*)-infected Col-0 WT leaves exhibited HR at 15 h.p.i. under our conditions (three with HR are shown), while only 3 out of 18 of the *se-1* leaves showed HR at 16 h.p.i. (three without HR are shown). A total of 12 out of 15 *Pst* (*avrRpt2*)-infected *se-1* leaves exhibited chlorosis, while only 3 out of 15 Col-0 WT leaves did. Only half of the leaf was inoculated. Bacterial inoculum concentration: 1×10^7 c.f.u. per ml. Scale bar, 10 mm. (**c**) The *se-1* mutant is more susceptible to the infection of *Pst* (EV) and *Pst* (*avrRpt2*) than Col-0 WT. Bacterial inoculum concentration: 5×10^5 c.f.u. per ml. Bacterial growth was measured 3 d.p.i. Error bars represent s.d. for at least 15 leaf discs. Similar results were obtained from three biological replicates. ***P* value <0.01 (Student's *t*-test). (**d**) PR1 protein levels in *Pst* (EV)- and *Pst* (*avrRpt2*)-infected Col-0 WT and *se-1* mutants were detected by western blot using an anti-PR1 antibody. Bacterial inoculum concentration: 1×10^7 c.f.u. per ml. Leaf tissue was collected 0 and 12 h.p.i. α-Tubulin was used as a loading control. Similar results were obtained from two biological

replicates. (**e**) Relative expression levels of *FRK1* in flg22-treated Col-0 WT and *se-1* mutant were detected by real-time RT–PCR. Leaf tissue was collected 0 and 30 min after treatment. Error bars indicate s.d. from three technical replicates. Similar results were obtained in three biological replicates. ***P* value <0.01 (Student's *t*-test). (**f**) MPK3 and MPK6 protein levels in flg22-treated Col-0 WT and *se-1* mutant were detected by western blot using monoclonal rabbit phospho-p44/42 MAPK (Erk1/2) (Thr202/Tyr204)(D13.14.4E) XP antibody. Samples were collected 0, 15 and 30 min after treatment. α-Tubulin was used as a loading control. Similar results were obtained from two biological replicates. (**g**) Phenotypes of 4-week-old FLAG-tagged SE overexpression lines (SE-OE), *se-1* mutants and Col-0 WT plants. (**h**) SE protein levels were detected in Col-0 WT and FLAG-tagged SE-OE lines by western blot using anti-FLAG and anti-SE antibodies. α-Tubulin was used as a loading control. Similar results were obtained from two biological replicates. (**i**) Bacterial growth in *Pst* (EV)- and *Pst* (*avrRpt2*)-infected Col-0 WT and SE-OE lines. Bacterial inoculum concentration: 5×10^5 c.f.u. per ml. Bacterial growth was measured 3 d.p.i. Error bars represent s.d. for at least 15 leaf discs. Similar results were obtained from three biological replicates. ***P* value <0.01 (Student's *t*-test).

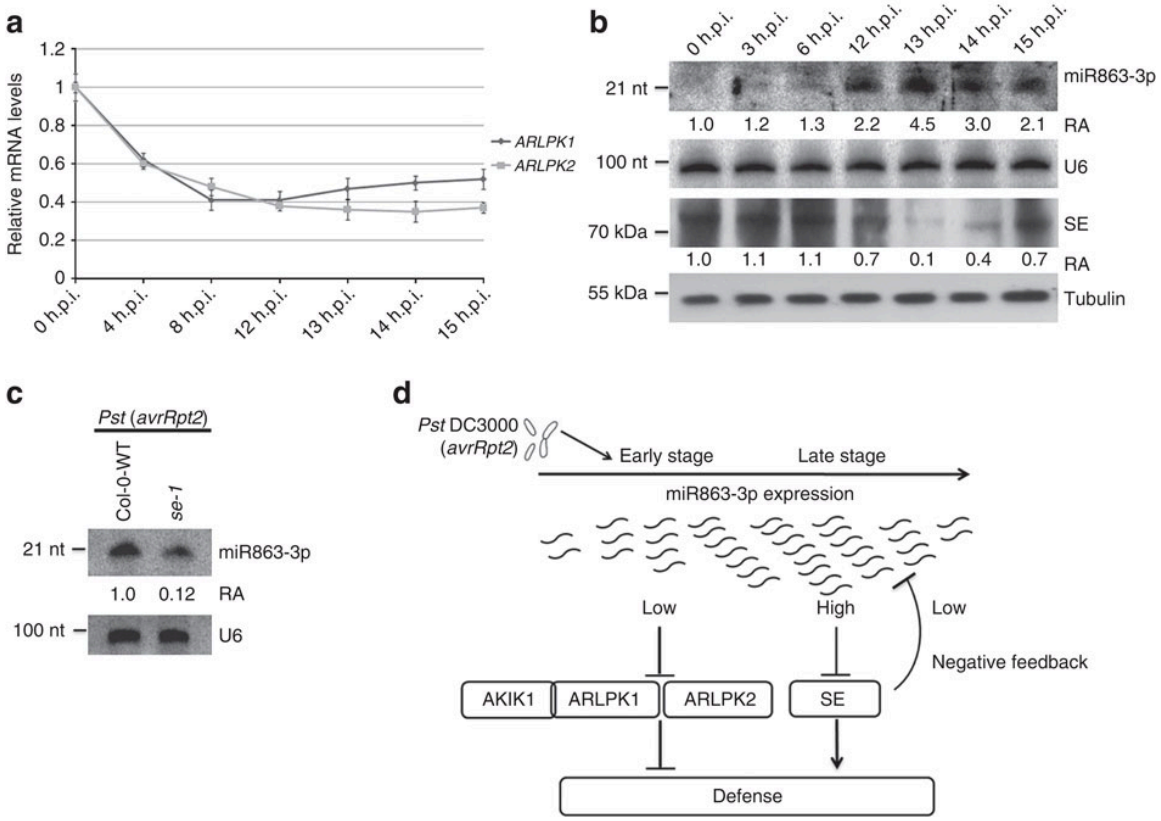

a
Relative mRNA levels
1.2
1
0.8
0.6
0.4
0.2
0
0 h.p.i.
4 h.p.i.
8 h.p.i.
12 h.p.i.
13 h.p.i.
14 h.p.i.
15 h.p.i.
ARLPK1
ARLPK2
b
0 h.p.i.
3 h.p.i.
6 h.p.i.
12 h.p.i.
13 h.p.i.
14 h.p.i.
15 h.p.i.
21 nt
miR863-3p
1.0 1.2 1.3 2.2 4.5 3.0 2.1
RA
100 nt
U6
70 kDa
SE
1.0 1.1 1.1 0.7 0.1 0.4 0.7
RA
55 kDa
Tubulin
c
Pst (avrRpt2)
Col-0-WT
se-1
21 nt
miR863-3p
1.0 0.12
RA
100 nt
U6
d
Pst DC3000
(avrRpt2)
Early stage
Late stage
miR863-3p expression
Low
High
Low
Negative feedback
AKIK1
ARLPK1
ARLPK2
SE
Defense

Figure 2.16: miR863-3p regulates ARLPK1, ARLPK2 and SE in a time-dependent manner.

(**a**) Time course of relative expression levels of *ARLPK1* and *ARLPK2* transcripts in *Pst* (*avrRpt2*)-infected Col-0 WT plants were detected by real-time RT–PCR. Bacterial inoculum concentration: 5×10^6 c.f.u. per ml. Error bars indicate s.d. from three technical replicates. Similar results were obtained in three biological replicates. ***P* value <0.01 (Student's *t*-test). (**b**) Time course of miR863-3p levels in *Pst* (*avrRpt2*)-infected Col-0 WT plants was detected by northern blot analysis. U6 was used as a loading control. SE protein levels in *Pst* (*avrRpt2*)-inoculated Col-0 WT plants were detected by western blot analysis using an anti-SE antibody. α-Tubulin was used as a loading control. Relative abundance (RA) levels are indicated. Bacterial inoculum concentration: 5×10^6 c.f.u. per ml. Similar results were obtained from two biological replicates. (**c**) miR863-3p levels in *Pst* (*avrRpt2*)-infected Col-0 WT and *se-1* mutants were detected by northern blot analysis. U6 was used as a loading control. Bacterial inoculum concentration: 1×10^7 c.f.u. per ml. Samples were collected 14 h.p.i. RA levels are indicated. Similar results were obtained from three biological replicates. (**d**) A model of miRNA863-3p downregulation of targets after infection with *Pst*(*avrRpt2*). During the early stage of infection, miR863-3p levels are upregulated and suppress ARLPK1 and ARLPK2 to enhance disease resistance. ARLPK1 interacts with LRR-RLK AKIK1 to negatively regulate defence. During the later stage of infection, miR863-3p downregulates SE. Downregulation of SE results in a decrease in miR863-3p levels, forming a negative feedback loop to suppress defence responses.

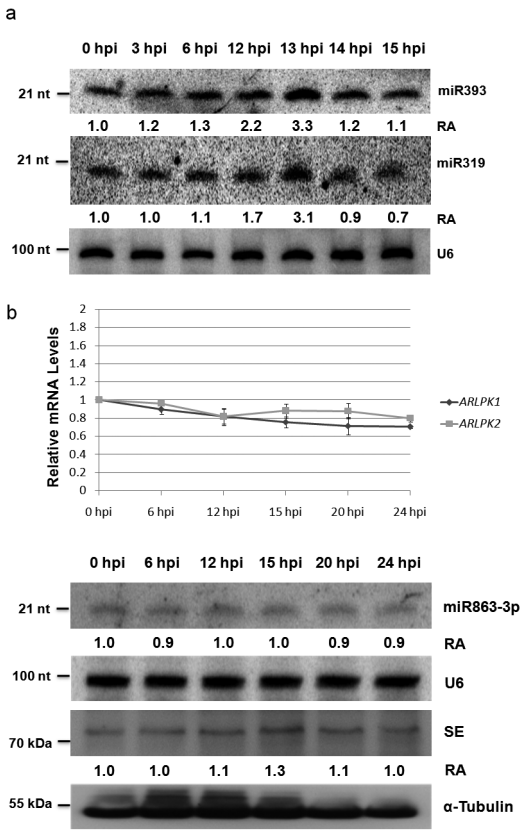


Figure 2.17. Expression levels of miR393 and miR319 and *ARLPK1*, *ARLPK2*, and SE in Col-0 WT plants infected with various strains of *Pst.*
(a) Time course of miR393 and mR319 levels in *Pst* (*avrRpt2*)-infected Col-0 WT plants were detected by Northern blot analysis. U6 was used as loading control. Relative abundance (RA) levels are indicated. Bacterial inoculum concentration: 5 x 10^6 CFU/ml. (b) Top: Time course of relative expression levels of *ARLPK1* and *ARLPK2* transcripts in *Pst* (EV)-infected Col-0 WT plants were detected by real-time RT-PCR. Bacterial inoculum concentration: 5 x 10^6 CFU/ml. Error bars indicate standard deviation from three technical replicates. Bottom: Time course of miR863-3p levels in *Pst* (EV)-infected Col-0 WT plants were detected by Northern blot. U6 was used as loading control. SE protein levels in *Pst* (EV)-inoculated Col-0 WT plants were detected by Western blot using an anti-SE antibody. α-Tubulin was used as a loading control. Relative abundance (RA) levels are indicated. Bacterial inoculum concentration: 5 x 10^6 CFU/ml.

Table 2: Primers used in this study.

Primer Name	Sequence
mARLPK1-F	5'-CTTTCAGCTTGCAATGAGCTGCTGTAGCCCTTCGCCTACTCTTAGG-3'
mARLPK1-R	5'-GAG TAGGCGAAGGGCTACAGCAGCTCATTGCAAGCTGAAAGTACTCG-3'
mARLPK2-F	5'-TTTTCAGCTTGCAATGAGCTGCTGTAGCCCTTCGCCTTCTCTTAGG-3'
mARLPK2-R	5'-GAGAAGGCGAAGGGCTACAGCAGCTCATTGCAAGCTGAAAATACTT-3'
mSE-3'UTR-F	5'-CTTTTGATGTCTGCGGGACTTCCCATACACCTTTTCACTCACTAA-3'
mSE-3'UTR-R	5'-AAGTATTGATAACAAACAATGTGGATAAAACGCATTATTCAATACAAG-3'
ARLPK1-R 5'RACE	5' TCATTTCCTGATCTCTTCAAGCTTCC 3'
ARLPK2-R 5'RACE	5' CTAAAATTTCCCAATCTCTTCAAG 3'
ACTIN2-F	5'-AGTGGTCGTACAACCGGTATTGT-3'
ACTIN2-R	5'-CTTGCCCATCGGGTAATTCATAG-3'
ARLPK1_OE-F	5'-CACCATGAGAAAATCCCATTTGGTAAA-3'
ARLPK1_OE-R	5'- TCATTTCCTGATCTCTTCAAGCTTC-3'
ARLPK2-OE-F	5'-CACCATGAGAAAATCTCTACTTCTAAC-3'
ARLPK2_OE-R	5'-CTAAAATTTCCCAATCTCTTCAAGTTT-3'
ARLPK1-qPCR-F	`5'-TTATTAGGAGATGTCTGAAGGAT-3'
ARLPK1-qPCR-R	5'-TCATTTCCTGATCTCTTCAAGCT-3'
ARLPK2-qPCR-F	5'-TGAGGAATGCTGTTCTTGATC-3'
ARLPK2-qPCR-R	5'-CTAAAATTTCCCAATCTCTTCAA-3'
AT5G59650-OE-F	5'-CACCATGGATAGTCCTTGTTGGCTTTTGCTG-3'
AT5G59650-OE-R	5'-CTACCTTGCCCTCGGAAACAA-3'
FRK1-F	5'-TGCACTTACCCTCCTTCG-3'
FRK1-R	5'-GACAGTAGAAGCCGGTTGGT-3'
LBb1.3	5'-ATTTTGCCGATTTCGGAAC-3'
SALK_022711-LP	5'-TTTGTTCCACATAGGTACCCG-3'
SALK_022711-RP	5'-GGAAGGGGACCACTAAGATTG-3'
CS848612-LP	5'-ACCTCCACTGAGTATGCCAATG-3'
CS848612-RP	5'-ATCCAGGAGTACCAGCAACCAC-3'
MIR863-3P-OE-F	5'-CACCAGAACCCGATGGAGACCAACA-3'
MIR863-3P-OE-R	5'-CAAACCCGTCAGCTTCCAGA-3'
MIR863-3P-probe	5'-ATTATGTCTTGTTGCTCTCAA-3'
MIR863-5P-probe	5'-TATTGAGATCAACAAGACATA-3'
SALK_144635-LP	5'-CCCTTACAAGGCCAAGAAATC-3'
SALK_144635-RP	5'-AGCTGTGTGGTTCTCTTTTGG-3'
SALK_040744C-LP	5'-TTTTGGGAGGTGATTTCGTAC-3'
SALK_040744C-RP	5'-AATCTTTTTCAGCTTCCTCGC-3'
SERRATE-qPCR-F	5'-ATGATCCTAATGCTCCAGGAG-3'
SERRATE-qPCR-R	5'-CGTCTAGGATCTTGTCTAAAG-3'

CHAPTER THREE

Polymerase IV-mediated RNA-directed DNA Methylation Regulates Systemic Acquired Resistance

ABSTRACT

In plants, DNA methylation plays an important role in disease resistance and transgenerational priming, and many mutants defective in RNA-directed DNA methylation (RdDM) components show altered disease phenotypes. So far, DNA methylation has not been implicated in systemic acquired resistance (SAR). Columbia-0 wild-type (WT) plants show increased resistance to bacterial pathogen *Psuedomonas* in upper leaves 3 d after pre-treatment of lower leaves with *Pseudomonas syringae* pv. *maculicoli* (*Psm*), a typical manifestation of SAR. We show that the *Arabidopsis polymerase IV* (*pol IV*) mutant is more resistant to virulent and avirulent bacterial infection compared to Col-0 WT plants, yet it does not exhibit SAR. We performed whole genome bisulfite sequencing to find differentially methylated regions (DMRs) specific to SAR that are not present in *pol IV*. We obtained a short list of genes that had DMRs located within 250 nt (upstream or downstream) of the transcriptional start site and at least three or more DMRs. From that list, we chose to further analyze a gene *SCR-LIKE* (*SCRL5*, At1g60987). In the upper leaves, Col-0 WT plants had increased DNA methylation directly upstream of a gene *SCR-LIKE 5* (*SCRL5*) after pre-treatment

of the lower leaves, which was concomitant with decreased relative gene expression. However, *pol IV* was lacking all methylation marks upstream of *SCRL5* and had higher *SCRL5* expression compared Col-0 WT after pre-treatment. Furthermore, Col-0 WT transgenic plants overexpressing *SCRL5* were attenuated in SAR. Further analysis in Col-0 WT plants showed that after infection with *Pst* strains in local tissue, *SCRL5* is upregulated. It is possible that SCRL5 is required after local inoculation with *Pst*, but somehow plays a negative role in SAR.

INTRODUCTION

DNA methylation is involved in many plant processes and is associated with changes in gene expression. In plants, DNA methylation occurs in three contexts, CG, CHG, and CHH (H being any base other than G), and is maintained, newly added (*de novo* methylation), and removed by the cooperative action of many different proteins. Small 24-nucleotide (nt) RNAs can direct DNA methylation in a canonical RNA-directed DNA methylation (RdDM) pathway involving Polymerase IV (Pol IV), Pol V, and many other associated proteins. In short, Pol IV transcribes a single-stranded transcript that is processed by RNA-DEPENDENT RNA POLYMERASE 2 (RDR2) into dsRNA that is then processed by DICER-LIKE 3 (DCL3) into 24-nt si-RNAs. One strand of the siRNA duplex associates with ARGONAUTE 4 (AGO4) and interacts with a nascent Pol V transcript. This association recruits other proteins, including DOMAINS REARRANGED METHYLTRANSFERASE (DRM2), which catalyzes DNA methylation at CHH sites. RdDM has a small role in silencing of transposons, as this is

mainly done through the DECREASED DNA METHYLATION 1 (DDM1) pathway, and is important for dynamic methylation in response to environmental changes (Matzke et al., 2015; Matzke and Mosher, 2014).

Many studies have shown *Arabidopsis thaliana* undergoes widespread DNA methylation changes during bacterial infection, and that mutants disrupted in global methylation have altered responses to virulent and avirulent bacterial pathogen *Pseudomonas syringae* pv. *tomato* (*Pst*) infection, salicylic acid (SA) application, fungal infection, and elicitor flg22 treatment. Most point to a negative role of DNA methylation in defense (Dowen et al., 2012; Lopez et al., 2011; Luna et al., 2012; Pavet et al., 2006; Yu et al., 2013). These studies have been detailed in Chapter 1—Introduction of this dissertation. There have been conflicting results regarding the role of Polymerase IV (Pol IV), possibly due to differences in infection and plant conditions (Dowen et al., 2012; Lopez et al., 2011). Here, we show that *pol IV* mutants are affected in local and systemic defense against bacterial pathogens: It has enhanced resistance to local infections with virulent and avirulent *Pst* and virulent *Pseudomonas syringae* pv. *maculicoli* (*Psm*). From whole genome bisulfite sequencing, we obtained a short list of genes with differentially methylated regions (DMRs) within 250 nt of the transcriptional start sites. One of the genes *S-LOCUS RECEPTOR-LIKE 5* (*SCRL5*, At1g60987), had increased CHH in Col-0 WT plants after pre-treatment with *Psm*, while *pol IV* was missing methylation of all cytosine contexts upstream of *SCRL5*. This DNA methylation is negatively correlated with the expression of *SCRL5* in Col-0 WT plants. Further

analysis shows that SCRL5 may have a positive role in local disease resistance, but has a negative role in SAR.

RESULTS

Systemic acquired resistance is abolished in Polymerase IV

Since previous studies showed that several mutants defective in RdDM components exhibited enhanced disease resistance (detailed in Chapter 1—Introduction of this dissertation and Table 1), we decided to investigate whether they could be altered in SAR phenotype. First, we confirmed the local disease response phenotypes of several RdDM mutants—*ddc*, *pol IV*, and *pol V*—to virulent *Pst*. The triple mutant *ddc* was more resistant to *Pst* (EV), consistent with previous studies (Figure 3.1a) (Dowen et al., 2012; Yu et al., 2013). The *pol IV* mutant also showed enhanced resistance; whereas the *pol V* mutant was the same as Col-0 WT (Figure 3.1b). This was similar to the findings in Dowen, et al. However, a different study showed opposite results, that *pol IV*, but not *pol IV* is indispensable for defense (Lopez et al., 2011). This prompted us to look further into the role of Pol IV and Pol V using other bacterial strains. We found that *pol IV*, but not *pol V*, shows enhanced resistance to *Pst* (*avrRpt2*) (Figure 3.1c) and mild increased resistance to *Pst* (*avrRpm1*) (Figure 3.1d). *pol IV* also has mild increased resistance to virulent *Psm* (Figure 3.1e). Altogether, our results confirmed previous studies that RdDM mutants have altered disease phenotypes, and that Pol IV is needed for disease resistance.

During pathogen infection, widespread hyper- and hypomethylation changes of all three contexts occur in the local tissue (Dowen et al., 2012). RdDM is mediated by 24-nt siRNAs, and studies have shown that mobile 24-nt siRNAs can direct transcriptional gene silencing in certain cases (Lewsey et al., 2016; Melnyk et al., 2011; Slotkin et al., 2009). However, it is not known whether pathogen-induced dynamic methylation changes can be carried to systemic tissue. Thus, we next looked at the SAR response in RdDM mutants. To do this, we pre-treated the lower leaves of plants with either a $MgCl_2$ (mock) solution or *Psm* and inoculated the upper leaves with *Psm* 3 d later. We then measured bacterial growth in the upper leaves 3 days post infection (dpi). We chose to pre-treat the plants with virulent *Psm* because it produced a more enhanced SAR effect in Col-0 WT plants compared to pre-treatment with virulent *Pst* DC3000 or avirulent *Pst* DC3000 containing *avRrpt2* (data not shown). In agreement with a previous study, Col-0 WT plants exhibited SAR (Figure 3.2a-c), while the *npr1* mutant, which is impaired in SAR, did not (Figure 3.2a) (Cao et al., 1994; Cao et al., 1997; Dong, 2004). To our surprise, the *pol IV* mutant, completely lost SAR (Figure 3.2b), while the *ddc* triple mutant exhibited reduced, but not completely lost, SAR (Figure 3.2c).

SAR is associated with the upregulation of marker gene PR1, so we measured the relative expression of PR1 in upper leaves of mock or Psm pre-treated RdDM mutants by real-time RT-PCR. As expected, Col-0 WT showed greater than 50-fold increased relative PR1 expression. This was not seen in the *pol IV* mutant, and in fact, the relative expression of PR1 in the *Psm* pre-treated plants was even lower than in the

mock pre-treated plants. The *ddc* mutant showed largely reduced induction of PR1 expression (Figure 3.2d).

Altogether, this data shows that *pol IV* cannot be induced by *Psm* to exhibit SAR and points to a possible role of methylation differences specific to *pol IV* that inhibits SAR, or a role of 24-nt hc-siRNAs that are missing in *pol IV* but not the other RdDM mutants that is needed for SAR. It has been suggested that there is a mechanistic separation between local and systemic resistance, and that some factors predominantly function in SAR (Breitenbach et al., 2014).

SCR-LIKE 5 **is methylated upstream of transcriptional start site in upper leaves during SAR in Col-0 WT but not** ***pol IV*** **plants**

We decided to focus on the *pol IV* mutant to uncover genes that are differentially methylated during SAR. To do this, we conducted whole genome bisulfite sequencing on Col-0 WT and *pol IV* plants in order to look at dynamic methylation specific to SAR that does not occur in *pol IV*. We either pre-treated the lower leaves of plants with mock solution (M) or *Psm*. We collected and sequenced the upper leaves 24 hours post infection (hpi), yielding a total of four treatments: M-M, Psm-M, M-Psm, and Psm-Psm (with the lower leaves treatment indicated first and the upper leaves treatment indicated second). A simple schematic of the treatments is shown in Figure 3.3.

To search for differentially methylated regions, the treatments were compared as such: M-Psm (control) vs. Psm-M and M-Psm (control) vs. Psm-Psm. It should be noted that the M-Psm vs. Psm-Psm comparison looks at DNA methylation changes due to

SAR and also local infection of the upper leaves. Thus, the changes during local infection may mask any previous changes due to pre-treatment of lower leaves. However, because our SAR bacterial growth assays involve secondary infection of the upper leaves, we wanted to capture the methylome even in these treatments.

We only looked at genes in which the DMRs were located ≤ 250 nt upstream of the transcriptional start site (TSS), in order to find genes that would most likely be affected by the changes in methylation. We also focused mainly on CHH methylation, since the RdDM *pol IV* mainly catalyzes CHH methylation. With a cut-off of three or more DMRs, we obtained a list of 14 genes with these criteria. One of the genes, *SCRL5* harbors a DMR just around 100 nt upstream its TSS in both the M-M vs. Psm-M as well as the M-Psm vs. Psm-Psm comparison in the Col-0 WT samples. DNA methylation increased after pre-treatment of the lower leaves with *Psm*. Interesting, the DNA methylation levels are lower when the upper leaves are treated with *Psm* compared to M (comparing M-M vs. M-Psm and Psm-M vs Psm-Psm). However, in all *pol IV* treatments, there was no methylation of any contexts upstream of SCRL5. Methylation in the CG context was not affected in all the treatments, as methylation in this context is predominantly maintained by factors not in the RdDM pathway. However, methylation in the CHG context also increased after pre-treatment of the lower leaves with *Psm* compared to mock pre-treatment (Figure 3.4a). While, two biological replicates for each treatment was sequenced, there are some expected differences between the replicates. For one, it may be due to the quality of that specific sample, for example in the "Col-0 WT ES-M 2" (Figure 3.4a).

Next, we looked at whether the changes in DNA methylation affected the relative expression of *SCRL5* using real-time RT-PCR. In Col-0 WT, *SCRL5* expression in upper leaves is lower when plants are pre-treated with *Psm* compared to mock (comparing M-M vs. M-Psm and Psm-M and Psm-Psm), and *SCRL5* expression is higher in the upper leaves infected with *Psm* compared to mock, when the lower leaves were mock- or *Psm*-treated (comparing M-M vs. M-Psm and Psm-M vs. Psm-Psm). This suggests that there is a negative correlation between DNA methylation and *SCRL5* expression. The fact that *pol IV* expression is higher than Col-0 in M-M and Psm-M treatments also supports this (Figure 3.4c). However, in the *pol IV* mutant, expression of SCRL5 is also lower in the Psm-M than in the M-M tissue, and expression is higher in Psm-Psm compared to M-Psm, similar to Col-0 WT (Figure 3.4c). Thus, there may be another level of control besides DNA methylation governing the expression of *SCRL5*. Furthermore, the *Psm* inoculation in the upper leaves does seem to mask the methylation and corresponding expression changes laid down from the primary infection of the lower leaves.

SCRL5 plays a complex role in plant defense

The *SCRL5* gene is a small (11 kDa), cysteine rich, secreted protein that is similar to S LOCUS CYSTEINE-RICH (SCR), a pollen coat protein that interacts with the female S-locus receptor kinase (SRK) to determine pollen self-incompatibility specificity in *Brassica* (Kemp and Doughty, 2007; Schopfer et al., 1999). SCRL5 has a signal peptide

and a defensin-like sequence containing four disulfide bonds (Silverstein et al., 2005) (Figure 3.5a).

The gene expression data in the above four treatments seems to indicate that SCRL5 may play a negative role in SAR, but a positive role in local resistance. In order to test this, we generated Col-0 WT and *pol IV* transgenic plants overexpressing *SCRL5*. To avoid altering the function of such a small protein, we chose to not use a tag for overexpression. Thus, we tested for SCRL5 expression by real-time RT-PCR, and we chose lines with the highest relative *SCRL5* expression for Col-0 WT (Col-0 SCRL5 OE lines #10 and #11) and for *pol IV* (*pol IV* SCRL5 OE lines #16 and #20) (Figure 3.5b) for analysis. Compared to their respective WT plants, the four-week-old overexpression lines were slightly smaller, the mature plants were shorter in stature and had fewer and smaller siliques (data not shown). Some T3 lines did not yield any viable seeds. The *SCRL5* overexpression lines had higher bacterial titers than their respective WT plants (comparing all the mock pre-treated plants). The Col-0 SCRL5 OE lines exhibited attenuated SAR compared to Col-0 WT. In the *pol IV* overexpression lines, SAR was still attentuated (Figure 3.5c).

Since the relative expression of *SCRL5* was higher in the Col-0 WT M-Psm treatment compared to M-M, we asked whether *SCRL5* may also have a role in local disease response. We found that *SCRL5* is upregulated by infection with *Pst* (EV) and *Pst* (*hrcC*-) over a course of 24 hpi, but only very slightly by infection with *Pst* (*avrRpt2*). Altogether, this data suggests that SCRL5 may have a negative role in SAR

initiated by *Psm*, but it also may have a positive role in local PTI, but not RPS2-mediated ETI.

The available T-DNA insertion lines for *SCRL5* that I examined are not knock-out lines (data not shown). *SCRL5* is located in a gene cluster with several other *SCR-LIKE* genes, two of which have a high percentage of amino acid identity with *SCRL5:* SCRL4 (~70%) and SCRL6 (~60%) (Vanoosthuyse et al., 2001). These genes are likely to have functional redundancy. Thus, I have generated separate RNAi knock-down lines knocking out SCRL5 only, two of the genes, and all three genes, which are in the process of seed collection and selection. More studies need to be done to further understand the functional role of SCRL5 in plant immunity (discussed in the next section).

DISCUSSION

During infection, plants undergo massive gene reprogramming to initiate and control defense against the pathogen. Bacterial infection triggers widespread changes in the host DNA methylation status, and data suggests that DNA methylation plays a negative role in defense (Dowen et al., 2012; Yu et al., 2013). We found that the *pol IV* mutant has enhanced local resistance (Figure 3.1) but has completely lost SAR after *Psm* pre-treatment (Figure 3.2). We performed whole genome bisulfite sequencing to search for DMRs involved in SAR that are lost in *pol* IV. We obtained a short list of genes with three or more DMRs within a 250 nt of the TSS. Many of these genes are unknown proteins, and *SCRL5* had the most DMRs; thus we decided to focus on SCRL5. In Col-0

WT plants, after pre-treatment of lower leaves with *Psm*, we saw increased CHH and CHG methylation directly upstream of SCRL5, along with decreased relative expression (Figure 3.4). Overexpression of SCRL5 in Col-0 WT also attenuated SAR (Figure 3.5c), suggesting SCRL5 may play a negative role in SAR. On the other hand, the higher expression of SCRL5 in Col-0 WT M-Psm vs. M-M treatments (Figure 3.4) and the upregulation of SCRL5 after infection with *Pst* (EV) and *Pst* (*hrcC*-) after 24 hpi suggest that SCRL5 may play a positive role in local PTI (Figure 3.5). The discrepancy may also be due to the timing. While we tested the short-term (24 hpi) response of SCRL5 in local infection, we looked at upper leaf SCRL5 expression 4 d after pre-treatment of the lower leaves. Analysis of the methylation and expression of SCRL5 in both the lower and upper leaves over a time course may reveal a better picture of the dynamic activity of SCRL5 resulting from DNA methylation.

In the *pol IV* mutant, there were no methylation marks of any contexts upstream of *SCRL5*. *SCRL5* expression was higher in *pol IV* than in Col-WT, though its expression did decrease after pre-treatment with *Psm* (in M-M vs M-Psm comparison), suggesting SCRL5 may also be controlled by factors other than DNA methylation (Figure 3.4).

In order to understand the function of SCRL5, current and future work will focus on examining local disease resistance phenotypes in these SCRL5 overexpression lines, analysis of artificial RNAi lines knocking-down SCRL5, as well as its close homologues SCRL4 and SCRL6, in both Col-0 and *pol IV* plants (these lines have been generated

and are in the process of selection). Bisulfite PCR sequencing of the DMR region upstream of SCRL5 in *ddc* may also reveal whether it plays a role in SAR in this mutant.

In *Arabidopsis thaliana,* inactivation of SCR and SRK genes are thought to have led to the self-fertile feature of this species (Kusaba et al., 2001; Sherman-Broyles et al., 2007). A previous search for possible ligands for the S gene family group of receptor-like kinases turned up a family of 29 *SCRL* genes, in which the majority are predicted to be secreted and the cysteine residues (which form disulfide bonds to increase stability in the extracellular environment) are mostly conserved (Vanoosthuyse et al., 2001). Yeast two-hybrid could be used to find possible interactors of SCRL5, focusing first on kinase receptors.

Defensins are small, cysteine-rich, peptides the function as antimicrobial compounds in mammals, insects, and plants (De Coninck et al., 2013; Ganz, 2003; Lacerda et al., 2014; Oppenheim et al., 2003; van der Weerden et al., 2013). Some plant defensins, like PDF1.2 have antifungal properties, and it is possible that SCRL5, as defensin-like protein (Silverstein et al., 2005), may have a positive role in antifungal immunity.

Although there are no DMRs in our treatments that correspond to known genes involved in SAR, such as PR1, EDS1, PAD4, SAG101, and SA biosynthetic genes (data not shown), analysis of the expression of these genes can tell us whether these genes are related to the loss of SAR in *pol IV*. It is possible that DNA methylation may affect other genes that are upstream or parallel to these pathways. Or these genes may be controlled by histone modification, as in the case of PR1, in which higher levels of active histone

marks such as H3K4me3 and H3K9ac were found after bacterial infection. Interestingly, the *pol V* mutant is reported to have a higher level of active histone marks even prior to local bacterial infection (Luna et al., 2012). The activity of RdDM or histone modification proteins may also be dynamic during SAR induction, and because RdDM and histone modification can be linked (Matzke and Mosher, 2014), studying both together may reveal a clearer picture of epigenetic control of gene regulation during pathogen infection.

METHODS

Plant Materials and growth conditions

Arabidopsis thaliana plants were grown in a controlled growth room at 23±1 °C in a 12-h light/12-h dark photoperiod. All experiments were performed on 4-week-old *Arabidopsis* plants. The following mutants seeds were used in this study: *drm1-2 drm2-2 cmt3-11* (*ddc*) (Chan et al., 2006), *ros1-3 dml2-1 dml3-1* (*rdd*) (Penterman et al., 2007), *pol IV* (*nrpd1a-3*, received from David Baulcombe) (Herr et al., 2005), *pol V* (*nrpd1b-11*) (Pontes et al., 2006) *, npr1* (Cao et al., 1994). Genotyping for *pol IV* and *pol V* mutants (Alonso et al., 2003) were done using primers listed in Table 3 following the PCR set-up recommended by T-DNA Primer Design (http://signal.salk.edu/tdnaprimers.2.html).

Bacterial inoculations

Bacterial strains used include: *Pseudomonas syringae* pv. *tomato* DC3000 carrying broad host range vector pVSP61 (EV) (Innes et al., 1993), pVSP61 plasmid containing avirulence gene *avrRpt2* (Innes et al., 1993), *avrRpm1* (Bisgrove et al., 1994), and a strain that has a mutation in its type III secretion system (*hrcC*-) (Yuan and He, 1996). Local inoculation bacterial growth assays were performed as previously described using bacterial inoculum concentration of 2.5×10^4 cfu per ml (Niu et al., 2016). For SAR bacterial growth assays, lower leaves were syringe-infiltrated with a bacterial inoculum concentration of 5×10^4 cfu per ml or a 10 mM $MgCl_2$ solution (mock), and 3 d later, upper leaves were syringe-infiltrated with a bacterial inoculum concentration of 2.5 x 10^4 cfu per ml. Bacterial growth in the upper leaves was assessed as in local inoculation bacterial growth assays. For inoculations for systemic tissue methylome sequencing and gene expression analysis, lower leaves were syringe-infiltrated with a bacterial inoculum concentration of 5×10^4 cfu per ml or a 10 mM $MgCl_2$ solution (mock), and 3 d later, upper leaves were syringe-infiltrated with a bacterial inoculum concentration of 1 x 10^5 cfu per ml or a 10 mM $MgCl_2$ solution (mock). Upper leaves were collected 1 d after inoculation, frozen in liquid nitrogen, and stored at –80° C until further processing. For inoculations for local tissue gene expression analysis, leaves were syringe-infiltrated with a bacterial inoculum concentration of 1 x 10^6 cfu per ml for *Pst* (EV) and *Pst* (*hrcC*-) and 5 x 10^5 cfu per ml for *Pst* (*avrRpt2*) or a 10 mM $MgCl_2$ solution (mock). Leaves were collected at 0 hpi, 2 hpi, 6 hpi, and 24 hpi, frozen in liquid nitrogen, and stored at –80° C until further processing.

Methylome library preparation

Libraries were prepared as described in Urich, et al. (Urich et al., 2015).

High-throughput sequencing and analysis

Sequencing, alignments, methyl-calling, identification of differentially methylated regions (DRMs), and comparisons were done as previously described (Dowen et al., 2012) with some modifications.

Generation of transgenic lines

To generate the SCRL5 overexpression lines, PCR was performed to amplify the entire coding sequence of SCRL5 using Phusion High-Fidelity DNA Polymerase (Thermo Fisher Scientific), ligated to pENTR vector (Life Technologies), and cloned into pEarleyGate (pEG) 100 destination vector (Earley et al., 2006) using LR Clonase II (Life Technologies). *Arabidopsis* plants were transformed using floral dip method with *Agrobacterium tumefaciens* strain GV3101 carrying the carrying cloned vector and selected using glufosinate ammonium. The primers used are listed in Table 3.

RNA extraction and analysis of relative gene expression

Tissue was ground to a powder in liquid nitrogen, and RNA extraction was performed as previously described (Onate-Sanchez and Vicente-Carbajosa, 2008). DNase treatment was performed using DNase I (Roche). For quantification of relative gene expression,

cDNA was synthesized using Superscript III or Superscript IV (Invitrogen) and anchored oligo(dT) primers (IDTDNA), and real-time RT–PCR was performed using SYBR green dye (Bio-Rad) on a CFX system (Bio-Rad). The primers used are listed in Table 3.

REFERENCES

Alonso, J.M., Stepanova, A.N., Leisse, T.J., Kim, C.J., Chen, H., Shinn, P., Stevenson, D.K., Zimmerman, J., Barajas, P., Cheuk, R., *et al*. (2003). Genome-wide insertional mutagenesis of Arabidopsis thaliana. Science *301*, 653-657.

Breitenbach, H.H., Wenig, M., Wittek, F., Jorda, L., Maldonado-Alconada, A.M., Sarioglu, H., Colby, T., Knappe, C., Bichlmeier, M., Pabst, E., *et al*. (2014). Contrasting Roles of the Apoplastic Aspartyl Protease APOPLASTIC, ENHANCED DISEASE SUSCEPTIBILITY1-DEPENDENT1 and LEGUME LECTIN-LIKE PROTEIN1 in Arabidopsis Systemic Acquired Resistance. Plant physiology *165*, 791-809.

Cao, H., Bowling, S.A., Gordon, A.S., and Dong, X. (1994). Characterization of an Arabidopsis Mutant That Is Nonresponsive to Inducers of Systemic Acquired Resistance. Plant Cell *6*, 1583-1592.

Cao, H., Glazebrook, J., Clarke, J.D., Volko, S., and Dong, X.N. (1997). The Arabidopsis NPR1 gene that controls systemic acquired resistance encodes a novel protein containing ankyrin repeats. Cell *88*, 57-63.

Chan, S.W., Henderson, I.R., Zhang, X., Shah, G., Chien, J.S., and Jacobsen, S.E. (2006). RNAi, DRD1, and histone methylation actively target developmentally important non-CG DNA methylation in arabidopsis. PLoS genetics *2*, e83.

De Coninck, B., Cammue, B.P.A., and Thevissen, K. (2013). Modes of antifungal action and in planta functions of plant defensins and defensin-like peptides. Fungal Biol Rev *26*, 109-120.

Dong, X.N. (2004). NPR1, all things considered. Current Opinion in Plant Biology *7*, 547-552.

Dowen, R.H., Pelizzola, M., Schmitz, R.J., Lister, R., Dowen, J.M., Nery, J.R., Dixon, J.E., and Ecker, J.R. (2012). Widespread dynamic DNA methylation in response to biotic stress. Proceedings of the National Academy of Sciences of the United States of America *109*, E2183-2191.

Earley, K.W., Haag, J.R., Pontes, O., Opper, K., Juehne, T., Song, K., and Pikaard, C.S. (2006). Gateway-compatible vectors for plant functional genomics and proteomics. Plant J *45*, 616-629.

Ganz, T. (2003). Defensins: Antimicrobial peptides of innate immunity. Nature Reviews Immunology *3*, 710-720.

Herr, A.J., Jensen, M.B., Dalmay, T., and Baulcombe, D.C. (2005). RNA polymerase IV directs silencing of endogenous DNA. Science *308*, 118-120.

Kemp, B.P., and Doughty, J. (2007). S cysteine-rich (SCR) binding domain analysis of the Brassica self-incompatibility S-locus receptor kinase. The New phytologist *175*, 619-629.

Kusaba, M., Dwyer, K., Hendershot, J., Vrebalov, J., Nasrallah, J.B., and Nasrallah, M.E. (2001). Self-incompatibility in the genus Arabidopsis: characterization of the S locus in the outcrossing A. lyrata and its autogamous relative A. thaliana. Plant Cell *13*, 627-643.

Lacerda, A.F., Vasconcelos, E.A.R., Pelegrini, P.B., and de Sa, M.F.G. (2014). Antifungal defensins and their role in plant defense. Front Microbiol *5*.

Lewsey, M.G., Hardcastle, T.J., Melnyk, C.W., Molnar, A., Valli, A., Urich, M.A., Nery, J.R., Baulcombe, D.C., and Ecker, J.R. (2016). Mobile small RNAs regulate genome-wide DNA methylation. Proceedings of the National Academy of Sciences of the United States of America *113*, E801-E810.

Lopez, A., Ramirez, V., Garcia-Andrade, J., Flors, V., and Vera, P. (2011). The RNA silencing enzyme RNA polymerase v is required for plant immunity. PLoS genetics *7*, e1002434.

Luna, E., Bruce, T.J., Roberts, M.R., Flors, V., and Ton, J. (2012). Next-generation systemic acquired resistance. Plant physiology *158*, 844-853.

Matzke, M.A., Kanno, T., and Matzke, A.J. (2015). RNA-Directed DNA Methylation: The Evolution of a Complex Epigenetic Pathway in Flowering Plants. Annu Rev Plant Biol *66*, 243-267.

Matzke, M.A., and Mosher, R.A. (2014). RNA-directed DNA methylation: an epigenetic pathway of increasing complexity. Nature reviews Genetics *15*, 394-408.

Melnyk, C.W., Molnar, A., Bassett, A., and Baulcombe, D.C. (2011). Mobile 24 nt small RNAs direct transcriptional gene silencing in the root meristems of Arabidopsis thaliana. Current biology : CB *21*, 1678-1683.

Niu, D., Lii, Y.E., Chellappan, P., Lei, L., Peralta, K., Jiang, C., Guo, J., Coaker, G., and Jin, H. (2016). miRNA863-3p sequentially targets negative immune regulator ARLPKs and positive regulator SERRATE upon bacterial infection. Nature communications *7*, 11324.

Onate-Sanchez, L., and Vicente-Carbajosa, J. (2008). DNA-free RNA isolation protocols for Arabidopsis thaliana, including seeds and siliques. BMC research notes *1*, 93.

Oppenheim, J.J., Biragyn, A., Kwak, L.W., and Yang, D. (2003). Roles of antimicrobial peptides such as defensins in innate and adaptive immunity. Ann Rheum Dis *62*, 17-21.

Pavet, V., Quintero, C., Cecchini, N.M., Rosa, A.L., and Alvarez, M.E. (2006). Arabidopsis displays centromeric DNA hypomethylation and cytological alterations of heterochromatin upon attack by Pseudomonas syringae. Molecular Plant-Microbe Interactions *19*, 577-587.

Penterman, J., Zilberman, D., Huh, J.H., Ballinger, T., Henikoff, S., and Fischer, R.L. (2007). DNA demethylation in the Arabidopsis genome. Proceedings of the National Academy of Sciences of the United States of America *104*, 6752-6757.

Pontes, O., Li, C.F., Costa Nunes, P., Haag, J., Ream, T., Vitins, A., Jacobsen, S.E., and Pikaard, C.S. (2006). The Arabidopsis chromatin-modifying nuclear siRNA pathway involves a nucleolar RNA processing center. Cell *126*, 79-92.

Schopfer, C.R., Nasrallah, M.E., and Nasrallah, J.B. (1999). The male determinant of self-incompatibility in Brassica. Science *286*, 1697-1700.

Sherman-Broyles, S., Boggs, N., Farkas, A., Liu, P., Vrebalov, J., Nasrallah, M.E., and Nasrallah, J.B. (2007). S locus genes and the evolution of self-fertility in Arabidopsis thaliana. Plant Cell *19*, 94-106.

Silverstein, K.A.T., Graham, M.A., Paape, T.D., and VandenBosch, K.A. (2005). Genome organization of more than 300 defensin-like genes in arabidopsis. Plant physiology *138*, 600-610.

Slotkin, R.K., Vaughn, M., Borges, F., Tanurdzic, M., Becker, J.D., Feijo, J.A., and Martienssen, R.A. (2009). Epigenetic reprogramming and small RNA silencing of transposable elements in pollen. Cell *136*, 461-472.

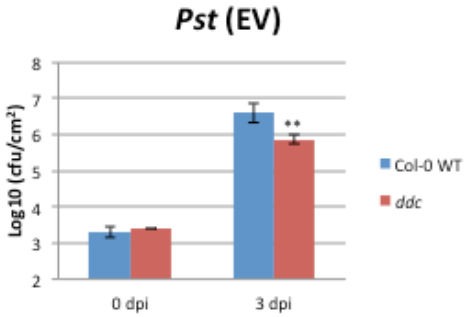
Urich, M.A., Nery, J.R., Lister, R., Schmitz, R.J., and Ecker, J.R. (2015). MethylC-seq library preparation for base-resolution whole-genome bisulfite sequencing. Nature protocols *10*, 475-483.

van der Weerden, N.L., Bleackley, M.R., and Anderson, M.A. (2013). Properties and mechanisms of action of naturally occurring antifungal peptides. Cellular and molecular life sciences : CMLS *70*, 3545-3570.

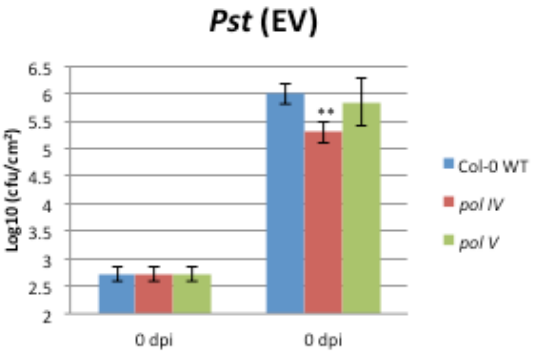
Vanoosthuyse, V., Miege, C., Dumas, C., and Cock, J.M. (2001). Two large Arabidopsis thaliana gene families are homologous to the Brassica gene superfamily that encodes pollen coat proteins and the male component of the self-incompatibility response. Plant Molecular Biology *46*, 17-34.

Yu, A., Lepere, G., Jay, F., Wang, J., Bapaume, L., Wang, Y., Abraham, A.L., Penterman, J., Fischer, R.L., Voinnet, O., *et al*. (2013). Dynamics and biological relevance of DNA demethylation in Arabidopsis antibacterial defense. Proceedings of the National Academy of Sciences of the United States of America *110*, 2389-2394.

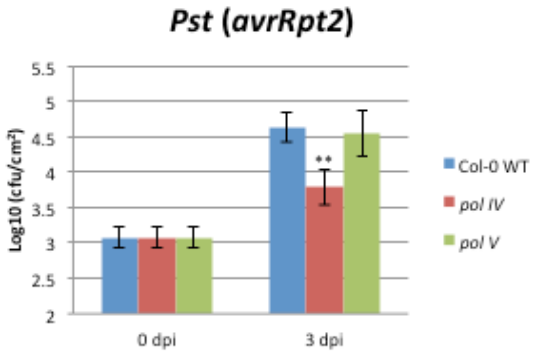
a


Pst (EV)
Log10 (cfu/cm²)
8
7
6
5
4
3
2
**
0 dpi
3 dpi
Col-0 WT
ddc

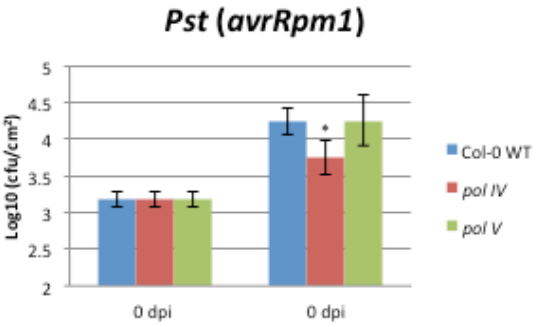
b


Pst (EV)
Log10 (cfu/cm²)
6.5
6
5.5
5
4.5
4
3.5
3
2.5
2
**
0 dpi
0 dpi
Col-0 WT
pol IV
pol V

c


Pst (*avrRpt2*)
Log10 (cfu/cm²)
5.5
5
4.5
4
3.5
3
2.5
2
**
0 dpi
3 dpi
Col-0 WT
pol IV
pol V

d


Pst (*avrRpm1*)
Log10 (cfu/cm²)
5
4.5
4
3.5
3
2.5
2
*
0 dpi
0 dpi
Col-0 WT
pol IV
pol V

e

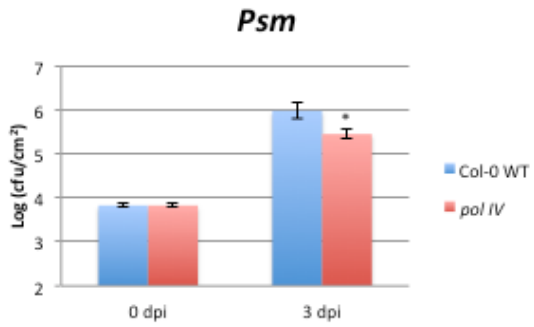

Psm
Log (cfu/cm²)
7
6
5
4
3
2
*
0 dpi
3 dpi
Col-0 WT
pol IV

Figure 3.1 RdDM mutants *ddc*, and *pol IV* have altered local disease resistance phenotypes to infection with *Pst*. *Pst* (EV) growth in **(a)** *ddc* triple mutant **(b)** *pol IV* and *pol V* single mutants; **(c)** *Pst* (*avrRpt2*) and **(d)** *Pst* (avrRpm1) growth in *pol IV* and *pol V* single mutants; **(e)** *Psm* growth in *pol IV* mutant. Bacterial inoculum concentration: 2.5×10^4 colony forming units [cfu] per ml. Bacterial growth was measured at 3 dpi. Error bars represent s.d. for at least 15 leaf discs. Similar results were obtained from at least two biological replicates. ***P* value <0.01; **P* value <0.05 (Student's *t*-test).

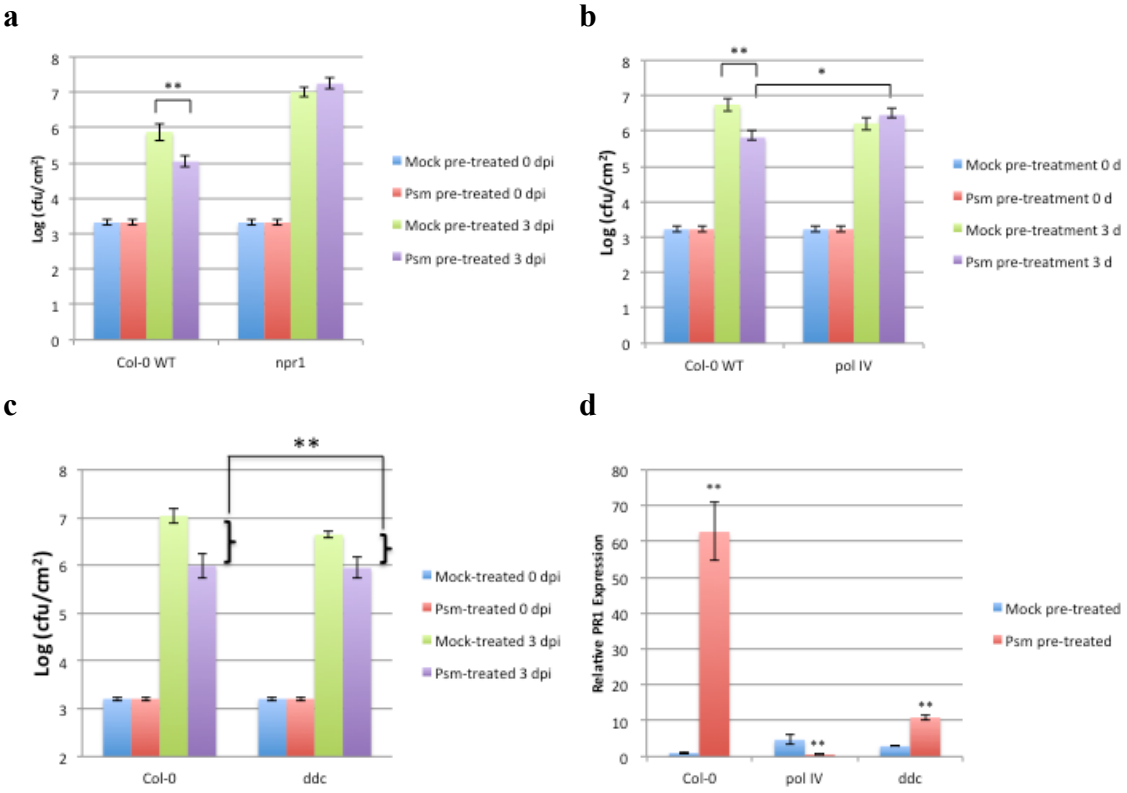


Figure 3.2 The *pol IV* mutant does not exhibit SAR and is missing PR1 induction. Bacterial growth in infected upper leaves were measured at 3 dpi. Lower leaves of **(a)** *npr1*, **(b)** *pol IV*, and **(c)** *ddc* were pre-treated with either a mock solution or *Psm* (inoculum concentration: 5 x 10^4 colony forming units [cfu] per ml), and 3 d later, the upper leaves were inoculated with *Psm* (inoculum concentration: 2.5 × 10^4 cfu per ml). Error bars represent s.d. for at least 15 leaf discs. Similar results were obtained from at least two biological replicates. ***P* value <0.01; **P* value <0.05 (Student's *t*-test). **(d)** The relative expression of PR1 was measured by real-time RT-PCR in upper leaves 4 d after either mock or *Psm* pre-treatment of lower leaves (inoculum concentration: 5 x 10^4 cfu per ml). Error bars indicate s.d. from three technical replicates. ***P* value <0.01 (Student's *t*-test).

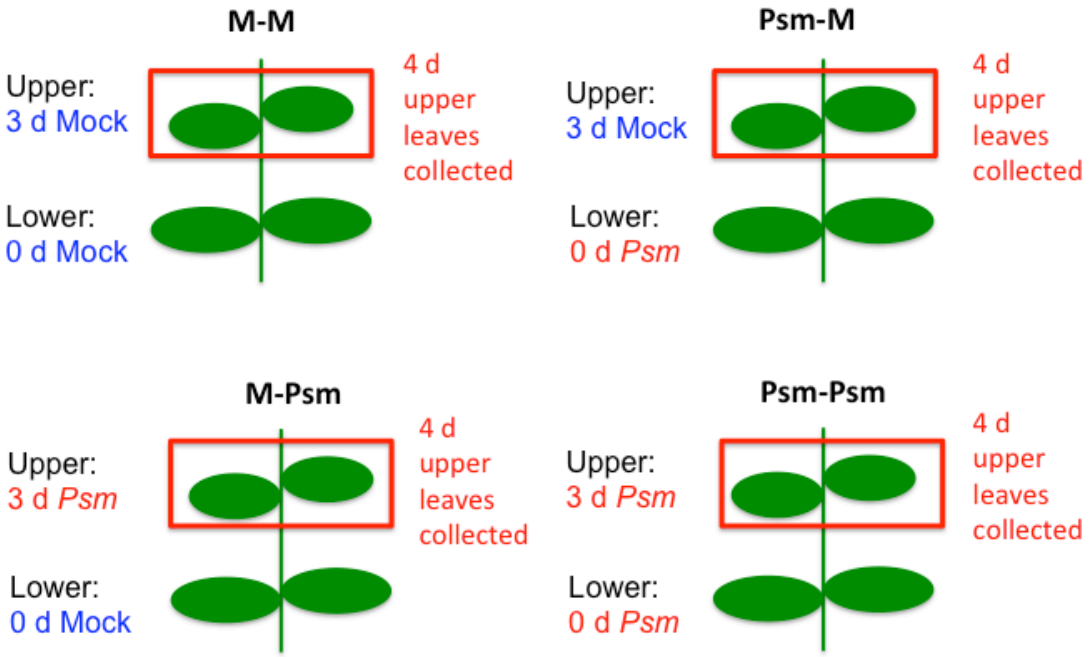
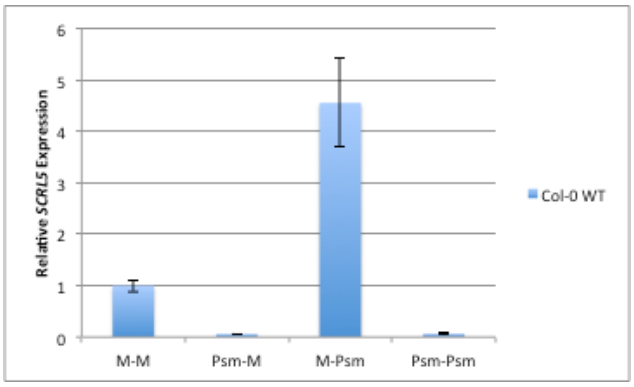


Figure 3.3. Simple schematic of the infection treatments for Col-0 WT and *pol IV* mutants used for whole genome bisulfite sequencing. Lower leaves of plants were treated with either 10 $MgCl_2$ (M) or *Psm* (inoculum concentration: 5 x 10^4 cfu per ml) (Psm). 3 d later, upper leaves were treated with either 10 $MgCl_2$ (M) or *Psm* (inoculum concentration: 1 x 10^5 cfu per ml) (Psm). 1 d later (4 d after the initial treatment), upper leaves were collected and used for further processing.

a


Gene Models (TAIR 9)
scrl5
scaling 1
AT1G60987.1
Ecker Col-0 mC
Col M-M 1 mC
Col M-M 2 mC
Col ES-M 1 mC
Col ES-M 2 mC
Col M-ES 1 mC
Col M-ES 3 mC
Col ES-ES 1
Col ES-ES 2 mC
sde4-3 mC
pol4 M-M 1 mC
pol4 M-M2 mC
pol4 ES-M 1
pol4 ES-M 2 mC
pol4 M-ES 1
pol4 M-ES 2 mC
pol4 ES-ES 1 mC
pol4 ES-ES 2 mC

b


Relative SCRL5 Expression
0
1
2
3
4
5
6
M-M
Psm-M
M-Psm
Psm-Psm
Col-0 WT

c

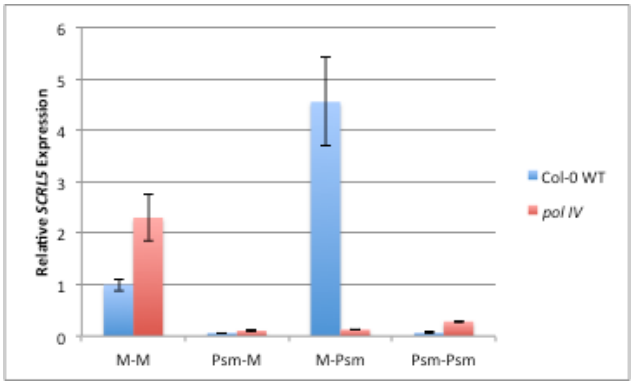
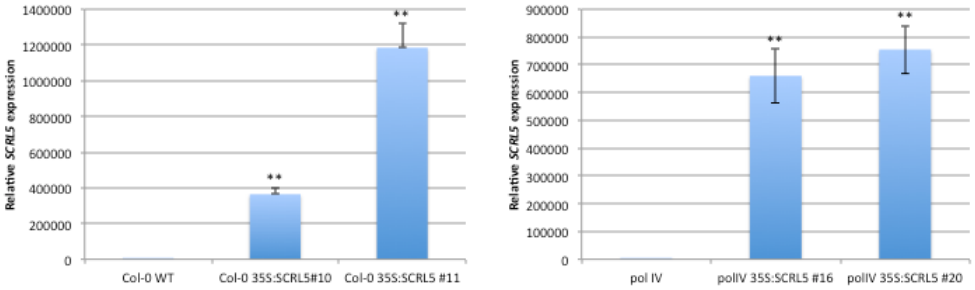

Relative SCRL5 Expression
0
1
2
3
4
5
6
M-M
Psm-M
M-Psm
Psm-Psm
Col-0 WT
pol IV

Figure 3.4. Increased DNA methlyation upstream of SCRL5 (At1G60987) is associated with downregulation of relative gene expression after *Psm* pre-treatment compared to mock pre-treatment in Col-0 WT.
(a) CHH (pink), CHG (blue), and CG (yellow) methylation marks of the upper leaves are shown in the respective treatments (M=mock, ES=Psm; lower leaves-upper leaves) of Col-0 WT and *pol IV* plants. Partial SCRL5 gene structure is shown at the top (red=5' UTR, green=exon). Two biological replicates are shown for each SAR treatment. Ecker Col-0 and sde4-3 (*pol IV*) were untreated tissue. The relative expression of *SCRL5* in upper leaves in the respective treatments (lower leaves-upper leaves) in **(b)** Col-0 WT and **(c)** Col-0 WT with *pol IV* plants was measured by real-time RT-PCR. Treatment conditions are indicated in Figure 3.3. Error bars indicate s.d. from three technical replicates. ***P* value <0.01 (Student's *t*-test).

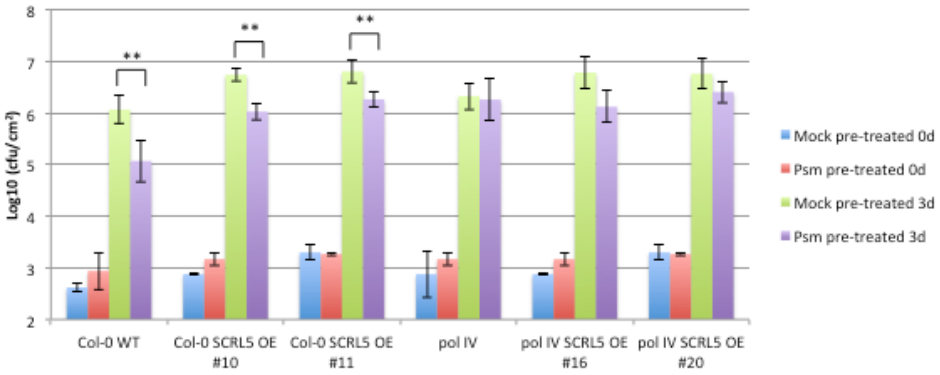
a

MKFVAIFLVTCVLFSLFPSHLSQGEESRMNINAERRPW**C**PSKIQMFDTN
CEVDGAKQ**C**LDLLISTWDPSVRLTRVS**C**I**C**SDFPYRNMM**C**S**C**PNMI**C**P

b



c



d

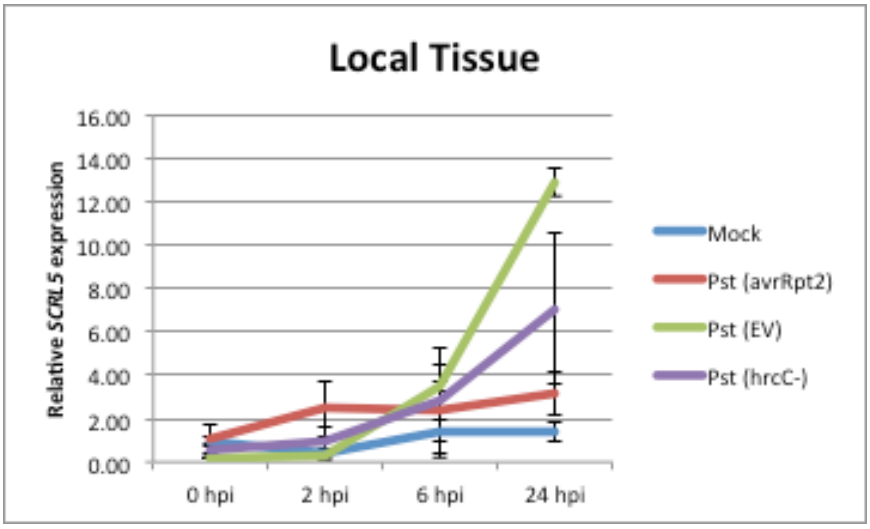


Figure 3.5 SCRL5 is a defensin-like protein with a complex role in plant defense. **(a)** Protein sequence of SCRL5 with the signal peptide in black bold letters and cysteines in red bold letters**. (b)** Relative *SCRL5* expression of Col-0 SCRL5 overexpression lines (#10 and #11) and pol IV SCRL5 overexpression lines (#16 and #20) measured by real-time RT-PCR. Error bars indicate s.d. from three technical replicates. ***P* value <0.01 (Student's *t*-test). **(c)** Bacterial growth was measured in infected upper leaves 3 dpi. Plants pre-treated with either a mock solution or *Psm* (inoculum concentration: 5 x 10^4 colony forming units [cfu] per ml), and 3 d later, the upper leaves were inoculated with *Psm* (inoculum concentration: 2.5 × 10^4 cfu per ml). Error bars represent s.d. for at least 15 leaf discs. ***P* value <0.01 (Student's *t*-test) **(d)** Relative *SCRL5* expression was measured in local tissue inoculated with mock, *Pst* (EV), *Pst* (*avrRpt2*), and *Pst* (*hrcC*-). at 0, 2, 6, and 24 hpi [inoculum concentration: 1 x 10^6 cfu per ml for *Pst* (EV) and *Pst* (*hrcC*-) and 5 x 10^5 cfu per ml for *Pst* (*avrRpt2*)].

Table 3. Primers used in this study.

For real-time RT-PCR	
Actin F for qPCR	AGTGGTCGTACAACCGGTATTGT
Actin R for qPCR	GATGGCATGAGGAAGAGAGAAAC
PR1 104F for qPCR	TCGAAAGCTCAAGATAGCCCA
PR1 523R for qPCR	TCATTAGTATGGCTTCTCGTTC
SCRL5 107F for qPCR	CCTTTTCCCAAGCCACCTGTCACA
SCRL5 291R for qPCR	AAGAGACTCGGGTGAGCCTTACAC
For genotyping SALK lines	
LBb1.3	ATT TTG CCG ATT TCG GAA C
nrpd1a-3 LP	GATCTGTTCAGCTTGCTCGTC
nrpd1a-3 RP	TTAATGTTCTTCATGCGGGAC
nrpd1b-11 LP	ATTTCTTCTTTGATGGGGGAG
nrpd1b-11 RP	TGTCGTGGATATGACCATTTG
Actin F for DNA	TCATACTAGTCTCGAGAGATGACTCAGATCATGTTTGAG
Actin R for DNA	TCATTCTAGAGGCGCGCCACAATTTCCCGTTCTGCGGTAG
For SCRL cloning	
SCRL5 F for cloning	CACCATGAAGTTTGTTGCAATCTTCTTGGTTACTTGTGTC TT
SCRL5 R for cloning	CTAGGGACAAATCATATTAGGACAACTACACATCATA
M13 Forward (−20)	GTAAAACGACGGCCAG
M13 Reverse	CAGGAAACAGCTATGAC
OCS3R	GCGCTCTATCATAGATGTCG
CaMV35SF	TAACAGAACTCGCCGTGAAGACTG

CHAPTER FOUR

Chemical Genetics Screen Targeting Small RNA Mediated Gene Silencing Pathways in *Arabidopsis Thaliana*

ABSTRACT

Plant small RNAs are short, non-coding RNAs involved in many processes, including development, maintenance of genome integrity, and response to abiotic and biotic stresses. They silence gene expression by directing mRNA degradation, translational inhibition, or by recruiting factors for chromatin modification and DNA methylation. There are many types of small RNAs, one of which is natural antisense transcripts-derived small-interfering RNA (nat-siRNA), so called because it is produced from overlapping sense and antisense transcripts from the same genomic loci. To complement genetic studies, we conducted a screen for compounds that interrupt a nat-siRNA pathway in *Arabidopsis* using a luciferase transgenic line exhibiting silencing. Chemicals from the "Library of AcTive Compounds on Arabidopsis" (LATCA) were used to perturb the silencing pathways to identify silencing-inhibition chemicals and new proteins or receptors involved in the biogenesis or function of nat-siRNAs. This approach was used due to its ability to overcome problems found in traditional genetic screens, such as duplicate or essential genes. After several rounds of screening, we found 11 putative hits disrupting the nat-siRNA pathway. These molecules effective at

perturbing these small RNA pathways could be further studied to discover their mode(s) of action. This cross-disciplinary project exemplifies the discovery potential that lies at the interface between chemistry and genetics.

INTRODUCTION

Plant small RNAs (sRNAs) are short non-coding RNA elements ranging from 20–24 nucleotides (nt) that regulate gene expression at transcriptional and posttranscriptional level. In plants, sRNAs mediate gene silencing by directing cytosine methylation and histone modifications (transcriptional gene silencing) or by mediating mRNA degradation and translational inhibition (posttranscriptional gene silencing or PTGS) (Bologna and Voinnet, 2014; Borges and Martienssen, 2015). Consequently, they are involved in a range of plant pathways and processes including development, abiotic and biotic stress response, genome maintenance, and genomic imprinting (Castel and Martienssen, 2013; Chen, 2012; Fei et al., 2013; Khraiwesh et al., 2012; Matzke et al., 2015; Pumplin and Voinnet, 2013; Seo et al., 2013; Sunkar et al., 2012; Weiberg and Jin, 2015; Weiberg et al., 2014).

Plant sRNAs are divided into two categories, each with distinct biogenesis and functional pathways involving several enzyme families: microRNAs (miRNAs) and short-interfering RNAs (siRNAs). siRNAs are then further classified as heterochromatic siRNAs (hc-siRNAs), phase seconary siRNAs (phasiRNAs, or trans-acting siRNAs, ta-siRNAs), and natural antisense transcript-derived siRNAs (nat-siRNAs). Although the biogenesis pathways differ, in general, they begin at the formation of double stranded

RNA (dsRNA) which are derived from viral RNA transcripts, endogenous transcripts producing stem-loop structures, inverted repeats, or RNA-dependent RNA polymerase (RDR) transcripts. RNase-III ribonuclease Dicer-like (DCL) proteins process the dsRNA into short duplexes, with the length dependent on the DCL type. From the resulting sRNA duplex, one strand is incorporated into Argonaute (AGO) protein to form the RNA-induced silencing complex (RISC), which targets complementary transcripts for post-transcriptional gene silencing, via mRNA cleavage or translational inhibition, or transcriptional gene silencing, via other recruited factors which mediate DNA methylation or histone modification (Bologna and Voinnet, 2014; Borges and Martienssen, 2015).

Natural antisense transcripts (NATs) are formed by the overlapping of antisense transcripts of the same (*cis*) or different loci (*trans*). *cis*-NATs can be processed by RNA silencing machinery to produce nat-siRNAs. They may also be dependent on DCL1 or DCL3, RDR2 or RDR6, and Polymerase IV (Pol IV), but their biogenesis is complex and varied. They can play a role in various processes in plants, such as fertilization, immunity, abiotic stress, cytokinin regulation (Borsani et al., 2005; Chen et al., 2010; Jin et al., 2008; Katiyar-Agarwal et al., 2006; Lu et al., 2012; Ron et al., 2010; Zhang et al., 2013; Zhang et al., 2012; Zhou et al., 2009; Zubko and Meyer, 2007).

Our lab previously discovered a 22-nt nat-siRNA called natsiRNAATGB2 that is specifically induced by *Pseudomonas syringae* pv. *tomato* (*Pst*) carrying effector gene *avrRpt2*. It is formed from the overlap of two transcripts, *ATGB2* (a Rab2-like small GTP-binding protein) and *PPRL* (a pentatricopeptide repeats protein-like gene). After

infection, *ATGB2* is upregulated, natsiRNAATGB2 is formed, and it targets the 3' UTR of *PPRL*, a putative negative regulator of plant defense, leading to its downregulation. The biogenesis of natsiRNAATGB2 depends on DCL1, RDR6, Pol IV, Hua Enhancer 1 (HEN1), Hyponastic 1 (HYL1), and Suppressor of gene silencing (SGS3); its induction depends on the cognate R gene *RPS2 (RESISTANT TO P. SYRINGAE 2*), which recognizes *avrRpt2*, as well as Non race-specific disease resistance 1 (NDR1). However, the study stated that other factors may also be involved in the generation of natsiRNATGB2 that still need to be uncovered.

Previously, many components of small RNA pathways and disease resistance pathways were uncovered using forward genetics screen involving mutants. In the past couple of decades, small molecules have been used to perturb signaling pathways in cells. This technology, termed chemical genetics has led to the discovery of many new components in various model systems. Forward chemical genetics screens offer many advantages by circumventing the limitations present in traditional forward genetics screens. One limitation is loss-of-function lethality. Chemical screens give the user temporal control over the activity of a small molecule: chemicals can be added after seed germination to prevent embryo lethality or even be removed at a desired time point to remove its effects if they are not permanent. Another limitation is gene redundancy, which may prevent the appearance of a desired phenotype. Chemicals may be able to target not only one protein but multiple proteins of a gene family (Blackwell and Zhao, 2003; Hicks and Raikhel, 2014; Norambuena et al., 2009; Sadhukhan et al., 2012; Schenone et al., 2013). Considering that *Arabidopsis* has four DCL and 10 AGO

proteins, most with structural homology and functional redundancy, an approach that enables one to turn off all proteins is useful in studying silencing pathways (Bologna and Voinnet, 2014; Borges and Martienssen, 2015; Mallory and Vaucheret, 2010). These chemicals may also be applied in agriculture to prevent desired transgenes (pathogen resistance, pesticide resistance, etc.) from being silenced in food crops (Repellin, et al. 2001).

To investigate the natsiRNAATGB2 pathway, and to discover factors involved in its biogenesis and induction, we conducted a forward chemical screen. Our goal was to find small molecules that would perturb this pathway and inhibit the silencing

RESULTS

Screening of small molecules targeting a nat-siRNA pathway

Katiyar-Agarwal, et al., discovered an endogenous nat-siRNA that is strongly induced by a *Pst* (*avrRpt2*). The 22-nucleotide nat-siRNA is generated from the overlapping region of a Rab2-like small GTP-binding protein gene (*ATGB2)* and a PPRL (pentatricopeptide) repeat protein-like gene. The PPRL gene is a putative negative regulator of the *RPS2*-mediated disease resistance pathway (Katiar-Agarwal, et al. 2006). R genes confer effector-triggered immunity for the plant under pathogen attack and results in a hypersensitive response (HR) in which the infected areas of the plant undergo cell death to stop the spread of the pathogen (Dodds and Rathjen, 2010).

To investigate this nat-siRNA pathway, we used a transgenic *Arabidopsis* line carrying two constructs: a *Pst* effector gene *avrRpt2* in a glucocorticoid-inducible

expression vector (Aoyama and Chua, 1997) and a Cauliflower Mosaic Virus (CaMV) 35S promoter driving a luciferase (LUC) reporter gene linked to the nat-siRNA target site (Figure 4.1) (Katiyar-Agarwal et al., 2006). With the addition of DEX and luciferin, the plants initially showed LUC expression that lasted until the nat-siRNA silenced the LUC reporter gene. At 17–18 hours after DEX exposure, the plants have no LUC expression. With the addition of a small chemical that perturbs the nat-siRNA biogenesis or functional pathway, LUC expression can be seen even at 20 hours post DEX exposure. Furthermore, plants in which the nat-siRNA silencing pathway is functional exhibit HR after four to five days and have wilted leaves. Plants were monitored for LUC expression and HR. 3,680 compounds were screened from the LACTA library (Figure 4.2). Because of the amount of DEX and luciferin applied to the plants may vary, duplicates of each chemical were screened, and several rounds of screening were conducted to narrow down the number of positive hits.

The first round of screening yielded 206 compounds, rescreening these yielded 55 compounds, and a final and third rescreening yielded 11 compounds (Figure 4.3). Four had antimicrobial antifungal properties, while others were involved in treatment of cancer, treatment of pain, fluorescent stain, vascular smooth muscle relaxant, antihypertensive, vasodilators, and ulcer inhibitors, or of unknown function. We have made efforts to acquire more of these compounds to perform follow-up experiments, but the chemicals were expensive to obtain; thus, we are seeking collaborations with chemists who can synthesize some of these compounds.

DISCUSSION

Future work will involve determining whether the compounds are indeed acting on the silencing pathway. Northern blot analysis will be used to detect the levels of small RNAs and small RNA precursors in plants grown with the chemical. If the levels of mature small RNAs are low or absent, it will confirm that the chemical interferes with the synthesis or processing of the small RNA. The presence of precursors (which are distinguishable in size from the final small RNAs products) would indicate which step of synthesis is affected by the chemical. If the mature small RNA levels have no obvious change, this suggests the chemical affects the function rather than the biogenesis of the small RNAs. This approach may give us target candidates, which can then be tested for interaction with the compound.

Structure-activity relationship studies of the compounds will reveal which moieties on the compounds are responsible for its activity. Analogs of the compounds may be purchased or synthesized and then tested. Knowing the responsible moieties and their properties (hydrophotic, charge, stearic features, etc.) would give us insight into the target.

The most successful way to identify targets is to use a genetics screen to search for mutants hypersensitive or insensitive to the compounds. Ethyl methanesulfonate will be used to mutagenize the *Arabidopsis* transgenic seeds used in this screen. These mutant seeds will then be grown with the compounds and screened for luciferase expression and hypersensitive response, or cell death. Insensitive mutants will not be affected by the compounds and will not show luciferase expression after 18 hours and

also will show hypersensitive response. Hypersensitive mutants may show just the opposite. Genetic mapping to determine the location of the mutations may reveal the target. Targets may be known proteins involved in the processing or function of the small RNAs (e.g. Dicer or Argonaute) or unknown proteins.

Compounds that do perturb the RNA silencing pathway may be applied in agriculture to prevent desired transgenes (pathogen resistance, pesticide resistance, etc.) from being silenced in food crops, provided that they do not have harmful effects. They also may be used in the research setting to study RNA silencing in mammalians or fungi.

METHODS

Plant Materials

Arabidopsis transgenic seeds were obtained from Brian Stastawicz (UC Berkeley). Seedlings were grown in a controlled Covarius growth chamber at 23±1 °C in a 12-h light/12-h dark photoperiod. Two-week-old seedlings were used for screening.

Chemical Screen

The transgenic *Arabidopsis* plants were screened with the chemicals from the "Library of AcTive Compounds on Arabidopsis" (LATCA, Sean Cutler) as previously described (Lii and Jin, 2014). Briefly, plants were grown in 96-well cell culture plates with a chemical in MS agar media. When the plants were two weeks old, DEX and luciferin was applied to cover the leaves. Plants were then monitored ~17–18 hours later

for LUC expression, using a charge coupled device (CCD) camera chilled to −70 °C (UCR Keen Hall Core Facility), and 4–5 d later for hypersensitive response (HR) using a dissecting scope.

REFERENCES

Aoyama, T., and Chua, N.H. (1997). A glucocorticoid-mediated transcriptional induction system in transgenic plants. The Plant journal : for cell and molecular biology *11*, 605-612.

Blackwell, H.E., and Zhao, Y. (2003). Chemical genetic approaches to plant biology. Plant physiology *133*, 448-455.

Bologna, N.G., and Voinnet, O. (2014). The diversity, biogenesis, and activities of endogenous silencing small RNAs in Arabidopsis. Annu Rev Plant Biol *65*, 473-503.

Borges, F., and Martienssen, R.A. (2015). The expanding world of small RNAs in plants. Nature reviews Molecular cell biology *16*, 727-741.

Borsani, O., Zhu, J., Verslues, P.E., Sunkar, R., and Zhu, J.K. (2005). Endogenous siRNAs derived from a pair of natural cis-antisense transcripts regulate salt tolerance in Arabidopsis. Cell *123*, 1279-1291.

Castel, S.E., and Martienssen, R.A. (2013). RNA interference in the nucleus: roles for small RNAs in transcription, epigenetics and beyond. Nature reviews Genetics *14*, 100-112.

Chen, D., Meng, Y., Ma, X., Mao, C., Bai, Y., Cao, J., Gu, H., Wu, P., and Chen, M. (2010). Small RNAs in angiosperms: sequence characteristics, distribution and generation. Bioinformatics *26*, 1391-1394.

Chen, X. (2012). Small RNAs in development - insights from plants. Current opinion in genetics & development *22*, 361-367.

Dodds, P.N., and Rathjen, J.P. (2010). Plant immunity: towards an integrated view of plant-pathogen interactions. Nat Rev Genet *11*, 539-548.

Fei, Q., Xia, R., and Meyers, B.C. (2013). Phased, secondary, small interfering RNAs in posttranscriptional regulatory networks. Plant Cell *25*, 2400-2415.

Hicks, G.R., and Raikhel, N.V. (2014). Plant chemical biology: are we meeting the promise? Frontiers in plant science *5*, 455.

Jin, H., Vacic, V., Girke, T., Lonardi, S., and Zhu, J.K. (2008). Small RNAs and the regulation of cis-natural antisense transcripts in Arabidopsis. BMC Mol Biol *9*, 6.

Katiyar-Agarwal, S., Morgan, R., Dahlbeck, D., Borsani, O., Villegas, A., Jr., Zhu, J.K., Staskawicz, B.J., and Jin, H. (2006). A pathogen-inducible endogenous siRNA in plant immunity. Proc Natl Acad Sci USA *103*, 18002-18007.

Khraiwesh, B., Zhu, J.K., and Zhu, J. (2012). Role of miRNAs and siRNAs in biotic and abiotic stress responses of plants. Biochimica et biophysica acta *1819*, 137-148.

Lii, Y., and Jin, H. (2014). Forward chemical screening of small RNA pathways. Methods in molecular biology *1056*, 95-101.

Lu, T., Zhu, C., Lu, G., Guo, Y., Zhou, Y., Zhang, Z., Zhao, Y., Li, W., Lu, Y., Tang, W.*, et al.* (2012). Strand-specific RNA-seq reveals widespread occurrence of novel cis-natural antisense transcripts in rice. BMC genomics *13*, 721.

Mallory, A., and Vaucheret, H. (2010). Form, function, and regulation of ARGONAUTE proteins. Plant Cell *22*, 3879-3889.

Matzke, M.A., Kanno, T., and Matzke, A.J. (2015). RNA-Directed DNA Methylation: The Evolution of a Complex Epigenetic Pathway in Flowering Plants. Annu Rev Plant Biol *66*, 243-267.

Norambuena, L., Raikhel, N.V., and Hicks, G.R. (2009). Chemical genomics approaches in plant biology. Methods in molecular biology *553*, 345-354.

Pumplin, N., and Voinnet, O. (2013). RNA silencing suppression by plant pathogens: defence, counter-defence and counter-counter-defence. Nature reviews Microbiology *11*, 745-760.

Ron, M., Alandete Saez, M., Eshed Williams, L., Fletcher, J.C., and McCormick, S. (2010). Proper regulation of a sperm-specific cis-nat-siRNA is essential for double fertilization in Arabidopsis. Genes Dev *24*, 1010-1021.

Sadhukhan, A., Sahoo, L., and Panda, S.K. (2012). Chemical genomics in plant biology. Indian journal of biochemistry & biophysics *49*, 143-154.

Schenone, M., Dancik, V., Wagner, B.K., and Clemons, P.A. (2013). Target identification and mechanism of action in chemical biology and drug discovery. Nature chemical biology *9*, 232-240.

Seo, J.K., Wu, J., Lii, Y., Li, Y., and Jin, H. (2013). Contribution of small RNA pathway components in plant immunity. Molecular plant-microbe interactions : MPMI *26*, 617-625.

Sunkar, R., Li, Y.F., and Jagadeeswaran, G. (2012). Functions of microRNAs in plant stress responses. Trends Plant Sci *17*, 196-203.

Weiberg, A., and Jin, H. (2015). Small RNAs-the secret agents in the plant-pathogen interactions. Curr Opin Plant Biol *26*, 87-94.

Weiberg, A., Wang, M., Bellinger, M., and Jin, H. (2014). Small RNAs: a new paradigm in plant-microbe interactions. Annu Rev Phytopathol *52*, 495-516.

Zhang, X., Lii, Y., Wu, Z., Polishko, A., Zhang, H., Chinnusamy, V., Lonardi, S., Zhu, J.K., Liu, R., and Jin, H. (2013). Mechanisms of small RNA generation from cis-NATs in response to environmental and developmental cues. Mol Plant *6*, 704-715.

Zhang, X., Xia, J., Lii, Y.E., Barrera-Figueroa, B.E., Zhou, X., Gao, S., Lu, L., Niu, D., Chen, Z., Leung, C.*, et al.* (2012). Genome-wide analysis of plant nat-siRNAs reveals insights into their distribution, biogenesis and function. Genome Biol *13*, R20.

Zhou, X., Sunkar, R., Jin, H., Zhu, J.K., and Zhang, W. (2009). Genome-wide identification and analysis of small RNAs originated from natural antisense transcripts in Oryza sativa. Genome research *19*, 70-78.

Zubko, E., and Meyer, P. (2007). A natural antisense transcript of the Petunia hybrida Sho gene suggests a role for an antisense mechanism in cytokinin regulation. The Plant journal : for cell and molecular biology *52*, 1131-1139.

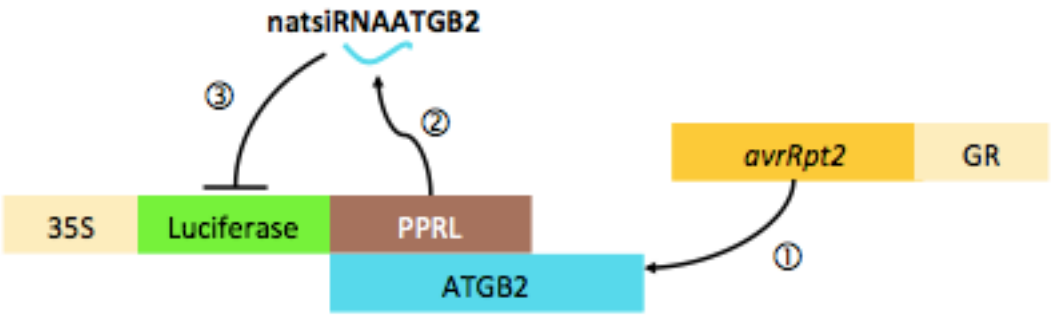


Figure 4.1 *Arabidopsis* transgenic plants containing two constructs were used for the screen. The first construct contains *Pst* effector gene *avrRpt2* attached to a glutocorticoid-inducible expression vector. The second contains a Cauliflower Mosaic Virus (CaMV) 35S promoter driving a luciferase (LUC) reporter green linked to the nat-siRNA target site—the 3' UTR of *PPRL*. Prior to addition of any chemicals, the CaMV promoter drives constitutive expression of LUC. With the addition of dexamethasone (DEX), *avrRtp2* is expressed, leading to the induction of *ATGB2* transcripts (Step 1). The formation of the *PPRL* and *ATGB2* NAT results in the production of natsiRNAATGB2 (Step 2) which targets the 3' UTR of PPRL and inhibits LUC expression (Step 3). A small chemical could target any of the steps (1–3), or possibly unknown proteins involved in this pathway.

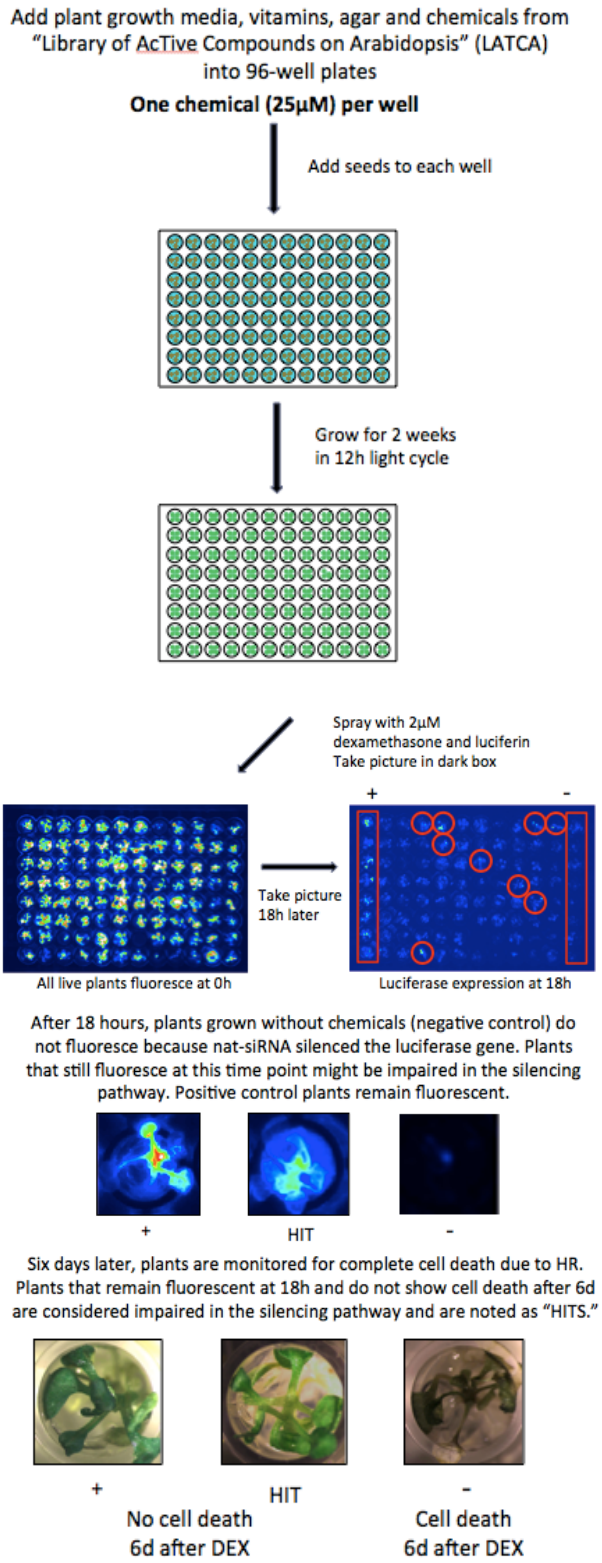


Figure 4.2. Schematic of screening process.

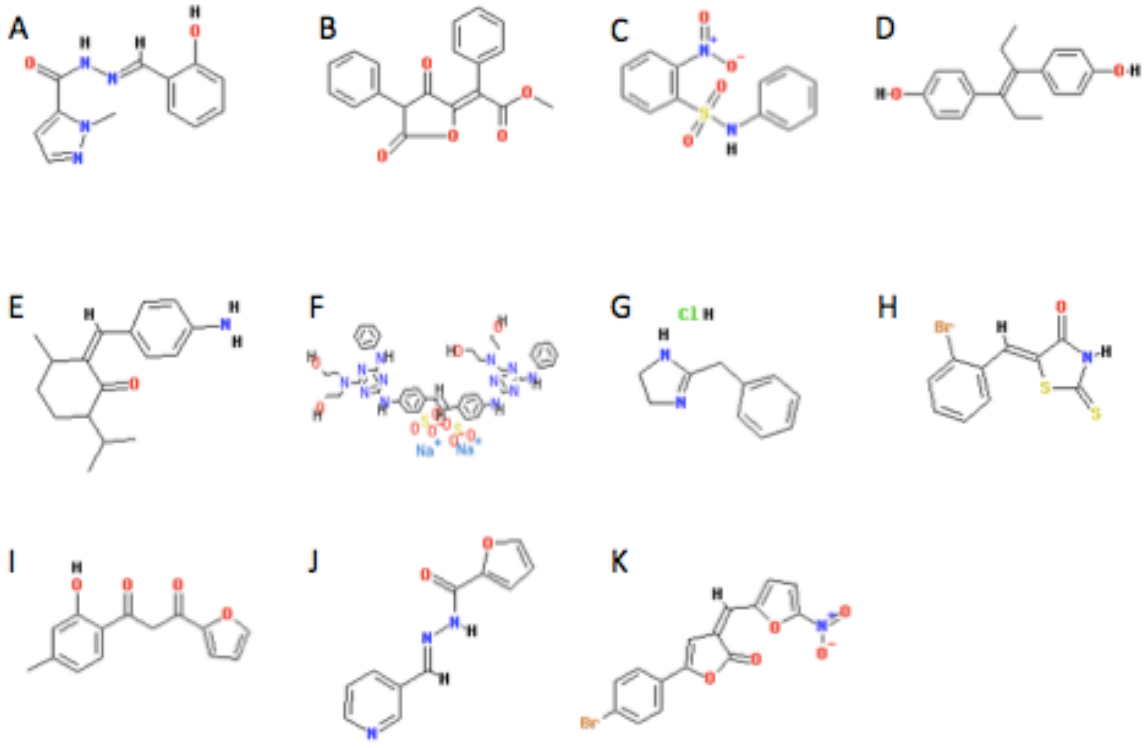


Figure 4.3. 11 putative hits from the LATCA library that perturb the natsiRNAATGB2 pathway. Chemicals are not shown in any particular order. The LATCA chemical identification number is given followed by the IUPAC name (if available) and other information (if available).
A. LAT011H06; 1H-Pyrazole-5-carboxylic acid, 1-methyl-, 2-[(2-hydroxyphenyl)-methylene]hydrazide; Other information: N/A
B. LAT001F06; Vulpinic Acid; Other information: produced from lichens, antimicrobial, antiherbivore
C. LAT014A04; name N/A; Other information: antifungal
D. LAT004B10; Diethylstilbestrol; Other information: Synthetic nonsteroidal estrogen, treatment of advanced prostate cancer, treatment of advanced breast cancer, carcinogen, teratogen
E. LAT024D11; Thiophene-2-carboxylic acid (4-phenylbutyl)amide; Other information: treatment of pain using selective antagonists of persistent sodium current
F. LAT006B07; Calcofluor white; Other information: fluorescent stain B, binds strongly to structures containing cellulose and chitin
G. LAT003A04; Tolazoline hydrochloride; Other information: alpha adrenergic blocking agent, treatment of persistent pulmonary hyper-tension in newborns, vascular smooth muscle relaxant

H. LAT013B05; 4-Thiazolidinone, 5-[(2-bromophenyl) methylene]-2-thioxo; Other information: Dopamine β-hydroxylase (II) inhibitor, useful as antihypertensives, vasodilators, and ulcer inhibitors
I. LAT015B04; 1,3-Propanedione, 1-(2-furanyl)-3-(2-hydroxy-4-methylphenyl); Other information: Some Intermediates in the synthesis showed fungicidal and bactericidal activity
J. LAT024G06; 2-Furancarboxylic acid, 2-(3-pyridinylmethylene)hydrazide; Other information: N/A
K. LAT026B04; 2(3H)-Furanone, 5-(4-bromophenyl)-3-[(5-nitro-2-furanyl)methylene]; Other information: antibacterial, inhibits transglycosylase (key enzyme in bacterial cell wall synthesis)